

Supporting information

Table of contents

1. Synthesis.....	S2
1.1. General methods.....	S2
1.2. Synthesis of phenylphosphonate-substituted 1,10-phenanthrolines.....	S2
1.3. Synthesis of the ruthenium complexes.....	S5
2. Photostability Studies.....	S10
3. X-ray diffraction of crystal structures.....	S11
4. Detailed NMR studies of complex Ru-4P.....	S13
5. Electrochemistry	S18
6. Study of photophysical properties.....	S24
7. DFT-studies.....	S26
8. Oxidation of sulfides.....	S75
9. NMR-spectra.....	S77
10. Mass-spectra of the complexes.....	S92
11. References.....	S97

1. Synthesis

1.1. Materials and methods

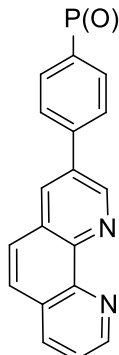
Unless otherwise noted, all chemicals and starting materials were obtained commercially from Acros and Aldrich–Sigma Co and used without further purification. 3-Bromo- and 3,8-dibromo-1,10-phenanthroline were prepared by using previously reported procedure¹ from 1,10-phenanthroline hydrochloride. 5-Bromo-1,10-phenanthroline was obtained from 1,10-phenanthroline by bromination in oleum.² 4,7-Dichloro-1,10-phenanthroline was prepared *via* three-step procedure from *o*-phenylenediamine and Meldrum's acid.³ 4-Chloro-1,10-phenanthroline was synthesized according to the same method.⁴ Phosphonate-substituted 1,10-phenanthrolines **3P**, **4P**, **5P**, **3,8P₂** and **4,7P₂** were obtained by using previously reported procedure.⁵ Diethyl 4-(4,4,5,5-tetramethyl-1,3,2-dioxaborolan-2-yl)phenylphosphonate was synthesized in two steps according to the known procedure.⁶ *cis*-[Ru(bpy)₂]Cl₂ was prepared from RuCl₃·H₂O as reported previously.⁷ Complex [Ru(phen)Ru(bpy)₂](PF₆)₂ (**Ru-phen**) was synthesized as reported in the previous work.⁸ Preparative column chromatography was carried out using Silica gel 60 (40–63 µm) from Merck Co. Dioxane was distilled successively over NaOH and sodium under argon; CH₂Cl₂ was distilled over CaH₂; DMF was distilled over CaH₂ under reduced pressure; EtOH was distilled over CaO; MeOH was used freshly distilled. All reactions were performed in argon. Preparation of Ru(II) complexes was conducted in Monowave 300 Microwave reactor (Anton Paar Co). ¹H and ¹³C NMR spectra were recorded with Bruker Avance-400 spectrometer in CDCl₃, CD₂Cl₂ or CD₃CN, using the residual signals of CHCl₃, CHDCl₂ or CHD₂CN as internal standards. MALDI TOF mass-spectra were obtained with Bruker Daltonics Autoflex II mass spectrometer in positive ion mode with dithranol matrix and polyethyleneglycols as internal standards. ESI mass measurements were obtained with a Thermo Scientific Orbitrap Elite high-field orbitrap hybrid mass spectrometer. FTIR spectra were registered on Nicolet iS 5 and Bruker Vector 22 spectrophotometers. Micro-ATR accessory (Pike) was used in order to obtain FTIR spectra of polycrystalline solid complexes. Elemental analysis was performed with a Thermo Electron Flash EA1112 CHNS analyzer.

1.2. Synthesis of phenylphosphonate-substituted 1,10-phenanthrolines

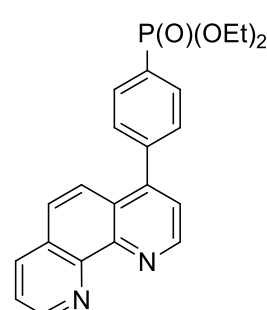
General procedure A.

A flask equipped with a magnetic stirrer, a condenser and a gas outlet was flushed with dry argon and charged with halogeno-substituted 1,10-phenanthroline (0.3–0.7 mmol), palladium catalyst (5–10 mol%), diethyl 4-(4,4,5,5-tetramethyl-1,3,2-dioxaborolan-2-yl)phenylphosphonate (1.25–2.5 equiv.) and absolute 1,4-dioxane. The mixture was stirred for 5 min at r.t. and cesium carbonate (2.5–5 equiv.) was added in stream of nitrogen. The reaction mixture was stirred under reflux for 24 h. After

cooling to r.t., the mixture was diluted in twice with dichloromethane and gravity filtered. The filtrate was concentrated under reduced pressure. The residue was taken up in dichloromethane and subjected to column chromatography on silica gel using a CH₂Cl₂/MeOH mixtures as eluents (gradual elution using pure CH₂Cl₂, CH₂Cl₂/MeOH, 200:1 to 20:1 v/v).

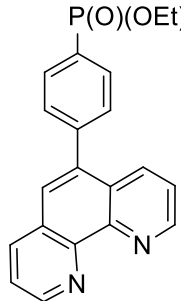


Diethyl 4-(1,10-phenanthrolin-3-yl)phenylphosphonate (3PPh) was obtained according to the general procedure A from 3-bromo-1,10-phenanthroline (124 mg, 0.48 mmol), diethyl 4-(4,4,5,5-tetramethyl-1,3,2-dioxaborolan-2-yl)phenylphosphonate (204 mg, 0.6 mmol) in the presence of Pd(PPh₃)₄ (27 mg, 5 mol%) and Cs₂CO₃ (391 mg, 2.5 equiv) in absolute dioxane (12 ml). Yield: 158 mg (84%); yellow oil; chromatography (CH₂Cl₂/MeOH, 200:3 v/v). ¹H NMR (CDCl₃, 400 MHz): δ 1.35 (t, 6H, J = 7.0 Hz, CH₃), 4.08–4.23 (m, 4H, CH₂O), 7.64 (dd, 1H, J = 8.0 Hz, J = 4.4 Hz, H8 (Phen)), 7.80–7.88 (m, 4H, H5 and H6 (Phen), H3 and H5 (Ph)), 7.98 (dd, 2H, $J_{H,P}$ = 12.9 Hz, $J_{H,H}$ = 8.4 Hz, H2 and H6 (Ph)), 8.25 (dd, 1H, J = 8.0 Hz, J = 1.7 Hz, H7 (Phen)), 8.45 (d, 1H, J = 2.2 Hz, H4 (Phen)), 9.20 (dd, 1H, J = 4.4 Hz, J = 1.7 Hz, H9 (Phen)), 9.41 (d, 1H, J = 2.2 Hz, H2 (Phen)). ¹³C{¹H} NMR (CDCl₃, 125 MHz): 16.3 (d, 2C, $J_{C,P}$ = 6.3 Hz), 61.9 (d, 2C, $J_{C,P}$ = 5.4 Hz), 123.2 (1C), 126.5 (1C), 127.3 (1C), 127.5 (d, 2C, $J_{C,P}$ = 15.1 Hz), 128.3 (1C), 128.8 (1C), 128.3 (d, 1C, $J_{C,P}$ = 189.6 Hz), 132.7 (d, 2C, $J_{C,P}$ = 10.0 Hz), 133.8 (1C), 134.6 (1C), 136.0 (1C), 141.5 (1C), 145.7 (1C), 146.0 (1C), 149.0 (1C), 150.5 (1C). ³¹P NMR (CDCl₃, 162.5 MHz): δ 18.2 (P(O)(OEt)₂). IR (neat): 3423 (H₂O), 3044, 2981 (CH), 2930, 2916, 2868, 1616, 1601, 1555, 1509, 1496, 1476, 1424, 1391, 1367, 1292, 1236 (P=O), 1162, 1132, 1098, 1046, 1015 (POC), 958, 873, 837, 780, 763, 732, 667, 658, 645, 627 cm⁻¹. HRMS (MALDI/TOF) m/z: [M + H]⁺ Calcd for C₂₂H₂₁N₂O₃P 393.1363; Found 393.1362.

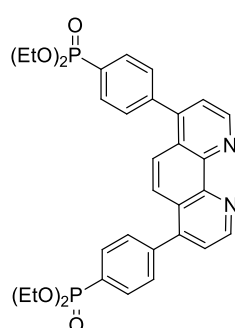


Diethyl 4-(1,10-phenanthrolin-4-yl)phenylphosphonate (4PPh) was obtained according to the general procedure A from 4-chloro-1,10-phenanthroline (69 mg, 0.32 mmol), diethyl 4-(4,4,5,5-tetramethyl-1,3,2-dioxaborolan-2-yl)phenylphosphonate (136 mg, 0.4 mmol) in the presence of Pd(OAc)₂ (7 mg, 10 mol%), PCy₃ (27 mg, 30 mol%) and Cs₂CO₃ (260 mg, 2.5 equiv) in absolute dioxane (8 ml). Yield: 65 mg (51%); red oil; chromatography (CH₂Cl₂/MeOH, 50:1 v/v). ¹H NMR (CDCl₃, 400 MHz): δ 1.37 (dt, 6H, $J_{H,H}$ = 6.5 Hz, $J_{H,P}$ = 1.8 Hz, CH₃), 3.95–4.12 (m, 4H, CH₂O), 7.30–7.38 (m, 1H, H8 (Phen)), 7.40–7.48 (m, 3H, H3 (Phen), H3 and H5 (Ph)), 7.51 (d, 1H, J = 9.2 Hz, H5 (Phen)), 7.59 (d, 1H, J = 9.2 Hz, H6 (Phen)), 7.82 (dd, 2H, $J_{H,P}$ = 13.1 Hz, $J_{H,H}$ = 8.1 Hz, H2 and H6 (Ph)), 8.02 (m, 1H, H7 (Phen)), 8.98–9.02 (m, 2H, H2 and

H9 (Phen)). $^{13}\text{C}\{\text{H}\}$ NMR (CDCl_3 , 125 MHz): 16.0 (d, 2C, $J_{\text{C},\text{P}} = 6.5$ Hz), 61.9 (d, 2C, $J_{\text{C},\text{P}} = 5.5$ Hz), 122.8 (1C), 123.9 (1C), 123.2 (1C), 125.8 (1C), 126.3 (1C), 128.2 (d, 1C, $J_{\text{C},\text{P}} = 189.6$ Hz), 127.8 (1C), 129.3 (d, 2C, $J_{\text{C},\text{P}} = 15.5$ Hz), 131.6 (d, 2C, $J_{\text{C},\text{P}} = 10.0$ Hz), 135.5 (1C), 141.5 (1C), 145.7 (1C), 146.1 (1C), 146.8 (1C), 149.2 (1C), 150.0 (1C). ^{31}P NMR (CDCl_3 , 162.5 MHz): δ 18.0 ($\text{P}(\text{O})(\text{OEt})_2$). HRMS (MALDI/TOF) m/z: [M + H]⁺ Calcd for $\text{C}_{22}\text{H}_{21}\text{N}_2\text{O}_3\text{P}$ 393.1363; Found 393.1362.



Diethyl 4-(1,10-phenanthrolin-5-yl)phenylphosphonate (5PPh) was obtained according to the general procedure A from 5-bromo-1,10-phenanthroline (124 mg, 0.48 mmol), diethyl 4-(4,4,5,5-tetramethyl-1,3,2-dioxaborolan-2-yl)phenylphosphonate (204 mg, 0.6 mmol) in the presence of $\text{Pd}(\text{PPh}_3)_4$ (27 mg, 5 mol%) and Cs_2CO_3 (391 mg, 2.5 equiv) in absolute dioxane (12 ml). Yield: 125 mg (66%); yellow oil; chromatography ($\text{CH}_2\text{Cl}_2/\text{MeOH}$, 50:1 v/v). ^1H NMR (CDCl_3 , 400 MHz): δ 1.33 (t, 6H, $J = 7.1$ Hz, CH_3), 4.07–4.23 (m, 4H, CH_2O), 7.55–7.60 (m, 3H, H8(Phen), H3 and H5 (Ph)), 7.65 (dd, 1H, $J = 8.1$ Hz, $J = 4.4$ Hz, H3 (Phen)), 7.71 (s, 1H, H6 (Phen)), 7.94 (dd, 1H, $J_{\text{H},\text{P}} = 13.4$ Hz, $J_{\text{H},\text{H}} = 8.2$ Hz, H2 and H6 (Ph)), 8.18 (dd, 1H, $J = 8.4$ Hz, $^4J = 1.7$ Hz, H7 (Phen)), 8.25 (dd, 1H, $J = 8.1$ Hz, $^4J = 1.7$ Hz, H4 (Phen)), 9.17 (dd, 1H, $J = 4.4$ Hz, $^4J = 1.7$ Hz, H9 (Phen)), 9.18 (dd, 1H, $J = 8.1$ Hz, $J = 4.4$ Hz, H2 (Phen)). $^{13}\text{C}\{\text{H}\}$ NMR (CDCl_3 , 125 MHz): δ 16.3 (d, 2C, $J_{\text{C},\text{P}} = 6.5$ Hz), 62.3 (d, 2C, $J_{\text{C},\text{P}} = 5.5$ Hz), 123.1 (1C), 123.6 (1C), 126.7 (1C), 127.3 (1C), 127.8 (1C), 128.2 (d, 1C, $J_{\text{C},\text{P}} = 189.6$ Hz), 129.8 (d, 2C, $J_{\text{C},\text{P}} = 15.5$ Hz), 131.9 (d, 2C, $J_{\text{C},\text{P}} = 10.5$ Hz), 134.5 (1C), 136.6 (1C), 137.7 (1C), 142.5 (1C), 144.7 (1C), 145.3 (1C), 149.4 (1C), 150.1 (1C). ^{31}P NMR (CDCl_3 , 162.5 MHz): δ 18.3 ($\text{P}(\text{O})(\text{OEt})_2$). IR (neat): 3461 (H_2O), 3029 (CH), 2980 (CH), 2929, 2903, 2867, 1596, 1580, 1549 1509, 1478, 1442, 1420, 1394, 1367, 1242 (P=O), 1164, 1139, 1124, 1097, 1048, 1015 (POC), 959, 934, 893, 875, 839, 792, 759, 743, 706, 611, 602 cm^{-1} . HRMS (MALDI/TOF) m/z: [M + H]⁺ Calcd for $\text{C}_{22}\text{H}_{21}\text{N}_2\text{O}_3\text{P}$ 393.1363; Found 393.1378.



Tetraethyl 4,4'-(1,10-phenanthroline-4,7-diy)bis(4,1-phenylene)diphosphonate (4,7(PPh)₂) was obtained according to the general procedure A from 4,7-dichloro-1,10-phenanthroline (169 mg, 0.68 mmol), diethyl 4-(4,4,5,5-tetramethyl-1,3,2-dioxaborolan-2-yl)phenylphosphonate (578 mg, 1.7 mmol) in the presence of $\text{Pd}(\text{OAc})_2$ (15 mg, 10 mol%), PCy_3 (57 mg, 30 mol%) and Cs_2CO_3 (1.1 g, 5 equiv) in absolute dioxane (17 ml). Yield: 229 mg (61%); pink oil; chromatography ($\text{CH}_2\text{Cl}_2/\text{MeOH}$, 20:1 v/v). ^1H NMR (CDCl_3 , 400 MHz): 1.36 (t, 12H, $J = 7.0$ Hz, CH_3), 4.11–4.27 (m, 8H, CH_2O), 7.58 (d, 2H, $J = 4.6$ Hz, H3 and H8 (Phen)), 7.63 (dd, 4H, $J_{\text{H},\text{P}}$

$J_{H,H} = 8.3$ Hz, H3 and H5 (Ph)), 7.77 (s, 2H, H5 and H6 (Phen)), 7.99 (dd, 4H, $J_{H,P} = 13.1$ Hz, $J_{H,H} = 8.3$ Hz, H2 and H6 (Ph)), 9.26 (d, 2H, $J = 4.6$ Hz, H2 and H9 (Phen)). $^{13}\text{C}\{\text{H}\}$ NMR (CDCl_3 , 125 MHz): 16.3 (d, 4C, $J_{\text{C},\text{P}} = 7.3$ Hz), 62.3 (d, 4C, $J_{\text{C},\text{P}} = 6.4$ Hz), 123.4 (2C), 124.0 (2C), 126.1 (2C), 128.9 (d, 2C, $J_{\text{C},\text{P}} = 189.9$ Hz), 129.7 (d, 4C, $J_{\text{C},\text{P}} = 15.4$ Hz), 132.1 (d, 4C, $J_{\text{C},\text{P}} = 10.0$ Hz), 141.8 (d, 2C, $J_{\text{C},\text{P}} = 3.8$ Hz), 146.8 (2C), 147.3 (2C), 150.0 (2C). ^{31}P NMR (CDCl_3 , 162.5 MHz): δ 17.8 ($\text{P}(\text{O})(\text{OEt})_2$). HRMS (MALDI/TOF) m/z: [M + H]⁺ Calcd for $\text{C}_{32}\text{H}_{35}\text{N}_2\text{O}_6\text{P}_2$ 605.1965; Found 605.1996.

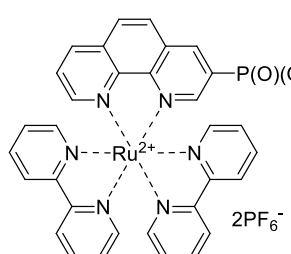
1.3. Synthesis of the ruthenium complexes

General procedure B.

A glass vessel G10 (Anton Paar) equipped with a magnetic stirrer was charged with *cis*-[Ru(bpy)₂Cl₂] (1 equiv.), substituted 1,10-phenanthroline ligand (1.1 equiv.) and dry ethanol (to C = 0.05 M). The mixture was stirred at 100°C in microwave reactor for 2 h, than mixture was concentrated under reduced pressure. The deionized water was added to the residue, the red solution was washed with equal volume of equal portions of dichloromethane until the purple color of the organic layer ceases. Methanol (60 vol%) and saturated aqueous solution of NH₄PF₆ (17 vol%) was added to the water fraction, the product was than extracted with 3 portions of dichloromethane. The combined organic layers were dried over 3Å and concentrated *in vacuo* giving the product as red glassy compound.

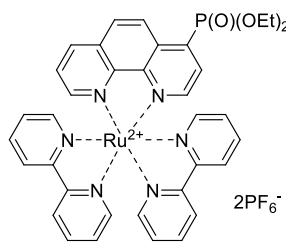
General procedure C.

Glass vessel G10 (Anton Paar) equipped with a magnetic stirrer was charged with *cis*-[Ru(bpy)₂Cl₂] (1 equiv.), substituted 1,10-phenanthroline ligand (1.1 equiv.) and dry ethanol (to C = 0.05M). The mixture was stirred at 100 °C in microwave reactor for 2 h, than hot mixture was diluted in twice with dry ethanol and poured through the glass filter and allowed to cool. The saturated aqueous solution of NH₄PF₆ was added (17 vol%). The product as red precipitate was collected by filtration and dried under reduced pressure at 80°C.

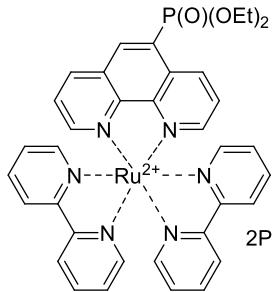


[Ru(3P)(bpy)₂](PF₆)₂ (**Ru-3P**) was prepared according to procedure C from **3P** (70 mg, 0.22 mmol) and *cis*-[Ru(bpy)₂Cl₂] (97 mg, 0.1 mmol). Yield: 197 mg (94%); red powder. ^1H NMR (CD_2Cl_2 , 400 MHz): 1.25 (t, 6H, $J = 7.0$ Hz, CH₃), 4.10–4.20 (m, 4H, CH₂O), 7.15–7.48 (m, 2H, H5 (bpy)), 7.48–7.56 (m, 4H, H5 and H6 (bpy)), 7.81 (d, 1H, $J = 5.3$ Hz, H6 (bpy)), 7.81–7.91 (m, 2H, H6 (bpy) and H8 (Phen)), 7.98–8.20 (m, 6H, H2 and H9 (Phen)),

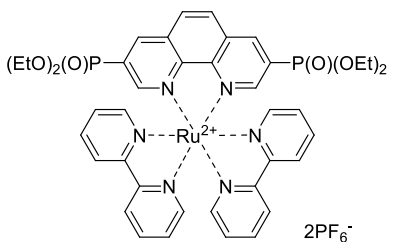
H6, H4 and H4' (bpy)), 8.23–8.32 (m, 2H, H5 and H6 (Phen)), 8.39–8.54 (m, 4H, H3 and H3' (bpy)), 8.61 (dd, 1H, J = 8.3 Hz, 4J = 1.1 Hz, H7 (Phen)), 8.88 (dd, 1H, J = 9.2 Hz, 4J = 1.3 Hz, H4 (Phen)). ^{31}P NMR (CD_2Cl_2 , 162.5 MHz): δ 10.2 (1P, P(O)(OEt)₂), 130.0–160.0 (m, 2P, PF₆). IR (neat): 3089 (CH), 2989 (CH), 1629, 1605, 1467, 1447, 1419, 1395, 1370, 1344, 1315, 1246 (P=O), 1161, 1136, 1098, 1047, 1017 (POC), 969 (POC), 878, 826, 761, 741, 721, 688 cm⁻¹. HRMS (ESI) m/z: [M–2PF₆]²⁺ Calcd for C₃₆H₃₃N₆O₃PRu 365.0697; Found 365.0705. Elemental analysis: Found C, 42.80; H, 3.15; N, 7.87; Calcd. for C₃₆H₃₃F₁₂N₆O₃P₃Ru C, 42.41; H, 3.26; N, 8.24 %.



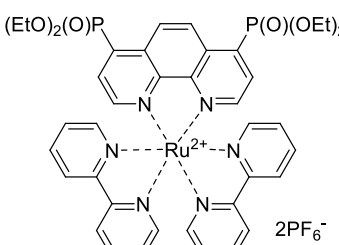
[Ru(**4P**)(bpy)₂](PF₆)₂ (**Ru-4P**) was prepared according to procedure **B** from **4P** (70 mg, 0.22 mmol) and *cis*-[Ru(bpy)₂Cl₂] (97 mg, 0.2 mmol). Yield: 102 mg (50%); red powder. ^1H NMR (CD_3CN , 400 MHz): 1.32 (td, 6H, $J_{\text{H,H}} = 6.2$ Hz, $J_{\text{H,P}} = 0.6$ Hz, CH₃), 4.15–4.32 (m, 4H, CH₂O), 7.21–7.23 (m, 2H, H5 and H5' (bpy)), 7.45–7.48 (m, 3H, H6, H5 and H5' (bpy)), 7.56–7.58 (m, 1H, H6 (bpy)), 7.79 (dd, 1H, J = 8.3 Hz, J = 5.3 Hz, H8 (Phen)), 7.81–7.84 (m, 1H, H6 and H6' (bpy)), 8.03 (dd, 1H, $J_{\text{H,P}} = 14.7$ Hz, $J_{\text{H,H}} = 5.3$ Hz, H3 (Phen)), 8.07–8.15 (m, 2H, H4 and H4' (bpy)), 8.14 (dd, 1H, J = 5.3 Hz, 4J = 1.1 Hz, H9 (Phen)), 8.23 (dd, 1H, $J_{\text{H,H}} = 5.3$ Hz, $J_{\text{H,P}} = 3.3$ Hz, H2 (Phen)), 8.36 (d, 1H, J = 9.2 Hz, H6 (Phen)), 8.50 (m, 2H, H3 and H3' (bpy)), 8.54 (m, 2H, H3 and H3' (bpy)), 8.66 (dd, 1H, J = 8.3 Hz, J = 1.2 Hz, H7 (Phen)), 8.77 (d, 1H, J = 9.2 Hz, H5 (Phen)). $^{13}\text{C}\{\text{H}\}$ NMR (CDCl_3 , 125 MHz): 16.51 (d, $J_{\text{C,P}} = 6.2$ Hz, 1C, CH₃), 16.57 (d, $J_{\text{C,P}} = 6.2$ Hz, 1C, CH₃), 64.4 (d, J = 5.8 Hz, 1C, CH₂O), 64.5 (d, J = 5.8 Hz, 1C, CH₂O), 125.1 (2C, C3 and C3' (bpy)), 125.2 (2C, C3 and C3' (bpy)), 127.4 (1C, C8 (Phen)), 127.6 (d, $J_{\text{C,P}} = 3.9$ Hz, 1C, C5 (Phen)), 128.4 (2C, C5 and C5' (bpy)), 128.5 (2C, C5 and C5' (bpy)), 130.2 (1C, C6 (Phen)), 130.6 (d, $J_{\text{C,P}} = 7.9$ Hz, 1C, C3 (Phen)), 131.1 (d, $J_{\text{C,P}} = 10.2$ Hz, 1C, C4a (Phen)), 131.9 (1C, C6a (Phen)), 136.1 (d, $J_{\text{C,P}} = 183$ Hz, 1C, C4 (Phen)), 137.8 (1C, C7 (Phen)), 138.8 (1C, C4 (bpy)), 138.9 (1C, C4' (bpy)), 139.0 (2C, C4 and C4' (bpy)), 148.4 (1C, C10a(Phen)), 149.1 (d, $J_{\text{C,P}} = 11.8$ Hz, 1C, C1a (Phen)), 152.7 (1C, C6 (bpy)), 152.8 (1C, C6 (bpy)), 152.9 (1C, C6 (bpy)), 153.0 (1C, C6 (bpy)), 153.3 (d, $J_{\text{C,P}} = 13.7$ Hz, 1C, C2 (Phen)), 153.9 (1C, C9 (Phen)), 157.7 (1C, C2 (bpy)), 157.8 (1C, C2' (bpy)), 157.9 (1C, C2 (bpy)), 158.1 (1C, C2' (bpy)). ^{31}P NMR (CD_3CN , 162.5 MHz): δ 11.7 (1P, P(O)(OEt)₂), 130.0–160.0 (m, 2P, PF₆). IR (neat): 3081 (CH), 2986 (CH), 1604, 1493, 1486, 1446, 1423, 1411, 1389, 1314, 1255, 1242 (P=O), 1227, 1200, 1161, 1035, 1014 (POC), 971, 829, 760, 728, 700, 670, 660, 648, 625 cm⁻¹. HRMS (MALDI/TOF) m/z: [M–PF₆]⁺ Calcd for C₃₆H₃₃F₁₂N₆O₃P₃Ru 875.1032; Found 875.0978. Detailed assignment of the signals in NMR spectra are given in the part 2.



$[Ru(5P)(bpy)_2](PF_6)_2$ (**Ru-5P**)⁹ was prepared according to procedure **C** from **5P** (35 mg, 0.11 mmol) and *cis*-[Ru(bpy)₂Cl₂] (49 mg, 0.1 mmol). Yield: 72 mg (88%); red powder. ¹H NMR (CD₃CN, 400 MHz): 1.34 (td, 6H, $J_{H,H} = 7.0$ Hz, $J_{H,P} = 5.5$ Hz, CH₃), 4.15–4.33 (m, 4H, CH₂O), 7.21–7.26 (m, 2H, H₅ (bpy)), 7.43–7.47 (m, 2H, H₅ (bpy)), 7.52 (ddd, 1H, $J = 5.7$ Hz, $^4J = 1.4$ Hz, $^5J = 0.4$ Hz, H₆ (bpy)), 7.57 (ddd, 1H, $J = 5.7$ Hz, $^4J = 1.4$ Hz, $^5J = 0.4$ Hz, H₆ (bpy)), 7.79 (dd, 1H, $J = 8.2$ Hz, J = 5.3 Hz, H₈ (Phen)), 7.80 (dd, 1H, $J = 8.6$ Hz, J = 5.3 Hz, H₃ (Phen)), 7.82–7.84 (m, 2H, H₆ (bpy)), 7.98–8.03 (m, 2H, H₄ (bpy)), 8.08–8.12 (m, 2H, H₄ (bpy)), 8.14 (dd, 1H, $J = 5.3$ Hz, $^4J = 1.2$ Hz, H₉ (Phen)), 8.19 (dd, 1H, $J = 5.3$ Hz, $^4J = 1.2$ Hz, H₂ (Phen)), 8.49 (br. d, 2H, $J = 8.2$ Hz, H₃ (bpy)), 8.53 (br. d, 2H, $J = 8.2$ Hz, H₃ (bpy)), 8.73 (dd, 1H, $J = 8.2$ Hz, $^4J = 1.2$ Hz, H₇ (Phen)), 8.85 (d, 1H, $J_{H,P} = 16.8$ Hz, H₆ (Phen)), 9.09 (dd, 1H, $J = 8.6$ Hz, $^4J = 1.2$ Hz, H₄ (Phen)). ³¹P NMR (CD₃CN, 162.5 MHz): δ 13.9 (1P, P(O)(OEt)₂), 130.0–160.0 (m, 2P). IR (neat): 3077 (CH), 2987 (CH), 1973, 1734, 1700, 1684, 1652, 1635, 1616, 1601, 1576, 1558, 1427, 1413, 1263, 1245 (P=O), 1224, 1153, 1096, 1043, 1015 (POC), 976, 876, 833, 720, 699, 688, 635 cm⁻¹. HRMS (MALDI/TOF) m/z: [M–PF₆]⁺ Calcd for C₃₆H₃₃F₆N₆O₃P₂Ru 875.1032; Found 875.1049.

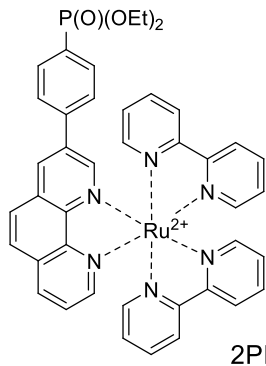


$[Ru(3,8P_2)(bpy)_2](PF_6)_2$ (**Ru-3,8P₂**) was prepared according to procedure **B** from **3,8P₂** (100 mg, 0.22 mmol) and *cis*-[Ru(bpy)₂Cl₂] (97 mg, 0.2 mmol). Yield: 188 mg (80%); red powder. ¹H NMR (CD₃CN, 400 MHz): 1.18 (t, 12H, $J = 7.0$ Hz, CH₃), 3.97–4.12 (m, 8H, CH₂O), 7.23–7.26 (m, 2H, H₅ (bpy)), 7.49–7.52 (m, 2H, H_{5'} (bpy)), 7.57 (d, 2H, $J = 5.4$ Hz, H₆ (bpy)), 7.89 (d, 2H, $J = 5.4$ Hz, H_{6'} (bpy)), 8.00–8.04 (m, 2H, H₄ (bpy)), 8.08–8.17 (m, 4H, H_{4'} (bpy), H₂ and H₉ (Phen)), 8.41 (s, 2H, H₅ and H₆ (Phen)), 8.51 (d, 2H, $J = 8.1$ Hz, H₃ (bpy)), 8.58 (d, 2H, $J = 8.1$ Hz, H_{3'} (bpy)), 8.99 (d, 2H, $J_{H,P} = 13.9$ Hz, H₄ and H₇ (Phen)). ³¹P NMR (CD₃CN, 162.5 MHz): δ 10.5 (2P, P(O)(OEt)₂), 130.0–160.0 (m, 2P). IR (neat): 2986 (CH), 1603, 1467, 1446, 1423, 1393, 1372, 1312, 1251 (P=O), 1161, 1144, 1097, 1047, 1016 (POC), 967, 876, 835, 766, 731, 722, 700, 688 cm⁻¹. HRMS (MALDI/TOF) m/z: [M–2PF₆]⁺ Calcd for C₄₀H₄₂N₆O₆P₂Ru 866.1674; Found 866.1658.

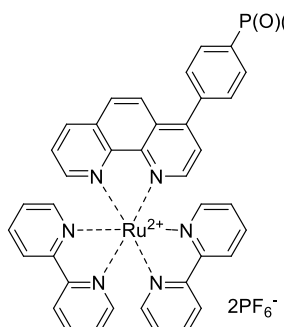


$[Ru(4,7P_2)(bpy)_2](PF_6)_2$ (**Ru-4,7P₂**) was prepared according to procedure **B** from **4,7P₂** (61 mg, 0.135 mmol) and *cis*-[Ru(bpy)₂Cl₂] (60 mg, 0.12 mmol). Yield: 72 mg (53%); red powder. ¹H NMR (CD₃CN, 400 MHz): 1.32 (td, 12H, $J_{H,H} = 7.0$ Hz, $J_{H,P} = 1.9$ Hz, CH₃),

4.15–4.32 (m, 8H, CH₂O), 7.24–7.27 (m, 2H, H5 (bpy)), 7.47–7.52 (m, 2H, H5' (bpy)), 7.52–7.54 (m, 2H, H6 (bpy)), 7.80–7.82 (m, 2H, H6 (bpy)), 8.01–8.15 (m, 6H, H4 and H4' (bpy), H3 and H8 (Phen)), 8.29 (dd, 2H, $J_{\text{H,P}} = 3.4$ Hz, $J_{\text{H,H}} = 5.3$ Hz, H2 and H9 (Phen)), 8.52 (br. d, 2H, $J = 8.0$ Hz, H3' (bpy)), 8.57 (br. d, 2H, $J = 8.0$ Hz, H3 (bpy)), 8.89 (s, 2H, H5 and H6 (phen)). ³¹P NMR (CD₃CN, 162.5 MHz): δ 11.5 (2P, P(O)(OEt)₂), 130.0–160.0 (m, 2P, PF₆). IR (neat): 2966 (CH), 1604, 1495, 1466, 1446, 1424, 1394, 1253 (P=O), 1234, 1197, 1162, 1129, 1096, 1038, 1011, 976, 827 cm⁻¹. HRMS (MALDI/TOF) m/z: [M–2PF₆]⁺ Calcd for C₄₀H₄₂N₆O₆P₂Ru 866.1674; Found 866.1647.

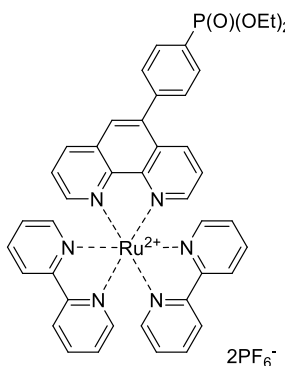


[Ru(3PPPPh)(bpy)₂](PF₆)₂ (**Ru-3PPPPh**) was prepared according to procedure **C** from **3PPPPh** (140 mg, 0.35 mmol) and *cis*-[Ru(bpy)₂Cl₂] (154 mg, 0.32 mmol). Yield: 295 mg (87%); red powder. ¹H NMR (CD₃CN, 400 MHz): 1.29 (t, 6H, $J = 7.0$ Hz, CH₃), 4.01–4.15 (m, 4H, CH₂O), 7.22–7.26 (m, 2H, H5 (bpy)), 7.44–7.48 (m, 2H, H5 (bpy)), 7.57 (br. d, 1H, $J = 5.4$ Hz, H6 (bpy)), 7.67–7.73 (m, 3H, H6 (bpy), H3 and H5 (Ph)), 7.76 (dd, 2H, $J = 8.3$ Hz, $J = 5.3$ Hz, H8 (Phen)), 7.84–7.90 (m, 3H, H6 (bpy), H2 and H6 (Ph)), 7.91 (ddd, 1H, $J = 5.7$ Hz, $^4J = 1.4$ Hz, $^5J = 0.6$ Hz, H6 (bpy)), 7.97–8.02 (m, 2H, H4 (bpy)), 8.08–8.13 (m, 3H, H4 (bpy) and H9 (phen)), 8.18 (d, 1H, $^4J = 1.8$ Hz, H2 (Phen)), 8.27–8.32 (m, 2H, H5 and H6 (Phen)), 8.47–8.52 (m, 4H, H3 and H3' (bpy)), 8.64 (dd, 1H, $J = 8.3$ Hz, $^4J = 1.0$ Hz, H7 (Phen)), 8.88 (d, 1H, $^4J = 1.8$ Hz, H4 (Phen)). ³¹P NMR (CD₃CN, 162.5 MHz): δ 16.8 (1P, P(O)(OEt)₂), 130.0–160.0 (m, 2P, PF₆). IR (neat): 2924 (CH), 2953, 1603, 1466, 1446, 1431, 1422, 1393, 1369, 1269, 1242 (P=O), 1162, 1132, 1098, 1048, 1018, 968, 876, 835, 761, 731, 722, 700, 674, 660, 648 cm⁻¹. HRMS (MALDI/TOF) m/z: [M–PF₆]⁺ Calcd for C₄₂H₃₇F₆N₆O₃P₂Ru 951.1345; Found 951.1349.

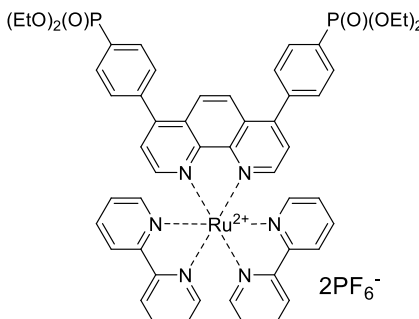


[Ru(4PPPPh)(bpy)₂](PF₆)₂ (**Ru-4PPPPh**) was prepared according to procedure **C** from **4PPPPh** (35 mg, 0.09 mmol) and *cis*-[Ru(bpy)₂Cl₂] (40 mg, 0.08 mmol). Yield: 81 mg (84%); red powder. ¹H NMR (CD₃CN, 400 MHz): 1.34 (t, 6H, $J = 7.0$ Hz, CH₃), 4.04–4.11 (m, 4H, CH₂O), 7.23–7.28 (m, 2H, H5 (bpy)), 7.44–7.48 (m, 2H, H5 (bpy)), 7.57–7.61 (m, 1H, H6 (bpy)), 7.62–7.65 (m, 1H, H6 (bpy)), 7.67 (d, 1H, $J = 5.4$ Hz, H3 (Phen)), 7.70–7.78 (m, 3H, H8 (Phen), H3 and H5 (Ph)), 7.87 (br. d, 2H, $J = 5.5$ Hz, H6 (bpy)), 7.97–8.04 (m, 4H, H4 (bpy), H2 and H6 (Ph)), 8.06–8.15 (m, 4H, H4 (bpy), H2 and H9 (Phen)), 8.17 (d, 1H, $J = 9.3$ Hz, H5 (Phen)), 8.21 (d, 1H, $J = 9.3$ Hz, H6

(Phen)), 8.48–8.57 (m, 4H, H3 and H3' (bpy)), 8.62 (dd, 1H, J = 8.2 Hz, 4J = 1.1 Hz, H7 (Phen)). ^{31}P NMR (CD_3CN , 162.5 MHz): δ 17.4 (1P, P(O)(OEt)₂), 130.0–160.0 (m, 2P, PF₆). IR (neat): 2928 (CH), 1604, 1446, 1426, 1312, 1241 (P=O), 1161, 1132, 1097, 1047, 1017 (POC), 969, 836 cm⁻¹. HRMS (MALDI/TOF) m/z: [M–PF₆]⁺ Calcd for C₄₂H₃₇F₆N₆O₃P₂Ru 951.1399; Found 951.1399.



[Ru(5PPh)(bpy)₂](PF₆)₂ (**Ru-5PPh**) was prepared according to procedure **B** from **5PPh** (125 mg, 0.32 mmol) and *cis*-[Ru(bpy)₂Cl₂] (141 mg, 0.29 mmol). Yield: 286 mg (90%); red powder. ^1H NMR (CD_3CN , 400 MHz): 1.34 (t, 6H, J = 7.0 Hz, CH₃), 4.10–4.20 (m, 4H, CH₂O), 7.23–7.28 (m, 2H, H5 (bpy)), 7.44–7.48 (m, 2H, H5 (bpy)), 7.57–7.61 (m, 2H, H6 (bpy)), 7.68 (dd, 1H, J = 8.5 Hz, J = 5.3 Hz, H8 (Phen)), 7.72–7.78 (m, 3H, H3 (Phen), H3 and H5 (Ph)), 7.86 (br. d, 2H, J = 5.6 Hz, H6 (bpy)), 7.95–8.05 (m, 4H, H2 and H9 (Phen), H2 and H6 (Ph)), 8.07–8.13 (m, 4H, H4 (bpy)), 8.23 (s, 1H, H6 (Phen)), 8.44 (dd, 1H, J = 8.5 Hz, 4J = 1.0 Hz, H4 (Phen)), 8.51 (br. d, 2H, J = 8.3 Hz, H3 (bpy)), 8.55 (br. d, 2H, J = 8.1 Hz, H3 (bpy)), 8.62 (dd, 1H, J = 8.3 Hz, 4J = 1.0 Hz, H7 (Phen)). ^{31}P NMR (CD_3CN , 162.5 MHz): δ 17.1 (1P, P(O)(OEt)₂), 130.0–160.0 (m, 2P, PF₆). IR (neat): 3082 (CH), 2989 (CH), 2359 (CO₂), 2341(CO₂), 1624, 1603, 1465, 1446, 1422, 1394, 1369, 1313, 1269, 1237 (P=O), 1161, 1127, 1096, 1047, 1018 (POC), 969, 831 cm⁻¹. HRMS (MALDI/TOF) m/z: [M–PF₆]⁺ Calcd for C₄₂H₃₇F₆N₆O₃P₂Ru 951.1345; Found 951.1350.



[Ru(4,7PPh)₂(bpy)₂](PF₆)₂ (**Ru-4,7(PPh)₂**) was prepared according to procedure **C** from **4,7(PPh)₂** (193 mg, 0.32 mmol) and *cis*-Ru(bpy)₂Cl₂ (141 mg, 0.29 mmol). Yield: 250 mg (83%); red powder. ^1H NMR (CD_3CN , 400 MHz): 1.32 (t, 12H, J = 7.0 Hz, CH₃), 4.10–4.20 (m, 8H, CH₂O), 7.28–7.32 (m, 2H, H5 (bpy)), 7.46–7.49 (m, 2H, H5 (bpy)), 7.66–7.77 (m, 8H, H6 (bpy), H3 and H8 (Phen), H3 and H5 (Ph)), 7.88 (br. d, 2H, J = 5.6 Hz, H6' (bpy)), 7.94–8.08 (m, 6H, H4 (bpy), H2 and H6 (Ph)), 8.09–8.17 (m, 4H, H4 (bpy), H5 and H6 (Phen)), 8.20 (d, 2H, J = 5.5 Hz, H2 and H9 (Phen)), 8.54 (br. d, 2H, J = 8.2 Hz, H3 (bpy)), 8.57 (d, 2H, J = 8.2 Hz, H3' (bpy)). ^{31}P NMR (CD_3CN , 162.5 MHz): δ 16.8 (2P, P(O)(OEt)₂), 130.0–160.0 (m, 2P, PF₆). IR (neat): 2983 (CH), 1700, 1695, 1684, 1652, 1603, 1595, 1569, 1559, 1465, 1446, 1419, 1391, 1269, 1240 (P=O), 1162, 1132, 1047, 1015 (POC), 963, 875, 827, 760, 728, 669, 604 cm⁻¹. HRMS (MALDI/TOF) m/z: [M–2PF₆]²⁺ Calcd for C₅₂H₅₀N₆O₃P₂Ru 1018.2300; Found 1018.2284.

2. Photostability studies

General procedure. A 0.01 mM solution of complex **Ru-Pcat** in acetonitrile/water (10:1 v/v) was stirred and irradiated by blue LED (15 W) at room temperature in a glass vial under air. The solution was diluted in 5–20 times and UV-vis spectra was recorded.

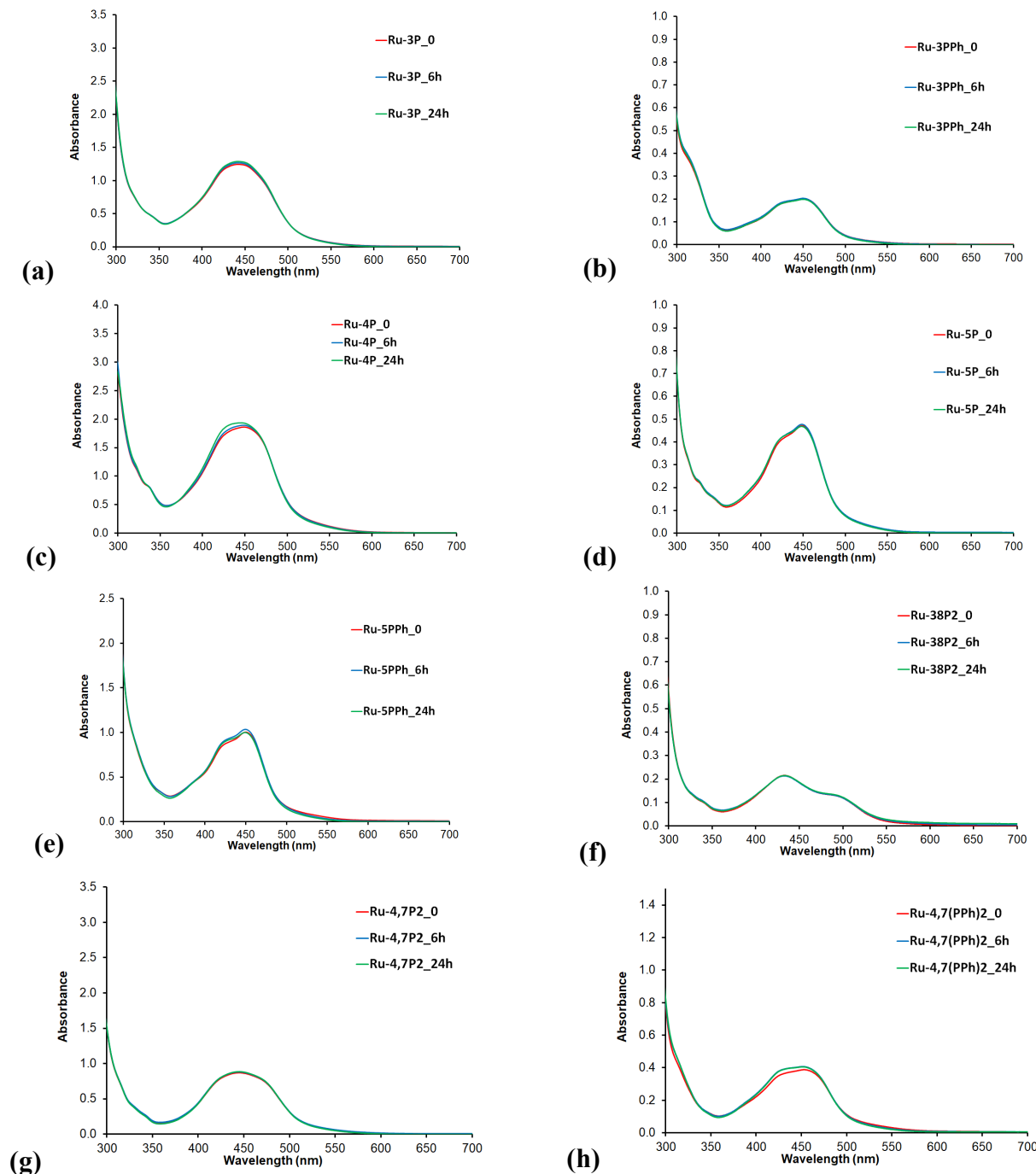


Figure S1. UV-vis spectra of the solutions **Ru-3P** (a), **Ru-3PPh** (b), **Ru-4P** (c), **Ru-5P** (d), **Ru-5PPh** (e), **Ru-3,8P₂** (f), **Ru-4,7P₂** (g), **Ru-4,7(PPh)₂** (h) in acetonitrile/water (10:1 v/v) before (red) and after irradiation (15W, blue LED) for 6 hours (blue) and 24 hours (green).

3. X-ray diffraction of crystal structures

Table S1. Crystal data and structure refinement for compounds **Ru-5P** and **Ru-4,7P₂**.

	Ru-5P	Ru-4,7P₂
empirical formula	C ₃₆ H ₃₃ F ₁₂ N ₆ O ₃ P ₃ Ru	C ₄₀ H ₄₃ F ₁₂ N ₆ O ₆ P ₄ Ru
fw	1019.66	1164.75
colour	dark orange	dark orange
temp (K)	150	150
crystal system	triclinic	triclinic
space group	P-1	P-1
<i>a</i> , Å	12.6664(6)	11.7648(4)
<i>b</i> , Å	13.0845(6)	12.884(4)
<i>c</i> , Å	13.0859(6)	c = 12.2028(6)
α , deg	108.787(2)	84.758(1)
β , deg	97.776(2)	74.787(1)
γ , deg	92.434(2)	84.262(1)
<i>V</i> , Å ³	2025.77(16)	2353.89(14)
Z	2	2
ρ_{calcd} , g/cm ³	1.672	1.643
μ , mm ⁻¹	0.606	0.570
radiation (λ , Å)	0.71073	0.71073
<i>R</i> 1 (F _o) ^a	0.0817	0.0795
<i>wR</i> 2 (F _o ²) ^b	0.1944	0.1975
GOF	1.062	1.023

^a $R1 = \sum |F_o - F_c| / \sum F_o$; ^b $wR2 = \sum [w(F_o^2 - F_c^2)^2] / \sum w(F_o^2)$ $\}^{1/2}$

Table S2. Comparison of selected bond length and angles in **Ru-phen** and phosphonate-substituted derivatives **Ru-5P** and **Ru-4,7P₂**.

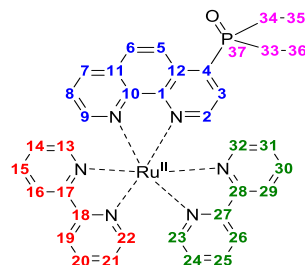
Structural parameter	Ru-phen^a	Ru-5P	Ru-4,7P
Ru–Nbpy, Å	2.04(1)	2.052(5)	2.056(5)
	2.054(9)	2.055(6)	2.058(5)
	2.07(1)	2.059(4)	2.062(5)
	2.09(1)	2.067(4)	2.067(5)
Ru–Nphen, Å	2.056(8)	2.059(6)	2.045(5)
	2.082(9)	2.067(5)	2.062(5)
Nphen–Ru–Nphen, deg	78.9(3)	79.3(2)	79.6(2)
Nbpy–Ru–Nbpy, deg	78.6(5)	79.0(2)	78.5(2)
	78.8(4)	79.0(2)	79.5(2)
Nphen–Ru–Nbpy(ax), deg	170.7(4)	172.0(2)	171.9(2)
	174.0(5)	174.5(2)	175.0(2)
Angle between pyridine planes in bpy ligand, deg	6.37	3.83	5.68
Angle between pyridine planes in phen ligand, deg	10.18	5.28	10.06
Angle between pyridine planes in phen ligand, deg	2.22	4.90	3.65

^a ref.¹⁰

4. Detailed NMR studies of complex Ru-4P

All NMR spectra were recorded with Agilent 400 MR spectrometer in CD₃CN; the residual signal of CHD₂CN was used as an internal standard.

Table S3. Signal assignment in NMR spectra of **4P-Ru**.



Assignment	Chemical shift (ppm)			J (Hz)		
	¹ H	¹³ C	³¹ P	H–H (atom)	H–P	C–P
1		149.1				11.8
2	8.24	153.3		5.3 (3)	3.3	13.7
3	8.03	130.6		5.3 (2)	14.7	7.9
4		136.1				183
5	8.76	127.6		9.21 (6)		3.9
6	8.36	130.2		9.21 (5)		1.1
7	8.66	137.8		8.3 (8) 1.2 (9)		
8	7.79	127.4		8.3 (7) 5.3 (9)		
9	8.14	153.9		5.3 (8) 1.2 (7)		
10		148.4				2.7
11		131.9				
12		131.1				10.2
13	7.82	152.7		5.6 (14) 0.8 (16)		
14	7.47	128.5		5.6 (13) 7.7 (15)		
15	8.12	139		8.2 (16) 7.7 (14)		
16	8.55	125.2		8.2 (15) 0.8 (13)		
17		157.9				
18		158.1				
19	8.54	125.2		8.2 (20) 0.8 (22)		
20	8.12	139		8.2 (19) 7.7 (21)		
21	7.46	128.5		5.6 (22) 7.7 (20)		
22	7.84	152.8		5.6 (21) 0.8 (20)		
23	7.48	152.9		5.6 (24) 0.8 (26)		
24	7.23	128.4		5.6 (23) 7.7 (25)		
25	8.00	138.9		8.2 (26) 7.7 (24)		
26	8.50	125.1		8.2 (25) 0.8 (23)		
27		157.8				
28		157.7				
29	8.50	125.1		8.2 (30) 0.8 (32)		
30	8.01	138.8		8.2 (29) 7.7 (31)		
31	7.23	128.4		5.6 (32) 7.7 (30)		
32	7.57	153.0		5.6 (31) 0.8 (29)		
33	4.23(2)	64.4			7.1 (36)	8.6
34	4.25(2)	64.5			7.1 (35)	8.6
35	1.323	16.57			7.1 (34)	0.6
36	1.318	16.51			7.1 (33)	0.6
37		11.6				6.2

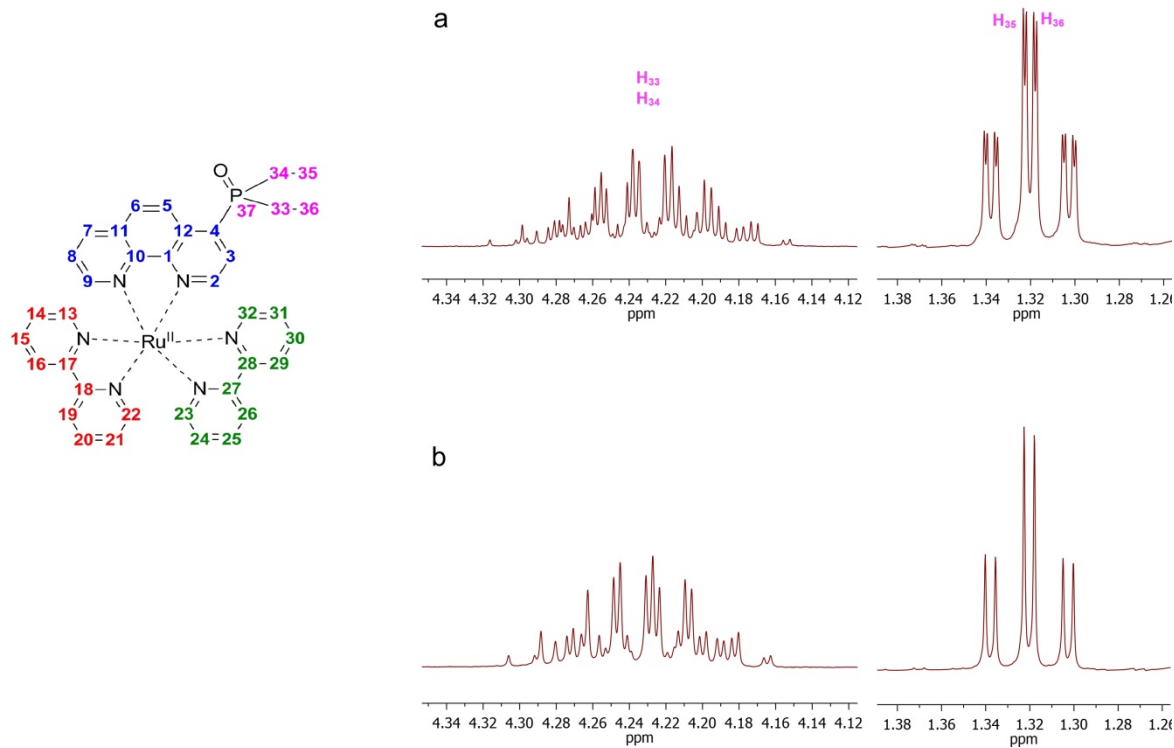


Figure S2. ^1H NMR spectrum of **Ru-4P** complex (CD₃CN, 400MHz, 298 K, aliphatic)
(a) ^1H - ^{31}P decoupled; (b) ^1H - ^{31}P decoupled.

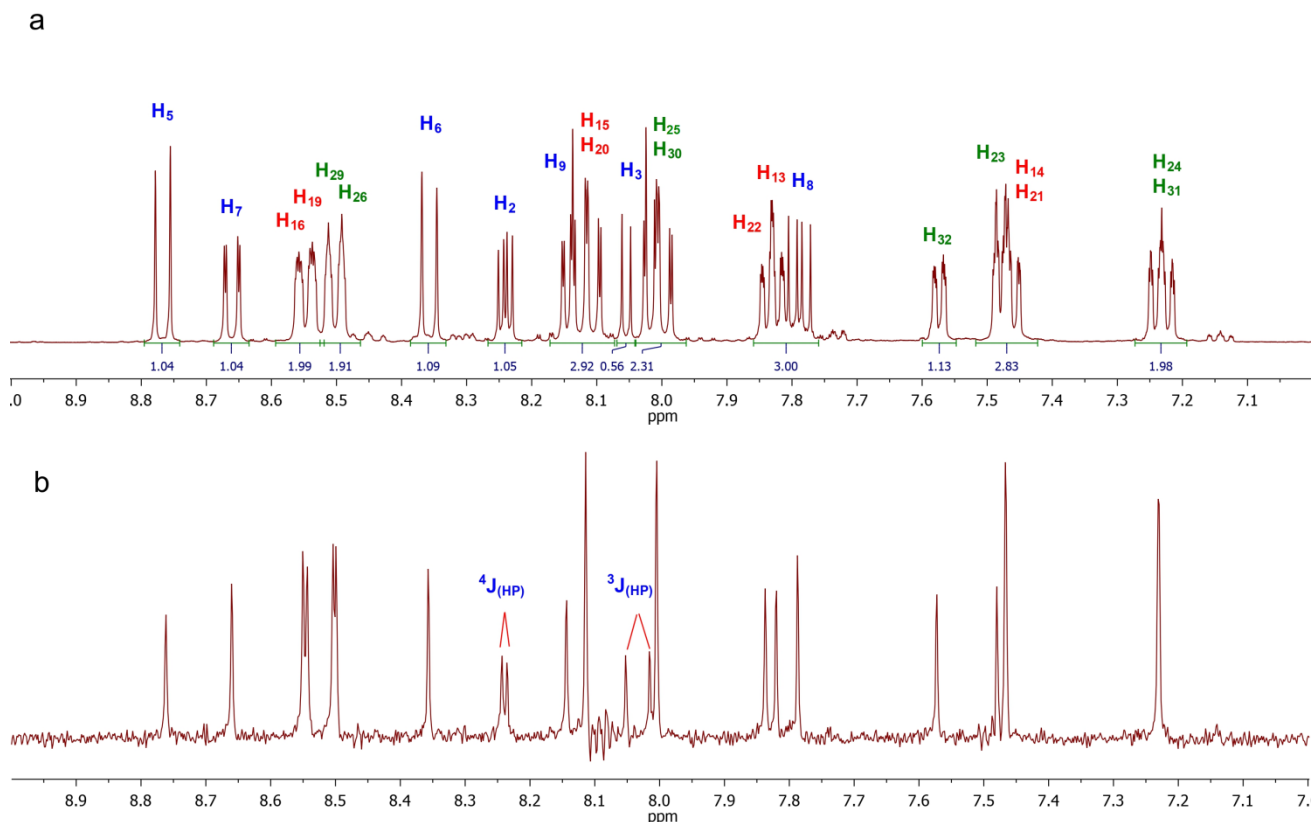


Figure S3. (a) ^1H NMR spectrum of **Ru-4P** complex (CD₃CN, 400MHz, 298K, aromatic).
(b) PSYCHE ^1H NMR spectrum of **Ru-4P** complex (CD₃CN, 100.6 MHz, 298 K, aromatic).

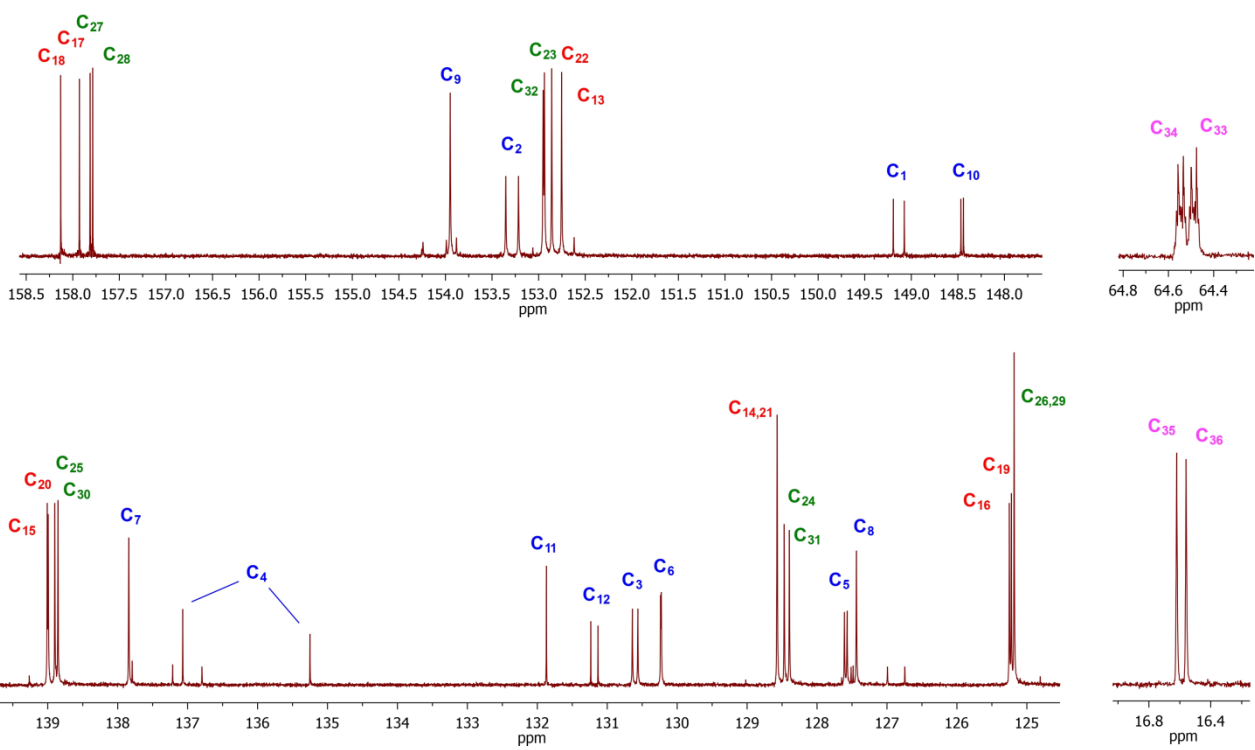


Figure S4. ¹³C NMR spectrum of Ru-4P complex (CD₃CN, 100.6 MHz, 298 K).

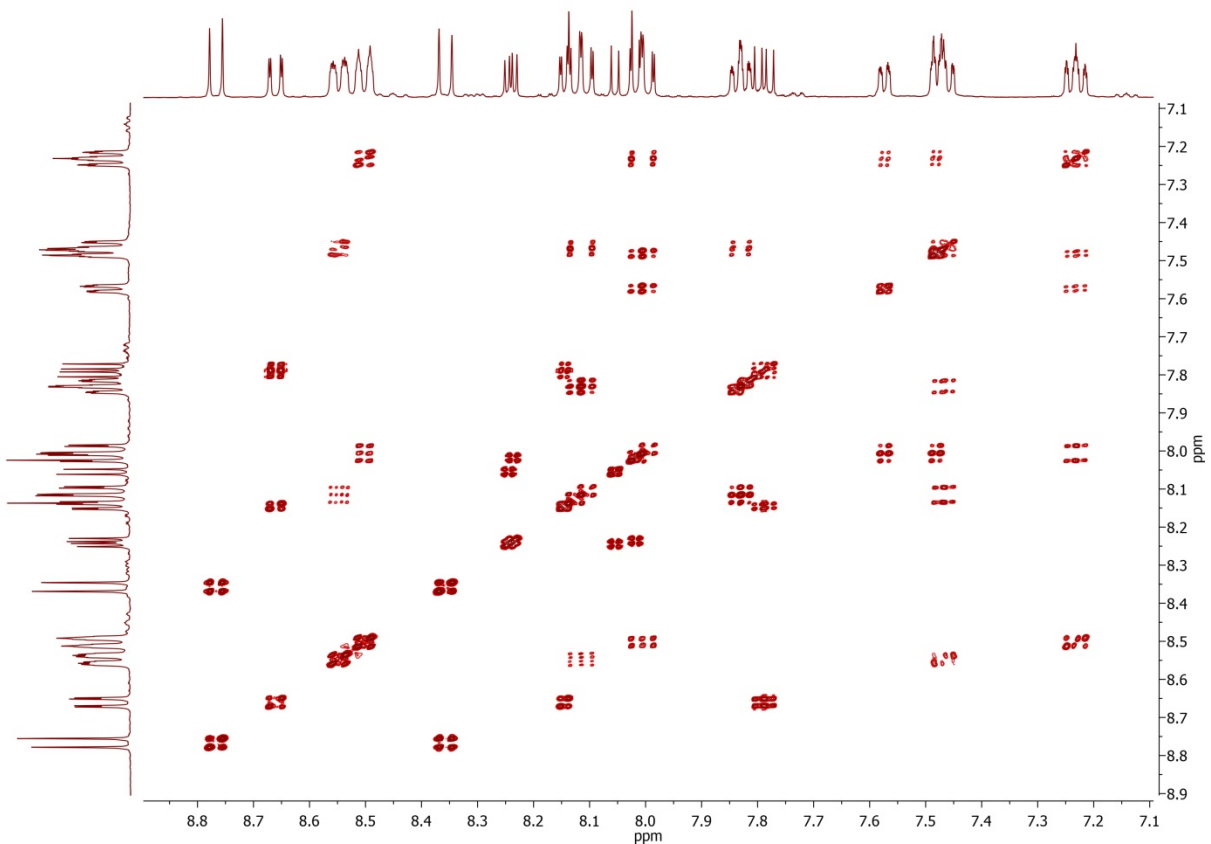


Figure S5. COSY ¹H NMR spectrum of Ru-4P complex (CD₃CN, 400 MHz, 298 K, aromatic).

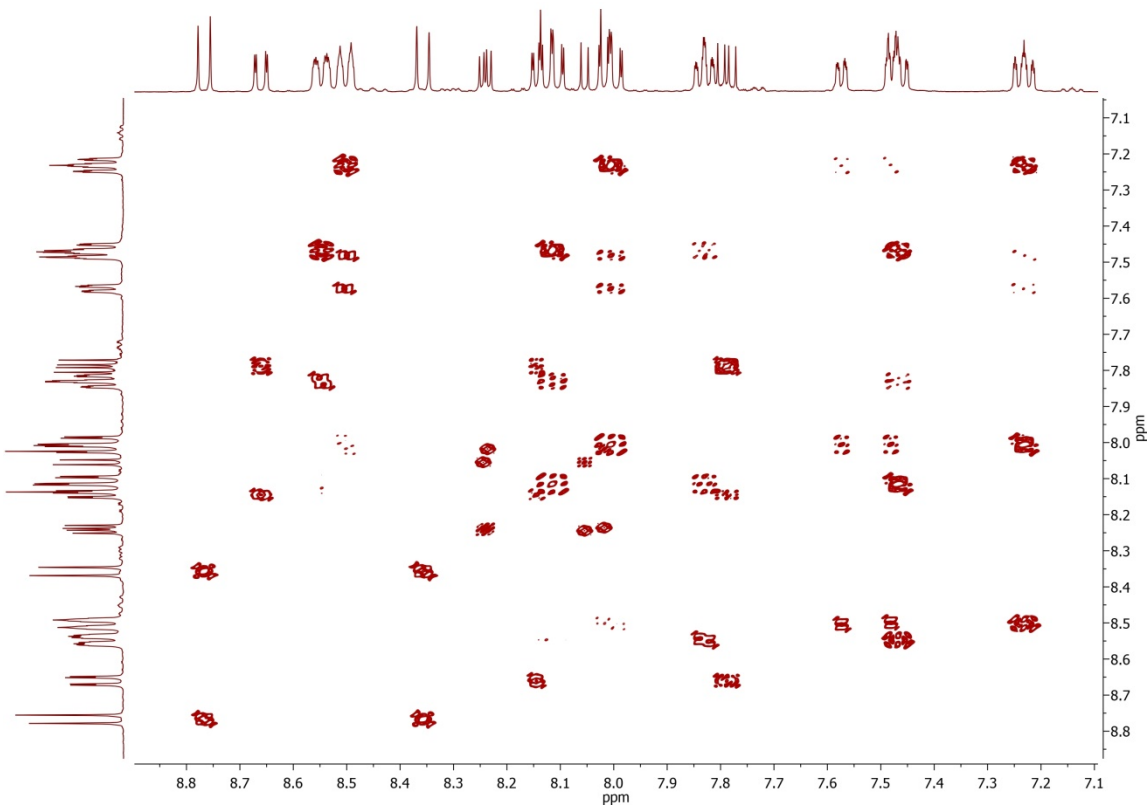


Figure S6. TOCSY spectrum of Ru-4P complex (CD₃CN, 298 K, aromatic).

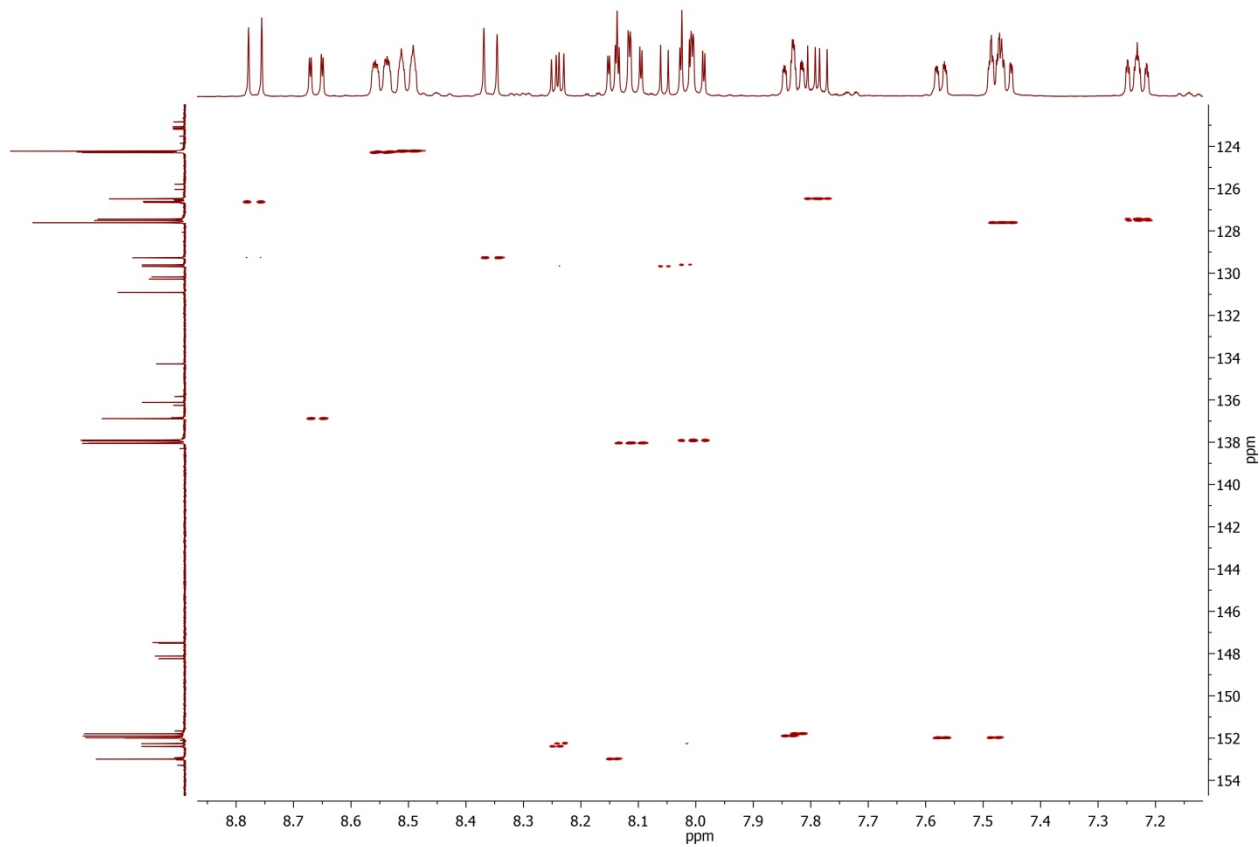


Figure S7. gHSQCAD spectrum of Ru-4P complex (CD₃CN, 298 K, aromatic).

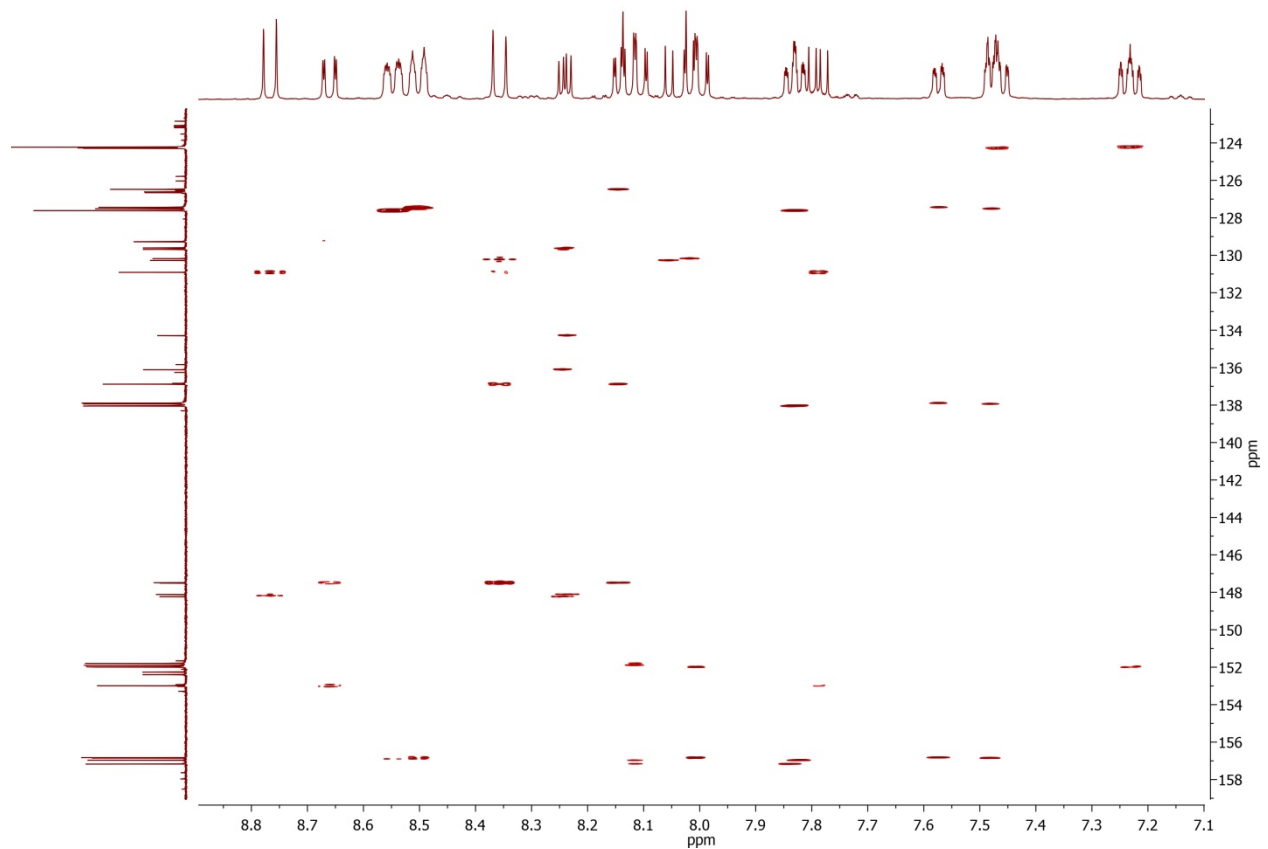


Figure S8. gHMBCAD spectrum of **Ru-4P** complex (CD_3CN , 298 K, aromatic).

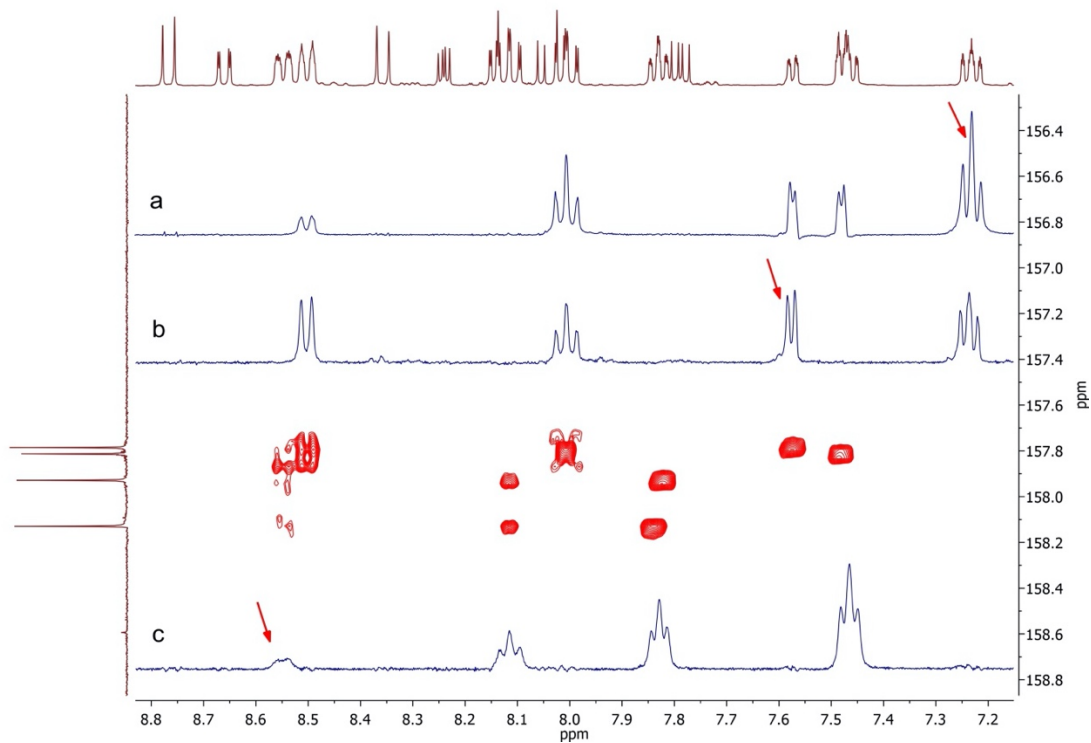


Figure S9. gHMBCAD spectrum of **Ru-4P** complex in (CD_3CN , 298 K, zoomed). Inset: selective 1D TOCSY NMR -spectra with excitation set on 7.23 ppm (a), 7.53 ppm (b) and 8.55 ppm (c).

5. Electrochemistry

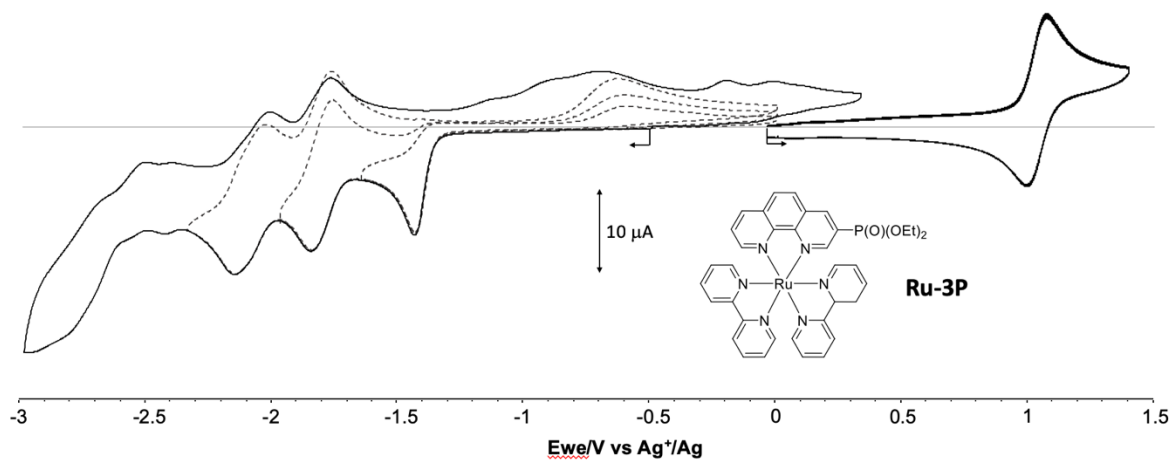


Figure S10. Voltamperometric curves of MeCN solutions of **Ru-3P** (1×10^{-3} M + 0.1 M in TBAPF₆) recorded at a vitreous carbon working electrode ($\varnothing = 3$ mm, 0.1 V.s^{-1}).

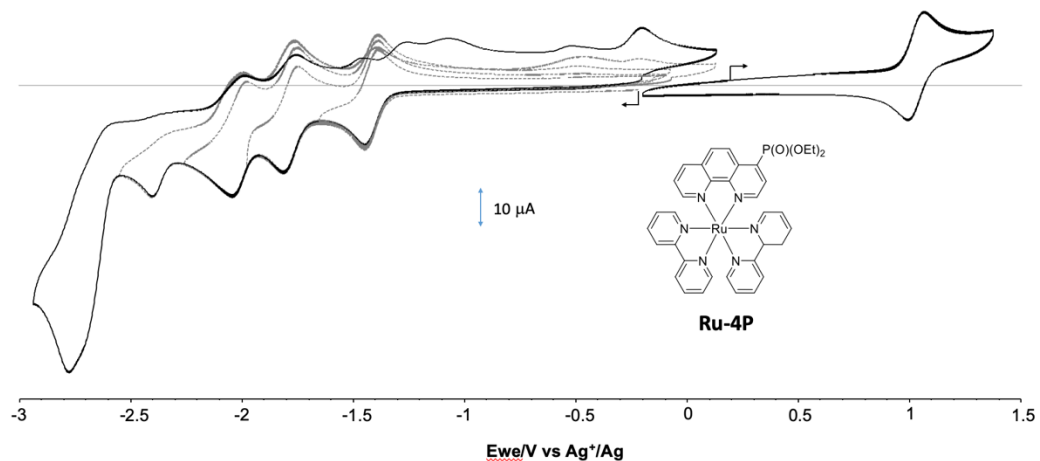


Figure S11. Voltamperometric curves of MeCN solutions of **Ru-4P** (1×10^{-3} M + 0.1 M in TBAPF₆) recorded at a vitreous carbon working electrode ($\varnothing = 3$ mm, 0.1 V.s^{-1}).

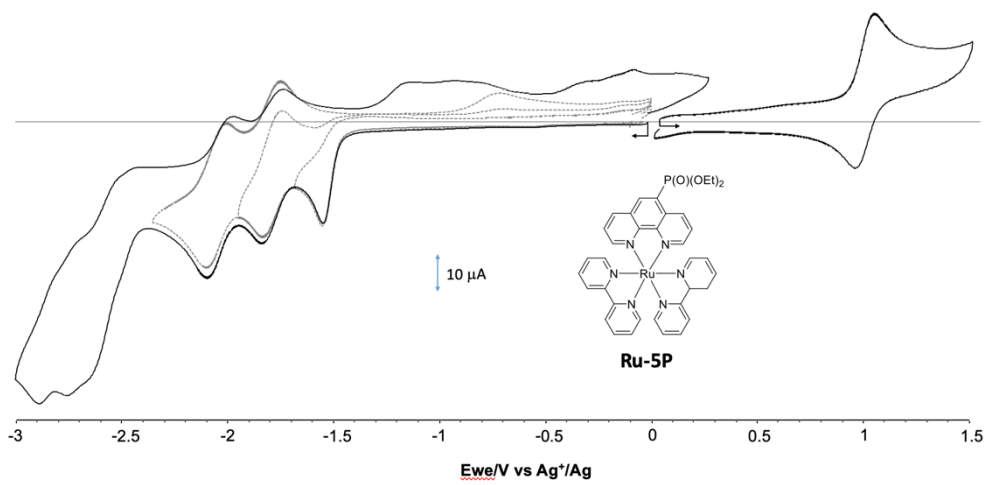


Figure S12. Voltamperometric curves of MeCN solutions of **Ru-5P** (1×10^{-3} M + 0.1 M in TBAPF₆) recorded at a vitreous carbon working electrode ($\varnothing = 3$ mm, 0.1 V.s^{-1}).

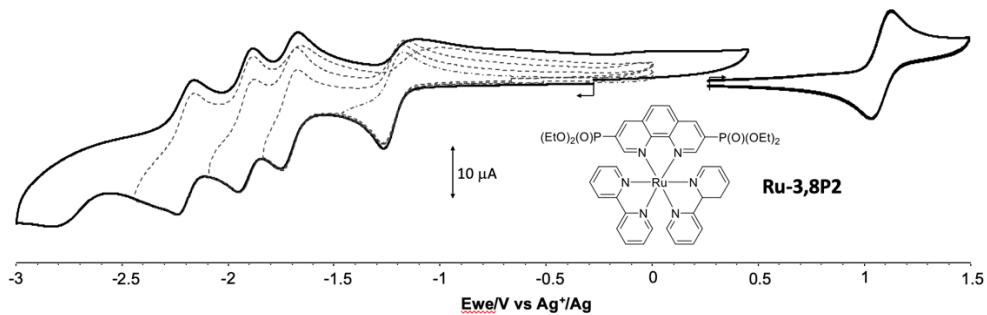


Figure S13. Voltamperometric curves of MeCN solutions of **Ru-3,8P2** (1×10^{-3} M + 0.1 M in TBAPF₆) recorded at a vitreous carbon working electrode ($\varnothing = 3$ mm, 0.1 V.s^{-1}).

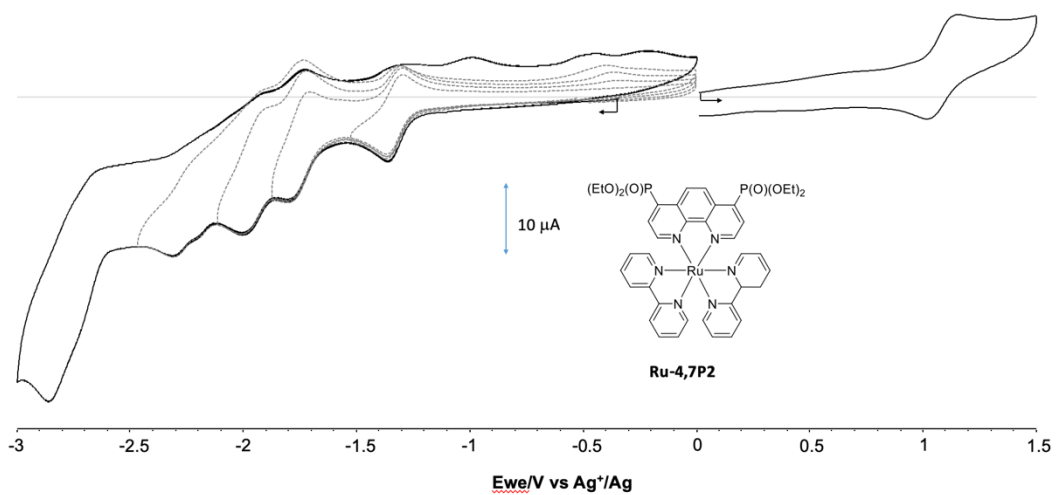


Figure S14. Voltamperometric curves of MeCN solutions of **Ru-4,7P₂** (1×10^{-3} M + 0.1 M in TBAPF₆) recorded at a vitreous carbon working electrode ($\varnothing = 3$ mm, 0.1 V.s^{-1}).

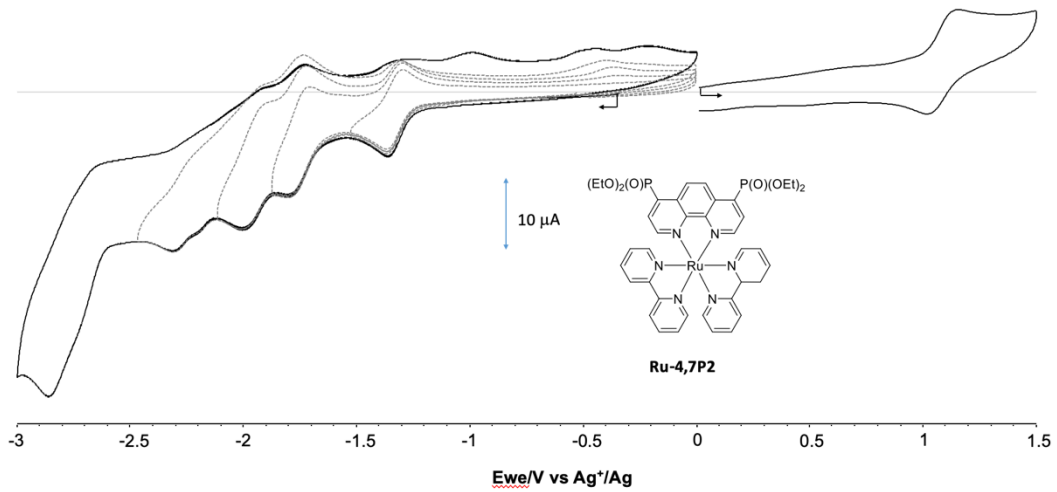


Figure S15. Voltamperometric curves of MeCN solutions of **Ru-3PPPh** (1×10^{-3} M + 0.1 M in TBAPF₆) recorded at a vitreous carbon working electrode ($\varnothing = 3$ mm, 0.1 V.s^{-1}).

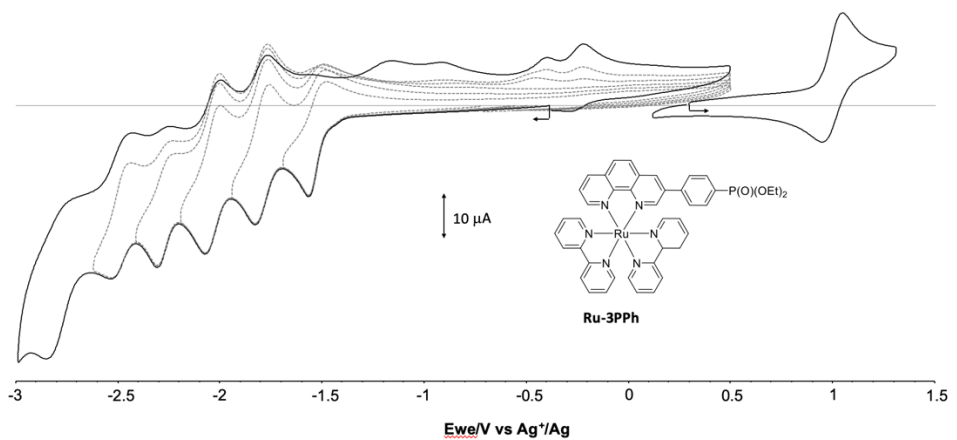


Figure S16. Voltamperometric curves of MeCN solutions of **Ru-4PPh** (1×10^{-3} M + 0.1 M in TBAPF₆) recorded at a vitreous carbon working electrode ($\varnothing = 3$ mm, 0.1 V.s^{-1}).

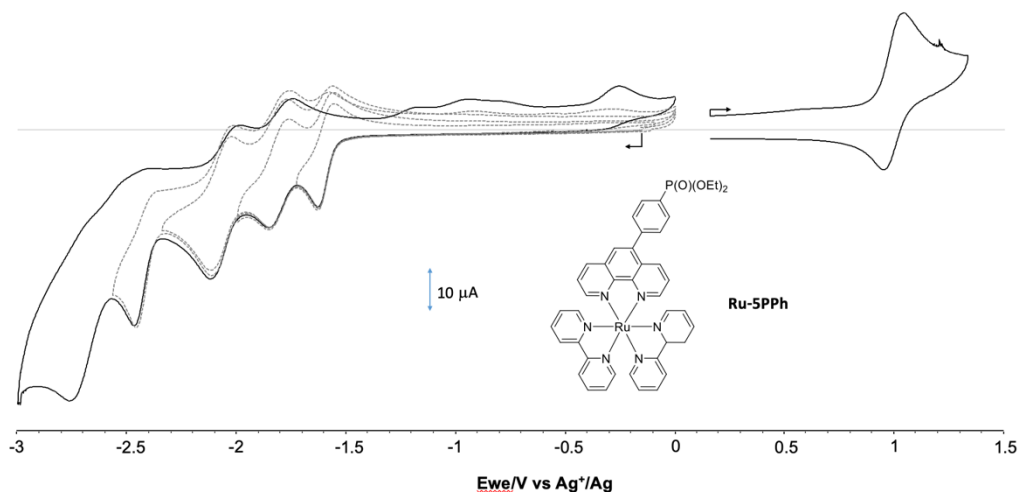


Figure S17. Voltamperometric curves of MeCN solutions of **Ru-5PPh** (1×10^{-3} M + 0.1 M in TBAPF₆) recorded at a vitreous carbon working electrode ($\varnothing = 3$ mm, 0.1 V.s^{-1}).

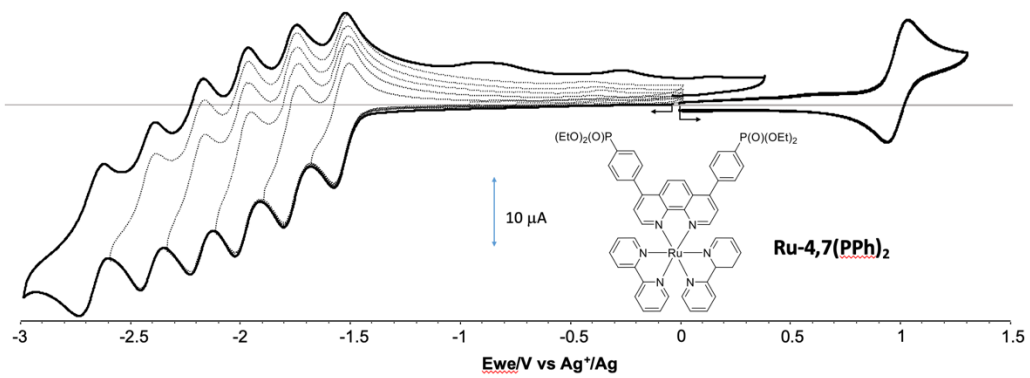


Figure S18. Voltamperometric curves of MeCN solutions of **Ru-4,7(PPh)₂** (1×10^{-3} M + 0.1 M in TBAPF₆) recorded at a vitreous carbon working electrode ($\varnothing = 3$ mm, 0.1 V.s⁻¹).

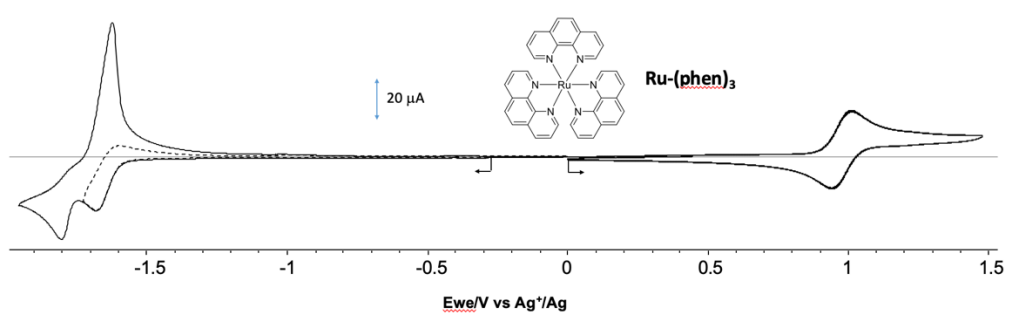


Figure S19. Voltamperometric curves of MeCN solutions of **Ru-(phen)₃** (1×10^{-3} M + 0.1 M in TBAPF₆) recorded at a vitreous carbon working electrode ($\varnothing = 3$ mm, 0.1 V.s⁻¹).

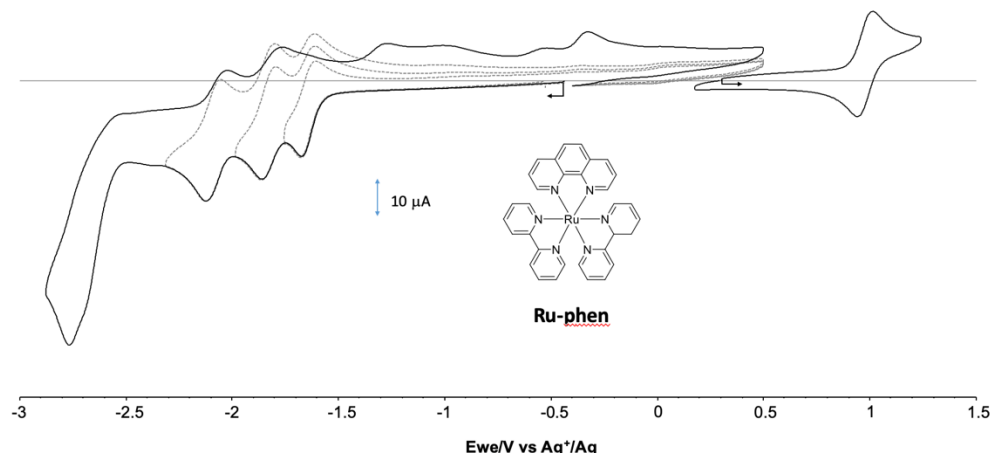


Figure S20. Voltamperometric curves of MeCN solutions of **Ru-phen** (1×10^{-3} M + 0.1 M in TBAPF₆) recorded at a vitreous carbon working electrode ($\varnothing = 3$ mm, 0.1 V.s⁻¹).

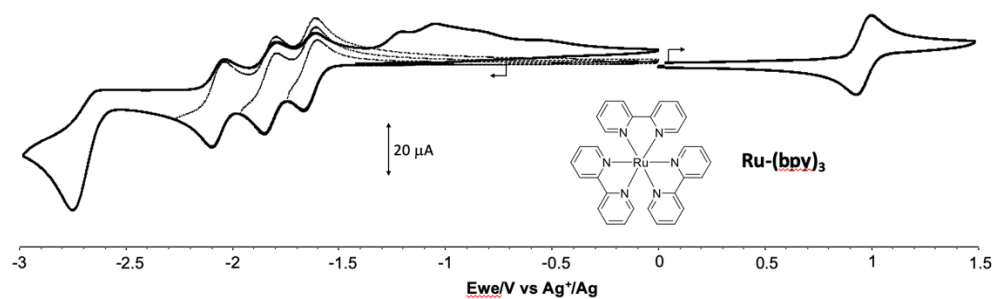


Figure S21. Voltamperometric curves of MeCN solutions of **Ru-phen** (1×10^{-3} M + 0.1 M in TBAPF₆) recorded at a vitreous carbon working electrode ($\varnothing = 3$ mm, 0.1 V.s^{-1}).

6. Study of photophysical properties

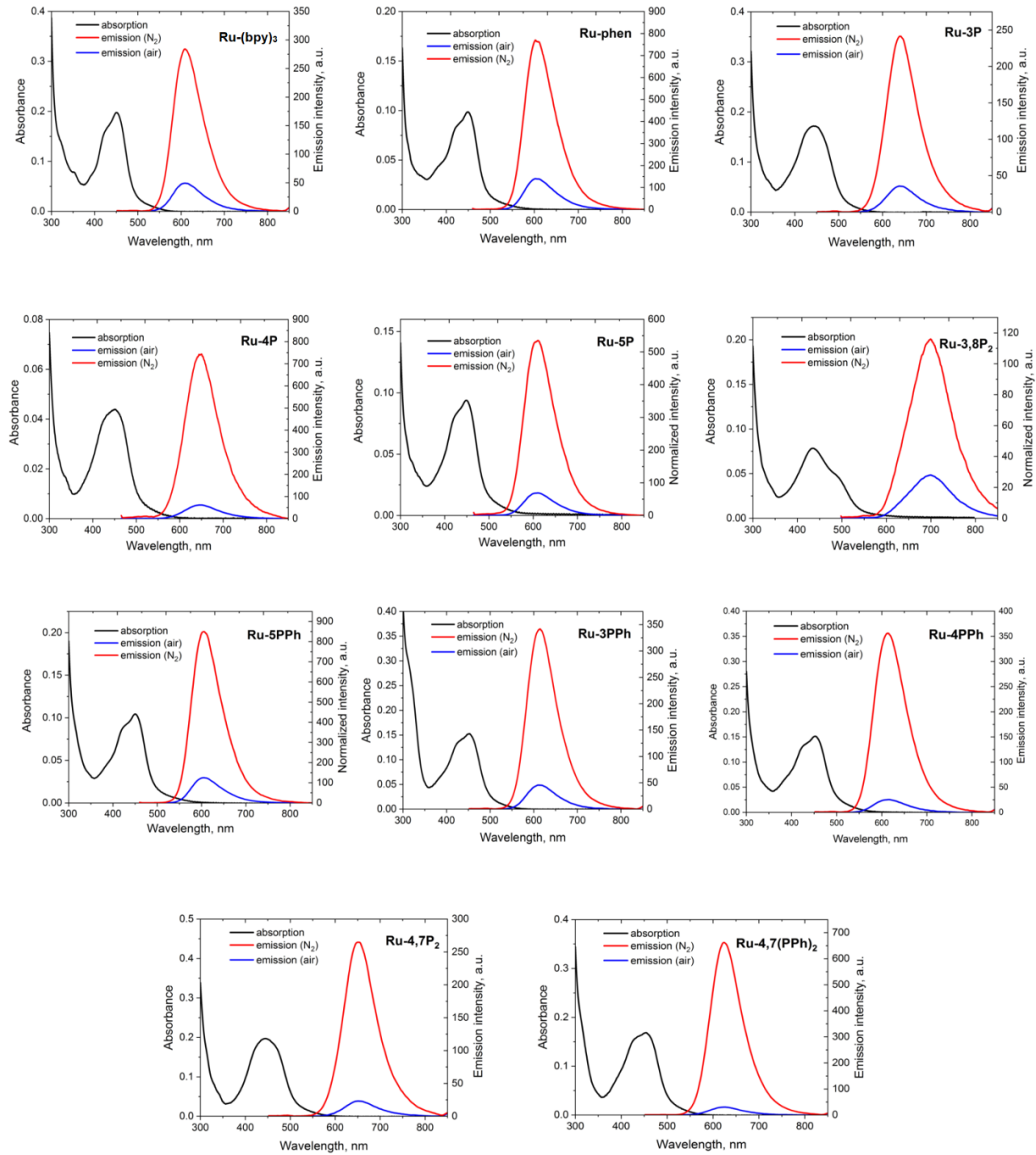


Figure S22. Absorption and emission spectra of complexes **Ru-Pcat** and reference compounds **Ru-(bpy)₃** in acetonitrile.

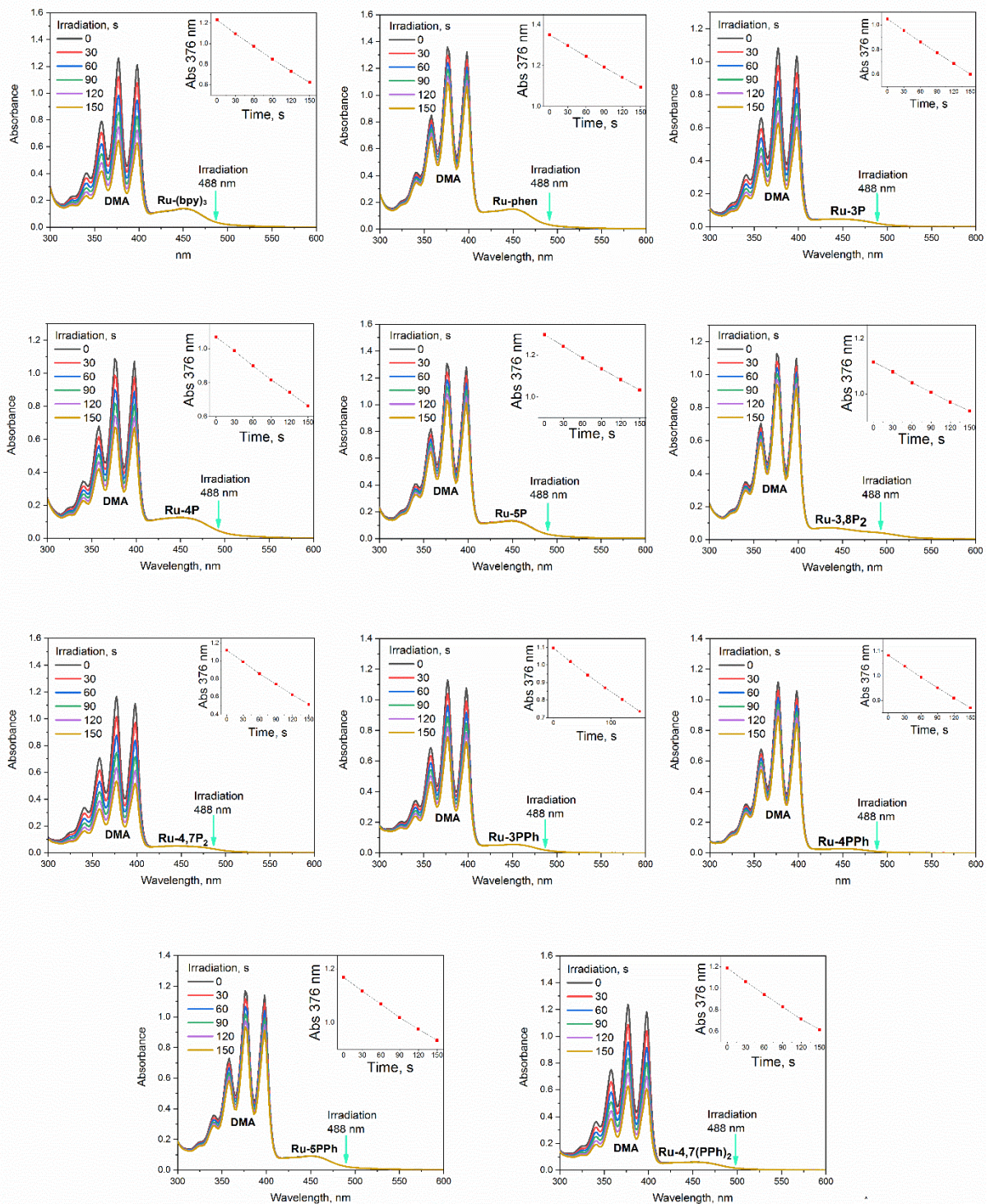


Figure S23. Photooxidation of 1,9-dimethylanthracene in air-saturated acetonitrile solution containing **Ru-Pcat** or reference photosensitizers **Ru-phen** and **Ru-(bpy)₃**. Inset: dependence of absorbance at 376 nm on the irradiation time.

7. DFT-studies

The structures of complexes was modelled using DFT calculations with Firefly quantum chemistry package,¹¹ which is partially based on the GAMESS (US)¹² source code. The calculations were performed using B3LYP functional with STO 6-31G(d,p) basis set for all elements except Ru, for which we have used the Stuttgart valence basis set and pseudopotential.¹³

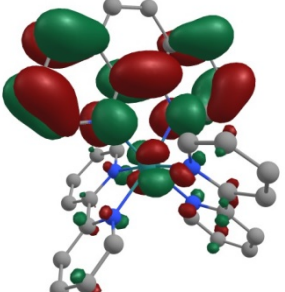
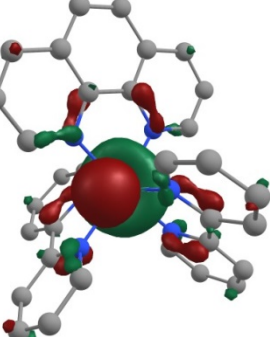
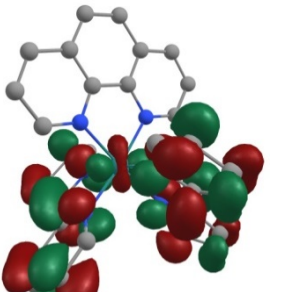
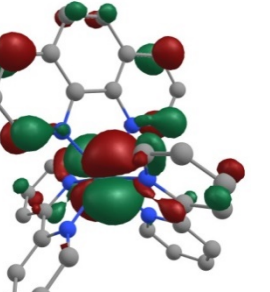
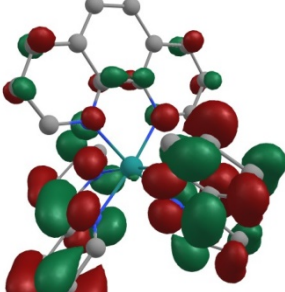
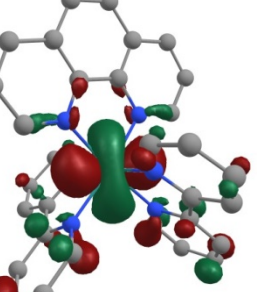
Table S4. Selected bond lengths [\AA] and angles [$^\circ$] for Ru-complexes obtained by DFT calculations and X-Ray analysis.

Complex	Parameters								
	Phen			bpy			bpy		
	Ru-N	Ru-N	$\theta_{\text{N}-\text{Ru}-\text{N}}$	Ru-N _{cis}	Ru-N _{trans}	$\theta_{\text{N}-\text{Ru}-\text{N}}$	Ru-N _{cis}	Ru-N _{trans}	$\theta_{\text{N}-\text{Ru}-\text{N}}$
Ru-Phen (DFT)	2.12	2.12	78.7	2.10	2.10	77.9	2.10	2.10	77.9
Ru-Phen (X-Ray)^a	2.07	2.08	79.8	2.07	2.07	78.3	2.07	2.06	78.5
Ru-5P (DFT)	2.11	2.11	78.7	2.10	2.10	77.9	2.10	2.10	77.9
Ru-5P (X-Ray)^b	2.07	2.06	79.3	2.07	2.05	79.0	2.06	2.05	79.0
Ru-4P (DFT)	2.11	2.11	78.7	2.10	2.10	77.9	2.10	2.10	77.9
Ru-3P (DFT)	2.11	2.12	78.6	2.10	2.10	78.0	2.10	2.10	77.9
Ru-4,7P₂ (DFT)	2.10	2.11	78.5	2.10	2.11	77.9	2.10	2.10	77.9
Ru-4,7P₂ (X-Ray)^b	2.06	2.04	79.6	2.06	2.06	78.5	2.07	2.06	79.4
Ru-3,8P₂ (DFT)	2.11	2.11	78.7	2.10	2.10	78.0	2.10	2.10	77.9
Ru-5PPh (DFT)	2.11	2.12	78.6	2.10	2.10	78.0	2.10	2.10	77.9
Ru-4PPh (DFT)	2.11	2.11	78.5	2.10	2.10	77.9	2.10	2.10	77.9
Ru-3PPh (DFT)	2.11	2.12	78.8	2.10	2.10	77.9	2.10	2.10	77.9
Ru-4,7(PPh)₂ (DFT)	2.11	2.11	78.2	2.10	2.10	77.9	2.10	2.10	77.9

^a experimental values for $[\text{Ru}(\text{bpy})_2(\text{Phen})](\text{BF}_4)_2 \cdot \text{H}_2\text{O}$ from ref.¹⁴

^b experimental values obtained in this work

Table S5. The electron-cloud distribution of the HOMO and LUMO calculated by DFT of the complex **Ru-Phen**

Orbital	E(eV)	The electron-cloud distribution	Orbital	E(eV)	The electron-cloud distribution
LUMO+2	-7.31		HOMO	-10.95	
LUMO+1	-7.37		HOMO-1	-11.08	
LUMO	-7.46		HOMO-2	-11.13	

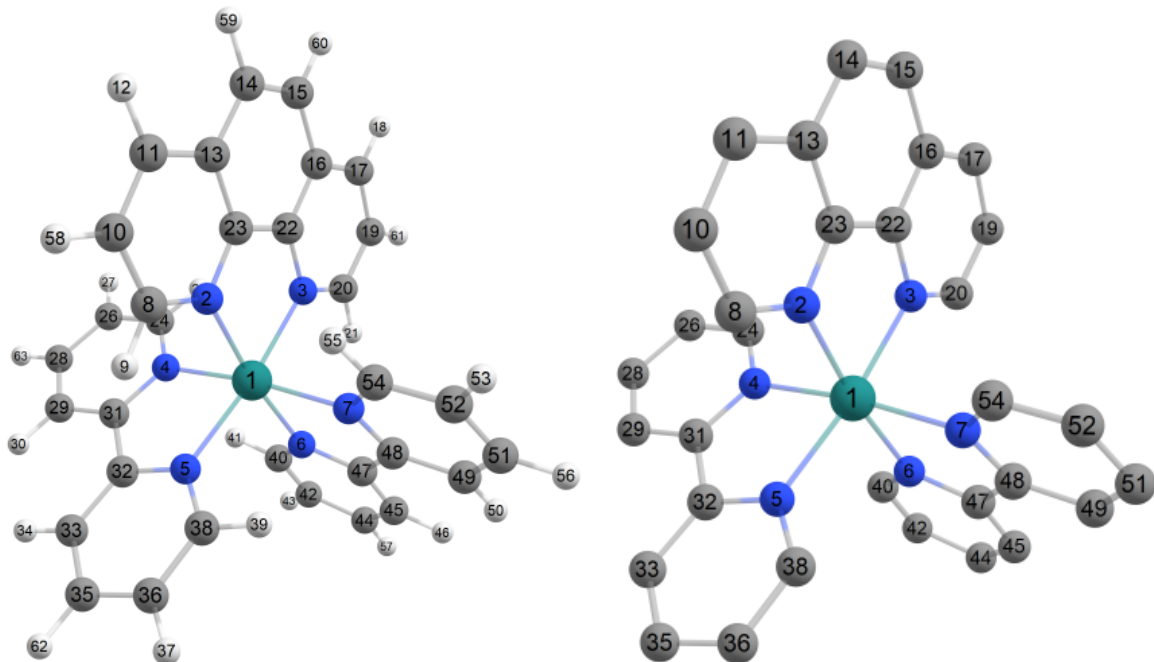


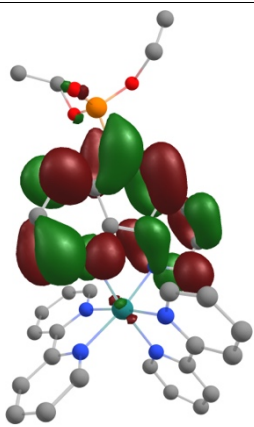
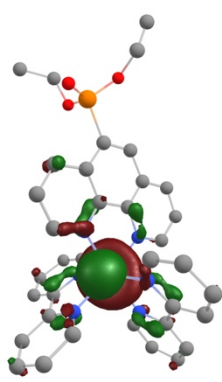
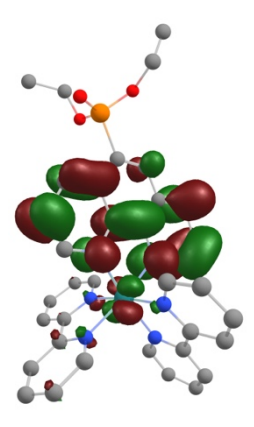
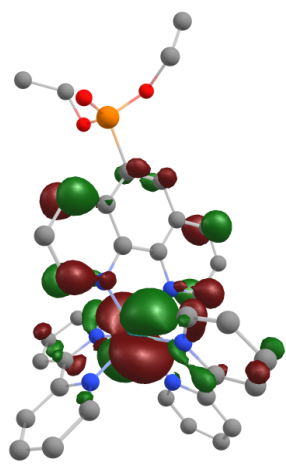
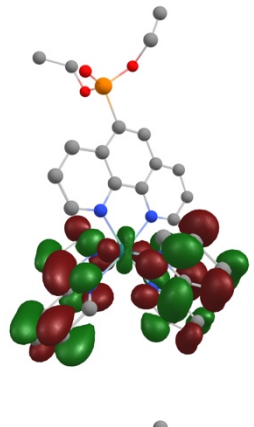
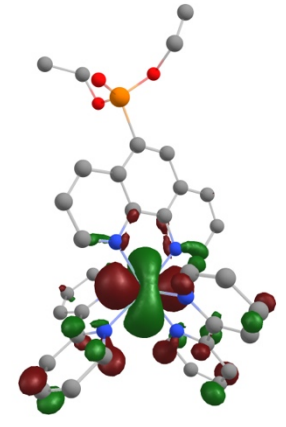
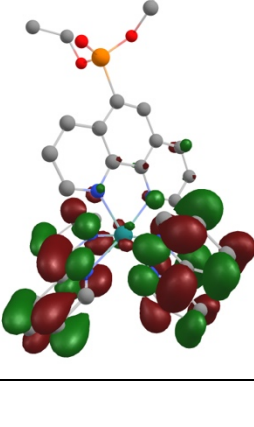
Figure S24. Optimized structure of the complex **Ru-Phen**.

1	44	8.701124853	24.120244663	0.260333510
2	7	10.728636692	24.508693039	0.719285104
3	7	8.780048612	23.555493211	2.297268324
4	7	9.298786134	22.267786424	-0.541947110
5	7	8.845276740	24.554299474	-1.790442641
6	7	6.629859850	23.850612079	0.032582559
7	7	7.944788522	25.984709065	0.874236451
8	6	11.689564864	24.971900379	-0.086583215
9	1	11.398455759	25.188162940	-1.107920127
10	6	13.009064754	25.181709348	0.346064257
11	6	13.350190653	24.903815111	1.656313902
12	1	14.363156091	25.061785655	2.013377746
13	6	12.362565128	24.407997968	2.536457803
14	6	12.613115618	24.089433277	3.914330868
15	6	11.620024801	23.614297250	4.718877706
16	6	10.289796277	23.415465930	4.215913740
17	6	9.223042236	22.925208219	5.001400017
18	1	9.389845819	22.677717794	6.045091471
19	6	7.976867849	22.767532192	4.424959141

20	6	7.792700266	23.093377064	3.071312030
21	1	6.824904272	22.974596943	2.597902394
22	6	10.016959353	23.721600396	2.861220856
23	6	11.058826544	24.222098898	2.017236012
24	6	9.532670086	21.144217864	0.165612676
25	1	9.363687395	21.212426941	1.233187841
26	6	9.961981446	19.959008636	-0.420123821
27	1	10.134126568	19.085114390	0.197831082
28	6	10.163870264	19.927601195	-1.799210214
29	6	9.925364069	21.082383681	-2.537912755
30	1	10.079638493	21.076152663	-3.609545417
31	6	9.492808787	22.244812057	-1.892230146
32	6	9.214580767	23.513888870	-2.592197575
33	6	9.313338800	23.673498830	-3.977991743
34	1	9.602142437	22.840818473	-4.606918730
35	6	9.034722048	24.908652835	-4.554812770
36	6	8.660091480	25.966775111	-3.728107100
37	1	8.433889770	26.947738644	-4.130175795
38	6	8.575885102	25.746954426	-2.358435970
39	1	8.287407251	26.540424041	-1.680291026
40	6	6.031640974	22.731963008	-0.424168840
41	1	6.691377493	21.909297461	-0.670719697
42	6	4.654262688	22.619260827	-0.571835358
43	1	4.226782358	21.694657538	-0.942997190
44	6	3.853234759	23.710190040	-0.237019232
45	6	4.461677371	24.870353244	0.232336758
46	1	3.853807580	25.727746104	0.493156949
47	6	5.853188832	24.923319975	0.361218322
48	6	6.586026562	26.107195692	0.850987214
49	6	5.962641367	27.288033260	1.266190434
50	1	4.883528339	27.373840373	1.246260970

51	6	6.732308874	28.358754079	1.710536079
52	6	8.119953266	28.225497262	1.730671452
53	1	8.761909594	29.031173356	2.068324391
54	6	8.682303475	27.026811680	1.307865250
55	1	9.755444253	26.881137337	1.307443358
56	1	6.256507640	29.277874206	2.035268020
57	1	2.774617158	23.660386979	-0.339569510
58	1	13.742235532	25.560903556	-0.356797267
59	1	13.614269070	24.236161210	4.306569679
60	1	11.821124939	23.375970328	5.758374074
61	1	7.136097074	22.395314905	4.999220749
62	1	9.108024307	25.040426762	-5.628917361
63	1	10.502074451	19.022493403	-2.292039908

Table S6. The electron-cloud distribution of the HOMO and LUMO calculated by DFT of the complex **Ru-5P**

Orbital	E(eV)	The electron-cloud distribution	Orbital	E(eV)	The electron-cloud distribution
LUMO+3	-7.02		HOMO	-10.81	
LUMO+2	-7.12		HOMO-1	-10.93	
LUMO+1	-7.26		HOMO-2	-10.99	
LUMO	-7.34				

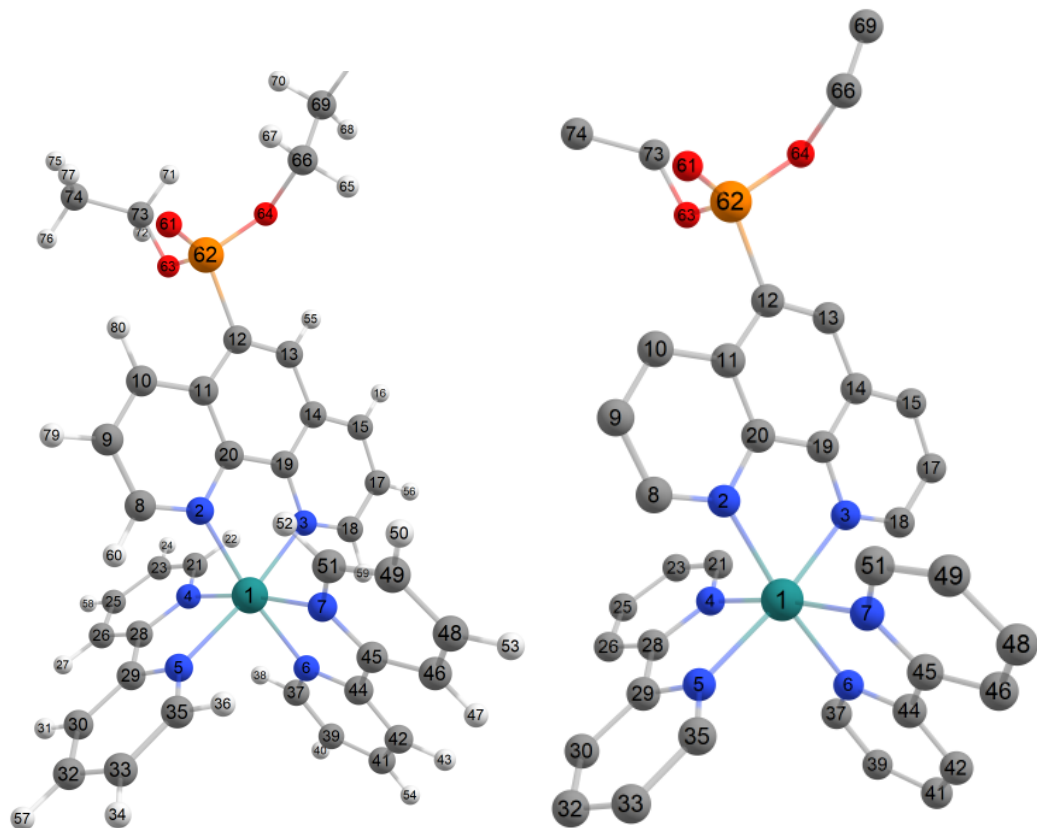


Figure S25. Optimized structure of the complex **Ru-5P**.

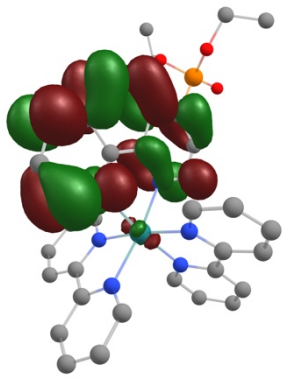
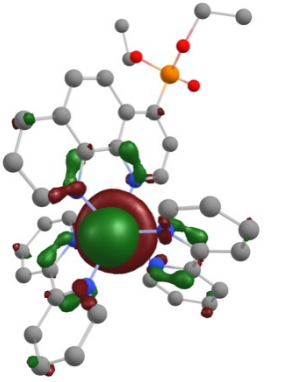
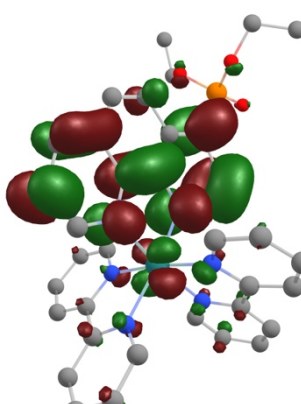
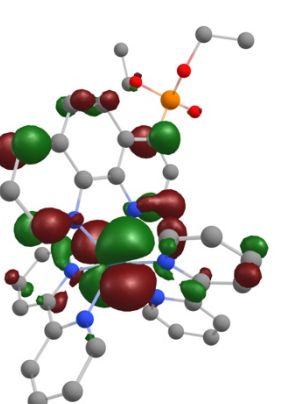
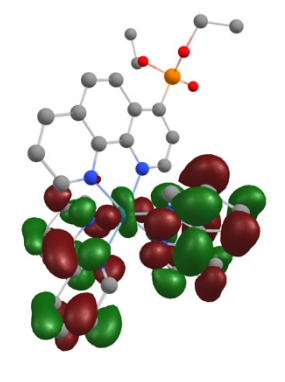
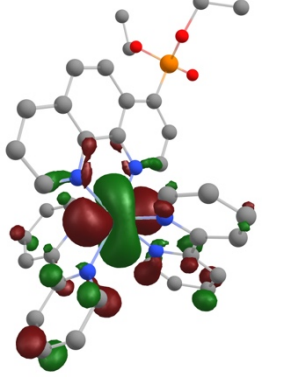
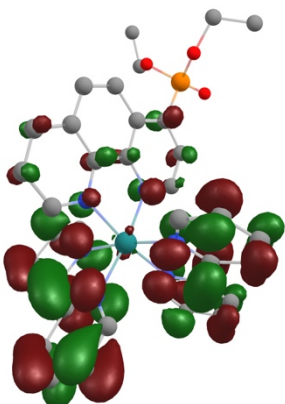
1	44	10.231960795	26.282116997	0.419865114
2	7	12.312324686	26.036801307	0.705016987
3	7	10.276028716	24.863499148	1.982484659
4	7	10.341159482	24.906262161	-1.165820852
5	7	10.384171733	27.548807317	-1.251433388
6	7	8.146038118	26.541404468	0.401799026
7	7	9.963253285	27.785211212	1.866018732
8	6	13.307196793	26.642271916	0.049548377
9	6	14.657095179	26.400254224	0.338546809
10	6	14.999834076	25.498782063	1.328740172
11	6	13.974579410	24.819089158	2.031942733
12	6	14.213069353	23.847444987	3.082737994
13	6	13.155015501	23.275529179	3.735992116
14	6	11.795272047	23.589532509	3.407059786
15	6	10.683034182	23.011497924	4.057798721
16	1	10.837296350	22.293441118	4.857184468

17	6	9.408680010	23.370209438	3.660569947
18	6	9.244701097	24.299281720	2.620887205
19	6	11.542476862	24.516844710	2.371397243
20	6	12.636737487	25.134225011	1.684128776
21	6	10.316198971	23.563994295	-1.041945384
22	1	10.202203352	23.183055354	-0.034638405
23	6	10.424237398	22.703736244	-2.128070230
24	1	10.396382035	21.631625184	-1.969931077
25	6	10.570008472	23.249149311	-3.402732858
26	6	10.596185263	24.633378693	-3.540756758
27	1	10.709214914	25.072667880	-4.523870535
28	6	10.478392125	25.448067323	-2.410360633
29	6	10.482332342	26.923053479	-2.460095816
30	6	10.574735478	27.658454744	-3.646009888
31	1	10.651662429	27.152405372	-4.600153010
32	6	10.564706105	29.049071704	-3.601795515
33	6	10.462631949	29.680697564	-2.363164117
34	1	10.450419406	30.761356678	-2.277291701
35	6	10.373743707	28.896844221	-1.218894288
36	1	10.294420797	29.347518130	-0.237368818
37	6	7.280840794	25.880835488	-0.393970810
38	1	7.715701249	25.145062694	-1.059228105
39	6	5.910521156	26.111613534	-0.374604905
40	1	5.261326082	25.549862422	-1.036567152
41	6	5.404617603	27.069566560	0.503145984
42	6	6.289692489	27.757509712	1.327500907
43	1	5.913109390	28.506351782	2.013071402
44	6	7.659226853	27.481101053	1.263370260
45	6	8.671712749	28.160497644	2.095500362
46	6	8.364074763	29.128602912	3.056670296
47	1	7.335913712	29.418326097	3.233661911

48	6	9.384575867	29.722437015	3.793179003
49	6	10.701497161	29.334329432	3.550803992
50	1	11.530700124	29.769300676	4.097136801
51	6	10.945528583	28.365772616	2.584282195
52	1	11.952990276	28.035530492	2.362961811
53	1	9.154611996	30.473345009	4.541430227
54	1	4.341201169	27.279315707	0.544935368
55	1	13.339828933	22.554226275	4.525547559
56	1	8.530946965	22.947188510	4.135915648
57	1	10.633457419	29.626536355	-4.517372230
58	1	10.661464485	22.610352148	-4.274444763
59	1	8.255258727	24.593307466	2.290237579
60	1	13.018169333	27.349114783	-0.719662936
61	8	16.898620446	24.454663835	3.424245393
62	15	15.918438138	23.342607958	3.540760200
63	8	16.073313967	22.071951504	2.583590595
64	8	15.781189831	22.689837474	5.002185767
65	1	15.403567842	23.915698986	6.631405971
66	6	16.259675576	23.382054312	6.205934337
67	1	17.018351116	24.109430897	5.909666378
68	1	16.043344033	21.606403213	7.425341713
69	6	16.804916793	22.346743868	7.167055649
70	1	17.665936836	21.828447840	6.737120838
71	1	17.539947801	21.082889704	3.701380829
72	1	16.882172342	20.230093350	2.296663947
73	6	17.250262168	21.193804527	2.652759425
74	6	18.386917021	21.716876895	1.795750012
75	1	19.215141757	21.001569353	1.819247570
76	1	18.068073015	21.832994071	0.756355137
77	1	18.750236017	22.679391276	2.163408339
78	1	17.129502385	22.841012415	8.087845441

79	1	15.421232444	26.932753652	-0.216511073
80	1	16.036168926	25.319510855	1.594919999

Table S7. The electron-cloud distribution of the HOMO and LUMO calculated by DFT of the complex **Ru-4P**.

Orbital	E(eV)	The electron-cloud distribution	Orbital	E(eV)	The electron-cloud distribution
LUMO+3	-7.02		HOMO	-10.83	
LUMO+2	-7.19		HOMO-1	-10.95	
LUMO+1	-7.27		HOMO-2	-11.01	
LUMO	-7.34				

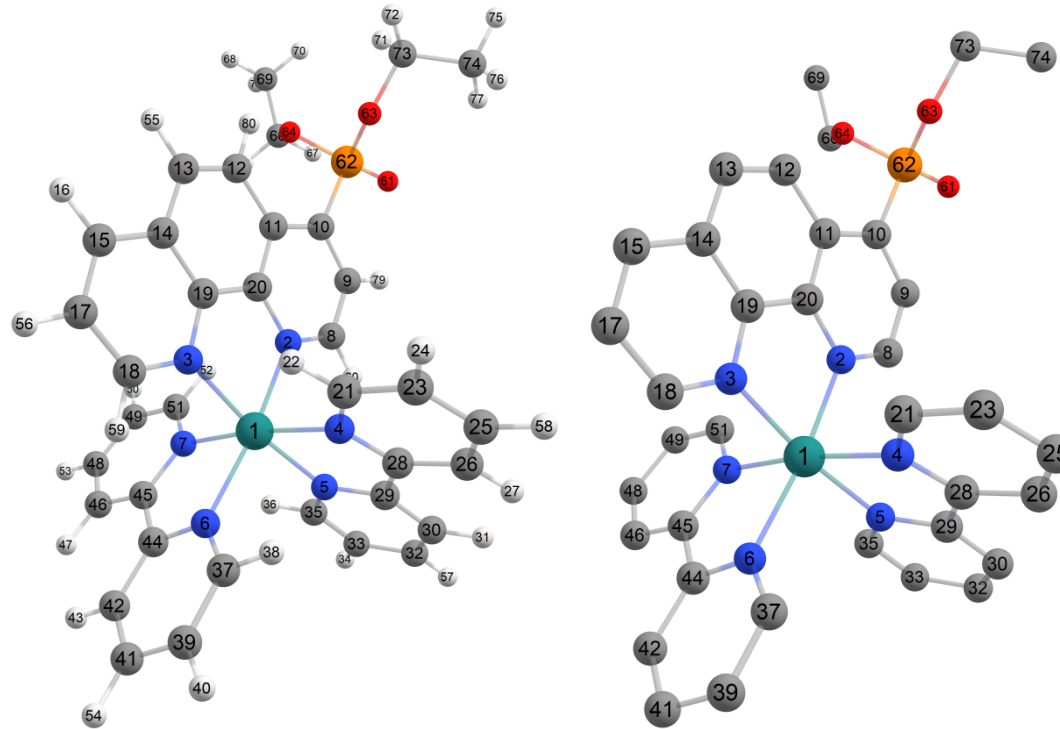


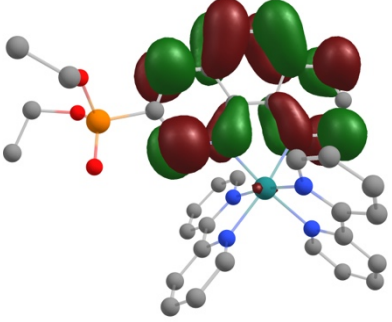
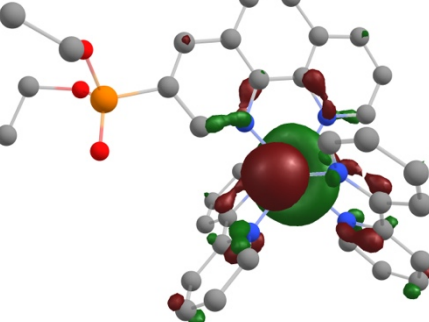
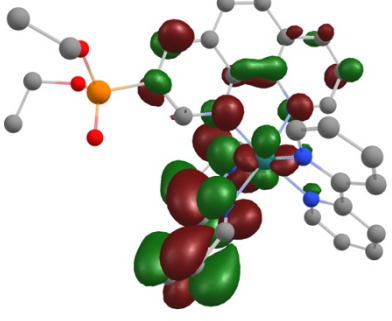
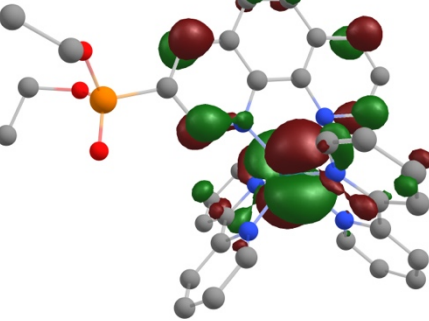
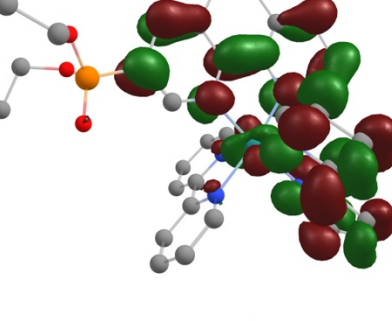
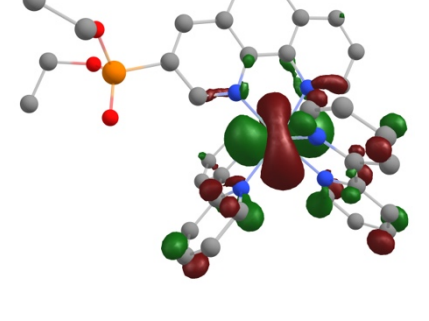
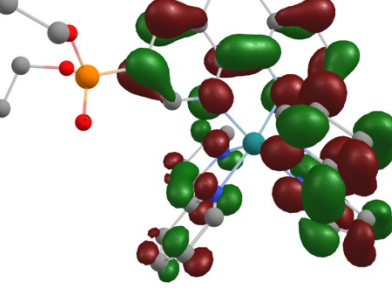
Figure S26. Optimized structure of the complex **Ru-4P**.

1	44	10.102535754	26.200010971	0.426976212
2	7	12.154815744	25.867413918	0.782348706
3	7	10.030132431	24.664169209	1.873531457
4	7	10.265474525	24.944175775	-1.254055153
5	7	10.373925097	27.583276722	-1.132377449
6	7	8.026932856	26.523311188	0.330736796
7	7	9.801266774	27.593315972	1.972044536
8	6	13.197868177	26.482454207	0.218903653
9	6	14.525773145	26.143059822	0.514410490
10	6	14.806594921	25.132973381	1.422024343
11	6	13.717678608	24.467854761	2.052119885
12	6	13.864660611	23.422628264	3.029065661
13	6	12.777438797	22.829570912	3.599683903
14	6	11.443160173	23.217207422	3.244458775
15	6	10.282953542	22.636123951	3.802230527
16	1	10.375917021	21.851443080	4.546549735
17	6	9.040574040	23.078646993	3.389827410
18	6	8.953188389	24.093196447	2.423074876

19	6	11.266908243	24.238826659	2.281923263
20	6	12.407458212	24.871633396	1.689941471
21	6	10.197880551	23.597828749	-1.236191218
22	1	9.998836787	23.145787829	-0.272427185
23	6	10.368180826	22.818569698	-2.374327037
24	1	10.300562023	21.738927387	-2.302198062
25	6	10.627041776	23.453615404	-3.588033590
26	6	10.697236009	24.843093087	-3.616787854
27	1	10.899053105	25.351589458	-4.551161126
28	6	10.510366888	25.573851623	-2.439322544
29	6	10.548156082	27.048021714	-2.375319961
30	6	10.738974576	27.868557858	-3.491611613
31	1	10.877324157	27.434739387	-4.473952284
32	6	10.746440142	29.251855503	-3.341665345
33	6	10.558190167	29.790463372	-2.069658321
34	1	10.551544025	30.861604440	-1.903220886
35	6	10.375648191	28.924787333	-0.997851342
36	1	10.228822303	29.300848056	0.007165144
37	6	7.186623110	25.961373621	-0.561401823
38	1	7.636067158	25.274601465	-1.268128323
39	6	5.823494450	26.231463259	-0.588226570
40	1	5.194219270	25.750743998	-1.328671892
41	6	5.298798843	27.124310118	0.345210325
42	6	6.158625353	27.712346850	1.267631284
43	1	5.767944928	28.412878754	1.995018162
44	6	7.521855807	27.401272190	1.245238449
45	6	8.509288187	27.980700007	2.176763045
46	6	8.179323079	28.870492796	3.203837897
47	1	7.150104155	29.167386979	3.361637121
48	6	9.178148697	29.374663627	4.031200902
49	6	10.496200944	28.976351967	3.812485177

50	1	11.309102260	29.342130031	4.429400271
51	6	10.762265627	28.086229081	2.778894826
52	1	11.770736742	27.748074976	2.575451788
53	1	8.930423737	30.063751987	4.831354713
54	1	4.240566682	27.361783816	0.354209740
55	1	12.908338391	22.045897042	4.339094360
56	1	8.129456333	22.656482652	3.798389109
57	1	10.893692748	29.895282400	-4.202411619
58	1	10.771395246	22.879163183	-4.496642099
59	1	7.989563765	24.451365529	2.079707557
60	1	12.970344486	27.268302381	-0.491723080
61	8	17.441996964	25.695708944	0.911093145
62	15	16.587142622	24.767187200	1.688809454
63	8	16.580466544	23.208262727	1.330613749
64	8	16.797370285	24.780321288	3.283453289
65	1	16.883088338	26.434867316	4.512943479
66	6	17.594215278	25.809413069	3.965283014
67	1	18.098242862	26.416353695	3.210106916
68	1	18.059458119	24.495946032	5.622217234
69	6	18.576078880	25.133479931	4.899979483
70	1	19.294240176	24.524617097	4.344045405
71	1	18.532322109	22.828517800	2.004095750
72	1	17.557088161	21.432579501	1.521105851
73	6	17.839769930	22.450343316	1.246067357
74	6	18.427040004	22.521669219	-0.149611276
75	1	19.326694825	21.899939871	-0.195984820
76	1	17.714171144	22.146249624	-0.888904811
77	1	18.699836028	23.547397400	-0.407807891
78	1	19.134117922	25.895649666	5.452848962
79	1	15.341746859	26.665030193	0.025532870
80	1	14.863889111	23.115555027	3.309636603

Table S8. The electron-cloud distribution of the HOMO and LUMO calculated by DFT of the complex **Ru-3P**

Orbital	E(eV)	The electron-cloud distribution	Orbital	E(eV)	The electron-cloud distribution
LUMO+3	-6.98		HOMO	-10.78	
LUMO+2	-7.17		HOMO-1	-10.91	
LUMO+1	-7.22		HOMO-2	-10.95	
LUMO	7.31				

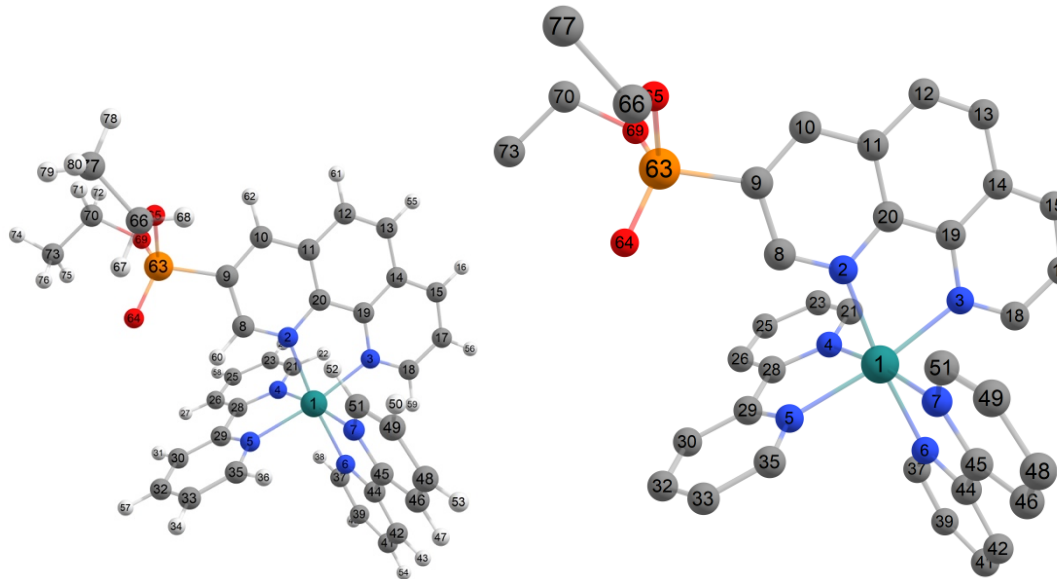


Figure S27. Optimized structure of the complex **Ru-3P**.

1	44	9.345199272	26.093423612	0.282259654
2	7	11.423638802	25.776248853	0.477710835
3	7	9.407984618	24.711708107	1.885335656
4	7	9.348877783	24.676821825	-1.271583753
5	7	9.496095825	27.312353042	-1.421542520
6	7	7.267884903	26.414892303	0.330498351
7	7	9.170484060	27.641765440	1.695185888
8	6	12.411830592	26.309506225	-0.244368563
9	6	13.768231613	25.977973788	-0.056849397
10	6	14.106631328	25.069195750	0.933314011
11	6	13.088848122	24.493357041	1.725876327
12	6	13.338884025	23.552895658	2.782708974
13	6	12.315715926	23.032066495	3.518953143
14	6	10.951778035	23.398509352	3.257272596
15	6	9.851382000	22.891617562	3.984009723
16	1	10.015757918	22.186812194	4.793190154
17	6	8.575017218	23.304388288	3.651480001
18	6	8.391694336	24.213661461	2.596486867
19	6	10.678301584	24.316713989	2.215081412

20	6	11.752980272	24.872766105	1.452828604
21	6	9.266555616	23.340387021	-1.114147268
22	1	9.171067582	22.988790891	-0.094278143
23	6	9.296981745	22.451765856	-2.182034647
24	1	9.223617812	21.386047103	-1.997415936
25	6	9.423744103	22.961463724	-3.473599667
26	6	9.511754165	24.339248178	-3.645540334
27	1	9.611927260	24.750883103	-4.641912577
28	6	9.471738520	25.184081126	-2.531813420
29	6	9.547194068	26.655520364	-2.616243021
30	6	9.665646390	27.357658305	-3.819129818
31	1	9.710011543	26.826884184	-4.761724616
32	6	9.731770503	28.747334178	-3.806485990
33	6	9.676824449	29.410657044	-2.582170230
34	1	9.727967091	30.491634010	-2.520121979
35	6	9.558370609	28.658722334	-1.419399204
36	1	9.517829059	29.135074469	-0.447853159
37	6	6.355184796	25.759174261	-0.414734116
38	1	6.743212567	24.993739325	-1.075336754
39	6	4.993454647	26.030268263	-0.352167497
40	1	4.304702928	25.470450829	-0.974633044
41	6	4.547035771	27.025484282	0.516171471
42	6	5.481095666	27.708505889	1.288627246
43	1	5.151558194	28.486129015	1.966217896
44	6	6.838866946	27.390341836	1.182785055
45	6	7.899401168	28.061019828	1.959533583
46	6	7.653669353	29.062643359	2.903907721
47	1	6.640717045	29.384861238	3.109947542
48	6	8.716391739	29.647895148	3.585084409
49	6	10.012439839	29.216450783	3.305764733
50	1	10.872389736	29.643566364	3.808868434

51	6	10.193926784	28.214035944	2.360257422
52	1	11.182589719	27.848531776	2.111338136
53	1	8.534353601	30.425292978	4.319310226
54	1	3.492357795	27.267605033	0.590507598
55	1	12.517601185	22.326058441	4.318170227
56	1	7.708308063	22.937339754	4.189428192
57	1	9.826377400	29.299692846	-4.735024511
58	1	9.453119871	22.299600450	-4.332365184
59	1	7.398698435	24.544756458	2.315021708
60	1	12.142798242	27.033133916	-1.004656115
61	1	14.365251918	23.265471751	2.987573434
62	1	15.144184223	24.798971312	1.106065973
63	15	14.972940510	26.794580636	-1.162690144
64	8	14.319889775	27.914445583	-1.890365453
65	8	16.232926465	27.176001305	-0.244382554
66	6	16.526965959	28.552591051	0.166423105
67	1	15.942078661	29.235113583	-0.454675560
68	1	16.200937046	28.645560962	1.207143274
69	8	15.494919623	25.516480095	-1.965821649
70	6	16.659726870	25.568861405	-2.858969975
71	1	17.453327902	26.126916320	-2.354646970
72	1	16.972235299	24.526650833	-2.943803297
73	6	16.308129818	26.162984586	-4.210070290
74	1	17.187540506	26.126159739	-4.860967147
75	1	15.506725936	25.592870221	-4.687764234
76	1	15.989017072	27.204168985	-4.117775968
77	6	18.015999183	28.794397050	0.028237384
78	1	18.588058122	28.074574375	0.619182728
79	1	18.330603416	28.721949308	-1.016347269
80	1	18.256761539	29.799904033	0.386964717

Table S9. The electron-cloud distribution of the HOMO and LUMO calculated by DFT of the complex **Ru-4,7P₂**

Orbital	E(eV)	The electron-cloud distribution	Orbital	E(eV)	The electron-cloud distribution
LUMO+3	-6.90		HOMO	-10.71	
LUMO+2	-7.04		HOMO-1	-10.81	
LUMO+1	-7.17		HOMO-2	-10.89	
LUMO	-7.25				

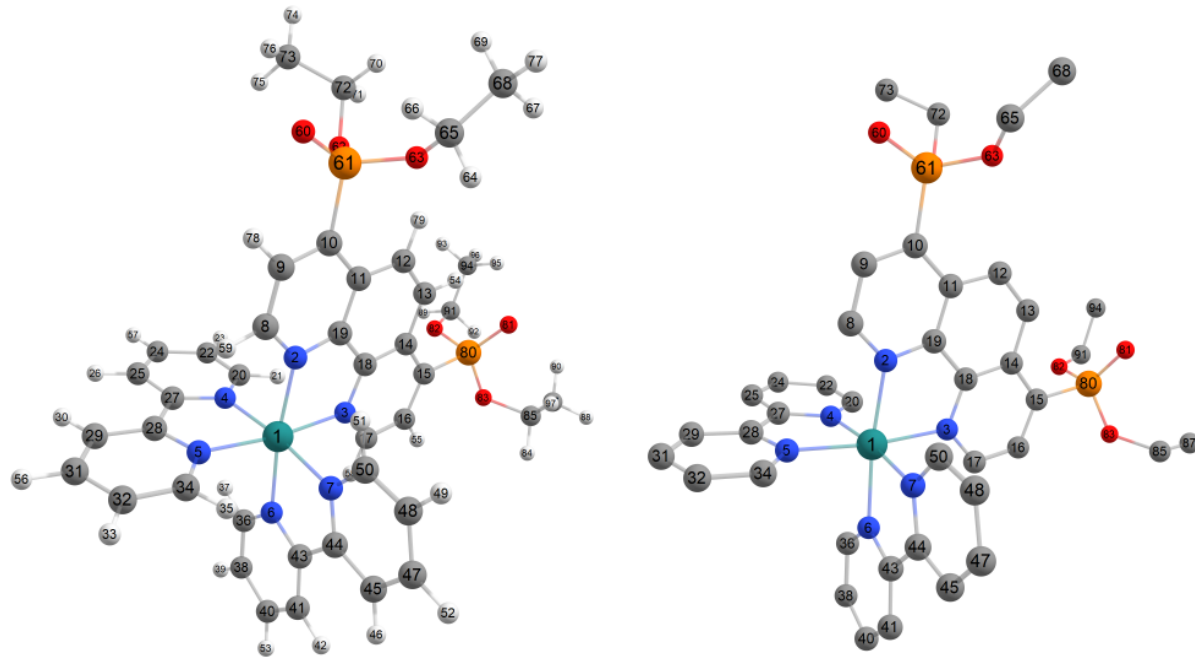


Figure S28. Optimized structure of the complex **Ru-4,7P₂**

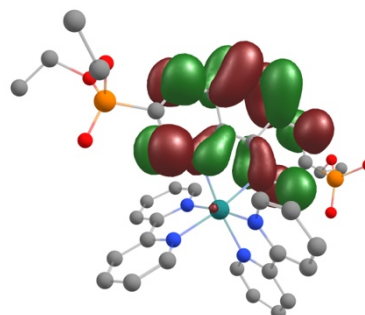
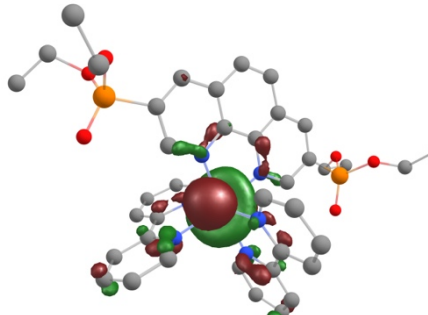
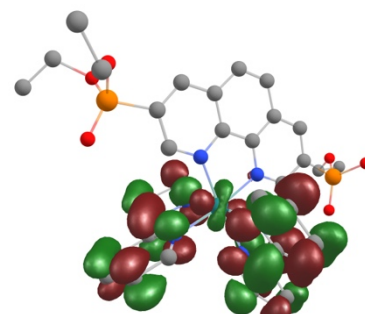
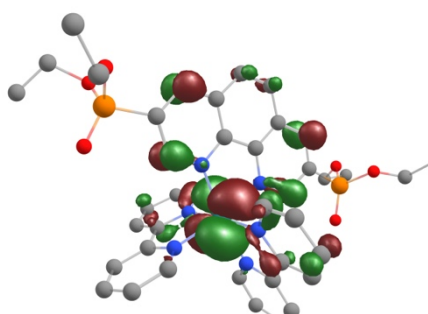
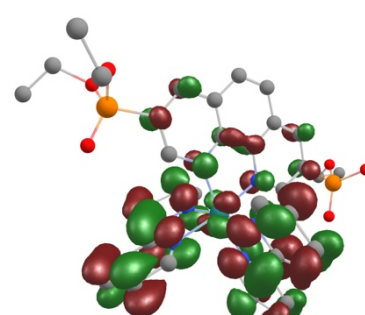
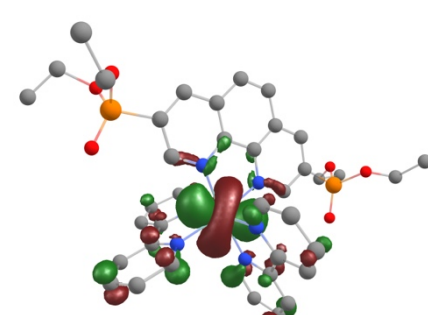
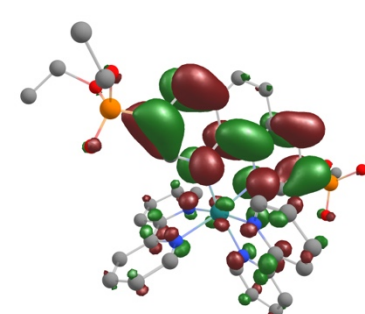
1	44	10.234613480	25.571022203	1.083347001
2	7	12.298491921	25.290931821	1.392510711
3	7	10.237492358	24.077850738	2.566265501
4	7	10.378902925	24.268502520	-0.561609291
5	7	10.424751481	26.913192555	-0.526823960
6	7	8.149319211	25.846669583	1.032985525
7	7	9.942407759	27.003990709	2.593002303
8	6	13.309864131	25.908792481	0.776776367
9	6	14.653026709	25.603760420	1.038017577
10	6	14.982201655	24.630303288	1.968546478
11	6	13.927515093	23.967015486	2.656245047
12	6	14.120983061	22.968709687	3.669885380
13	6	13.067117504	22.363492717	4.288749570
14	6	11.709243621	22.683294425	3.941844498
15	6	10.564681497	22.063675049	4.521776479
16	6	9.310548201	22.493873491	4.115377753
17	6	9.183298433	23.497467821	3.145329453
18	6	11.489200082	23.683458206	2.961480456
19	6	12.598513858	24.328680763	2.322104734

20	6	10.356563888	22.921960062	-0.498818861
21	1	10.213467452	22.494761085	0.486015780
22	6	10.504540987	22.112346929	-1.618831016
23	1	10.477787523	21.034171475	-1.509614748
24	6	10.689671147	22.714970947	-2.862145200
25	6	10.714852718	24.104110393	-2.936402524
26	1	10.861850880	24.588472965	-3.893515103
27	6	10.555341034	24.866246542	-1.775071134
28	6	10.556047038	26.341986587	-1.758855650
29	6	10.675607111	27.129260546	-2.908407240
30	1	10.775904096	26.665815059	-3.881802309
31	6	10.660443748	28.516484586	-2.802864457
32	6	10.521932689	29.092326185	-1.540784543
33	1	10.501734223	30.168029940	-1.407835564
34	6	10.405885557	28.258216718	-0.435016267
35	1	10.296770092	28.663867092	0.563304681
36	6	7.297273579	25.230836734	0.188861980
37	1	7.741798604	24.523230010	-0.500127123
38	6	5.928552314	25.471861004	0.188897486
39	1	5.289853231	24.946885156	-0.512341610
40	6	5.410445438	26.393203716	1.098150115
41	6	6.282294996	27.036635444	1.970926711
42	1	5.896510394	27.758293966	2.680006791
43	6	7.650672082	26.751057688	1.924738725
44	6	8.649268478	27.380975583	2.810497327
45	6	8.327371844	28.303198025	3.811129720
46	1	7.297989223	28.595246799	3.976759794
47	6	9.334819785	28.846191297	4.602610234
48	6	10.652999678	28.453531588	4.375019616
49	1	11.471828127	28.846882736	4.966491006
50	6	10.911847407	27.533926969	3.365497859

51	1	11.920616593	27.201492412	3.153810110
52	1	9.093375013	29.560799398	5.382103756
53	1	4.347804791	26.608972030	1.127271351
54	1	13.237259333	21.640307283	5.077799802
55	1	8.417404280	22.051393993	4.540920572
56	1	10.752604471	29.134017563	-3.689805523
57	1	10.813273144	22.116758498	-3.758445063
58	1	8.205942370	23.831938760	2.817343610
59	1	13.043787319	26.666885380	0.049449103
60	8	17.589386085	25.217946823	1.350024730
61	15	16.775916875	24.296586172	2.179773509
62	8	16.776758209	22.729362699	1.858397072
63	8	17.050064814	24.347020288	3.763873249
64	1	17.148454953	26.072173175	4.896122772
65	6	17.852970736	25.403502587	4.392339764
66	1	18.374066795	25.957798138	3.608686947
67	1	18.276141269	24.181459763	6.127775222
68	6	18.812714507	24.764668058	5.374812665
69	1	19.522093088	24.109215164	4.862371375
70	1	18.706941064	22.341577666	2.579857130
71	1	17.743148391	20.951511849	2.060280179
72	6	18.035005326	21.970584440	1.800004590
73	6	18.661216943	22.047942234	0.421196121
74	1	19.560643669	21.424507611	0.396032476
75	1	17.968077570	21.678117095	-0.339227392
76	1	18.942252331	23.074264925	0.174541299
77	1	19.381760438	25.546344887	5.887425602
78	1	15.442375621	26.122144465	0.503963204
79	1	15.133064629	22.708465760	3.951942421
80	15	10.706096570	20.711604852	5.759537491
81	8	11.802918485	20.927410123	6.737277370

82	8	10.797839761	19.478258493	4.746140447
83	8	9.230298074	20.600447451	6.384430707
84	1	8.040504331	21.488339917	7.788145055
85	6	8.966896016	20.909087549	7.797026630
86	1	8.039649029	18.991770336	8.177431481
87	6	8.819879941	19.631741499	8.598020617
88	1	8.541935650	19.877991428	9.627769561
89	1	10.450746872	17.508492969	4.386225228
90	1	9.761769112	19.076815252	8.628163968
91	6	10.843535337	18.088671172	5.222948860
92	1	10.151167958	17.986376079	6.063525435
93	1	12.928484273	17.796953388	4.734408208
94	6	12.255749563	17.671178491	5.587073421
95	1	12.638049624	18.255711202	6.427121166
96	1	12.258223226	16.613551360	5.868935062
97	1	9.779430159	21.530121242	8.180724207.

Table S10. The electron-cloud distribution of the HOMO and LUMO calculated by DFT of the complex **Ru-3,8P₂**

Orbital	E(eV)	The electron-cloud distribution	Orbital	E(eV)	The electron-cloud distribution
LUMO+3	-6.83		HOMO	-10.61	
LUMO+2	-7.03		HOMO-1	-10.74	
LUMO+1	-7.06		HOMO-2	-10.78	
LUMO	-7.22				

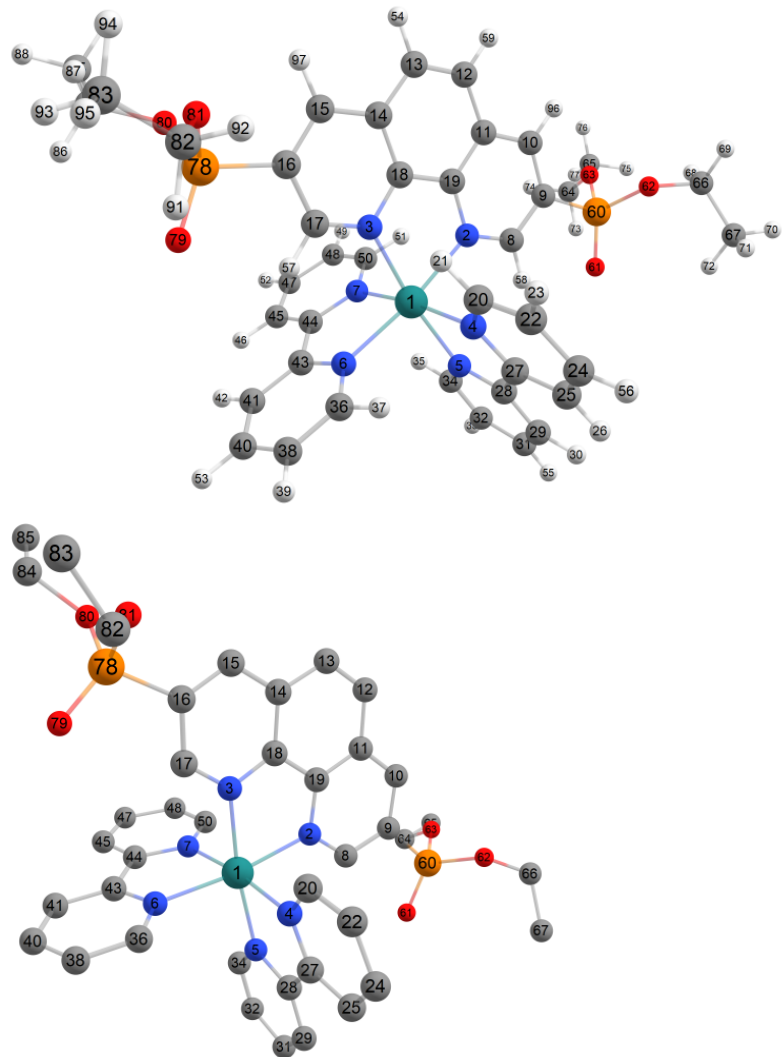


Figure S29. Optimized structure of the complex **Ru-3,8P₂**.

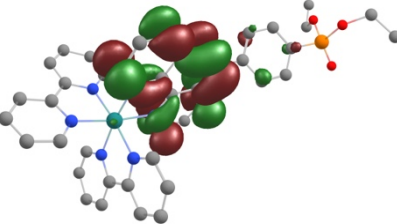
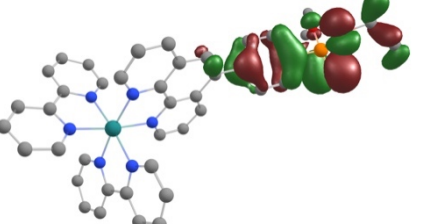
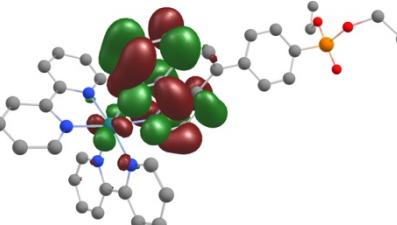
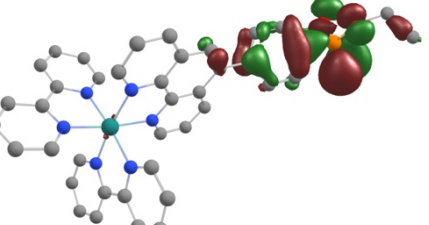
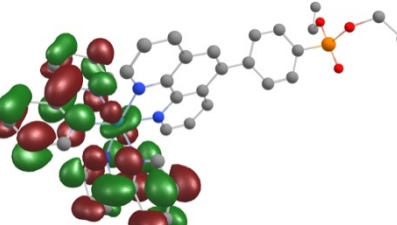
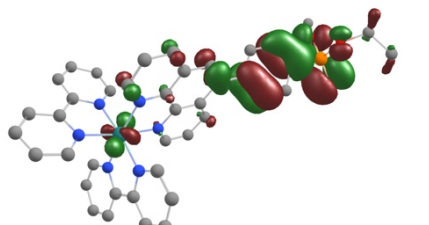
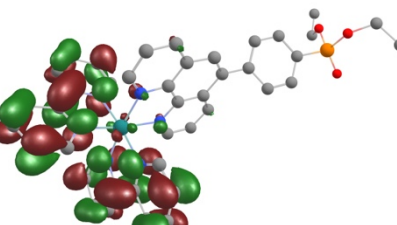
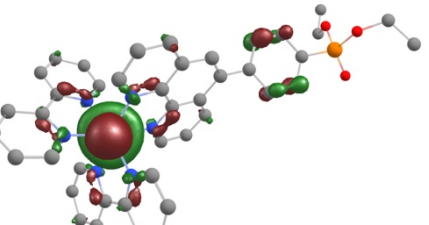
1	44	5.347930910	27.816456654	-2.951555441
2	7	7.450699130	28.002795120	-2.962394881
3	7	5.888481543	26.517132137	-1.372081468
4	7	5.524622556	26.398283293	-4.492972287
5	7	5.030613555	28.989643890	-4.663854990
6	7	3.270452131	27.656266766	-2.679981351
7	7	4.972600124	29.320139542	-1.530878915
8	6	8.212253491	28.721365423	-3.790181548
9	6	9.619065058	28.742148702	-3.718302462
10	6	10.253142296	27.997696089	-2.735960178
11	6	9.480384919	27.226291016	-1.839607619

12	6	10.042737661	26.416638294	-0.794839478
13	6	9.246801876	25.666153669	0.020469921
14	6	7.819987784	25.658874140	-0.140058667
15	6	6.948727255	24.867796483	0.641567000
16	6	5.585338655	24.912201469	0.400726616
17	6	5.094269821	25.762035594	-0.611196092
18	6	7.240993879	26.465338827	-1.146988965
19	6	8.073953682	27.252141960	-2.000499749
20	6	5.784840014	25.086153719	-4.324666675
21	1	5.881126573	24.748318378	-3.300280338
22	6	5.917944273	24.201818121	-5.388094237
23	1	6.127323865	23.156326296	-5.193434350
24	6	5.780139643	24.689924763	-6.686708215
25	6	5.515172766	26.043234815	-6.870162838
26	1	5.407678520	26.437782784	-7.872591954
27	6	5.389983167	26.884825052	-5.760381422
28	6	5.103416269	28.329419373	-5.855416510
29	6	4.918820287	29.006128474	-7.064672225
30	1	4.981755297	28.473711445	-8.005179156
31	6	4.655070792	30.372251303	-7.061469631
32	6	4.579055182	31.038189121	-5.839615006
33	1	4.377975246	32.101989708	-5.784711464
34	6	4.771618951	30.312146470	-4.670423131
35	1	4.725225771	30.790451933	-3.700201279
36	6	2.459767738	26.794615695	-3.326072023
37	1	2.942480663	26.122872513	-4.024992909
38	6	1.085973861	26.752169347	-3.120677463
39	1	0.483958119	26.038547635	-3.671433774
40	6	0.517409725	27.637063502	-2.205540576
41	6	1.346469925	28.528344230	-1.531795778
42	1	0.921525483	29.222017011	-0.817248238

43	6	2.721929376	28.526250018	-1.783339216
44	6	3.675120964	29.442413964	-1.127556877
45	6	3.307053870	30.389539434	-0.166498538
46	1	2.275350143	30.477609255	0.149905666
47	6	4.271737524	31.225109901	0.387631434
48	6	5.594537014	31.096387702	-0.033621878
49	1	6.379560743	31.727903292	0.366514225
50	6	5.900498384	30.134486044	-0.988943085
51	1	6.913566565	30.001748855	-1.347913848
52	1	3.994172273	31.964214170	1.131386963
53	1	-0.550954221	27.636194382	-2.017952079
54	1	9.681831050	25.051407756	0.801983968
55	1	4.513911855	30.904885703	-7.995664926
56	1	5.876101497	24.030556686	-7.542499256
57	1	4.032122796	25.818846084	-0.817459557
58	1	7.711194954	29.310062725	-4.549343466
59	1	11.120854231	26.406893974	-0.670089448
60	15	10.493153924	29.754505005	-4.963310071
61	8	9.517937690	30.517434383	-5.786098178
62	8	11.391478509	28.615372710	-5.630247445
63	8	11.576309793	30.624552325	-4.156192805
64	6	11.402452543	32.056265347	-3.903060659
65	6	12.775364279	32.681586817	-3.769097963
66	6	12.451688047	28.921777491	-6.599335585
67	6	11.899417442	29.032454686	-8.007734326
68	1	12.961769677	29.834521572	-6.278809695
69	1	13.149436320	28.088006153	-6.502171545
70	1	12.724595028	29.201087394	-8.706635039
71	1	11.391310191	28.108909200	-8.297723152
72	1	11.195468625	29.863797910	-8.095831056
73	1	10.829565077	32.488914735	-4.726330882

74	1	10.824757597	32.160657400	-2.977958147
75	1	13.343087988	32.579751477	-4.697308620
76	1	13.342101226	32.216415951	-2.958624831
77	1	12.671014401	33.748219568	-3.548416015
78	15	4.490077635	23.834772004	1.382583230
79	8	5.233399255	23.056682800	2.401025499
80	8	3.779384519	23.047761128	0.175030311
81	8	3.344440783	24.823795644	1.934731722
82	6	3.108356256	24.994760247	3.374163860
83	6	1.868935908	24.233983888	3.801139814
84	6	2.935083330	21.883024882	0.458830233
85	6	2.633140069	21.194422434	-0.855046887
86	1	3.476530883	21.225704322	1.143671001
87	1	2.023417002	22.237756638	0.949398082
88	1	1.990870393	20.328109619	-0.673462868
89	1	2.112269027	21.867574030	-1.542261934
90	1	3.553636519	20.844458229	-1.330268543
91	1	3.991789245	24.655381571	3.919599618
92	1	2.990884246	26.072175266	3.514025323
93	1	2.012452463	23.155256441	3.692387709
94	1	0.997032593	24.536596195	3.214437604
95	1	1.660073668	24.439142405	4.855746590
96	1	11.336057386	27.995526023	-2.656516792
97	1	7.335766621	24.213638780	1.418000879

Table S11. The electron-cloud distribution of the HOMO and LUMO calculated by DFT of the complex **Ru-5PPh**.

Orbital	E(eV)	The electron-cloud distribution	Orbital	E(eV)	The electron-cloud distribution
LUMO+3	-6.92		HOMO	-10.31	
LUMO+2	-7.10		HOMO-1	-10.52	
LUMO+1	-7.24		HOMO-2	-10.71	
LUMO	-7.33		HOMO-3	-10.79	

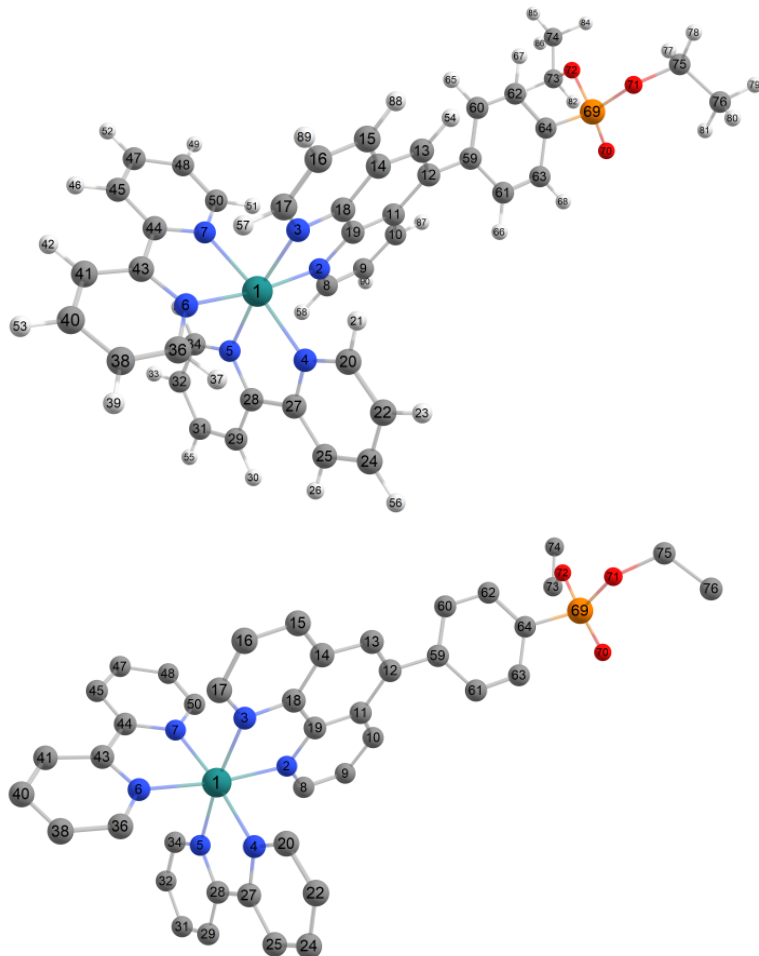


Figure S30. Optimized structure of the complex **Ru-5PPh**.

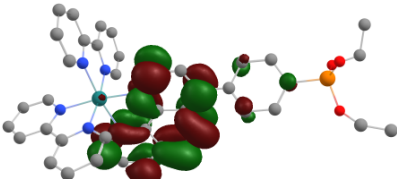
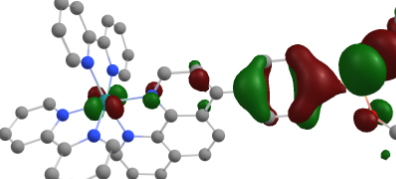
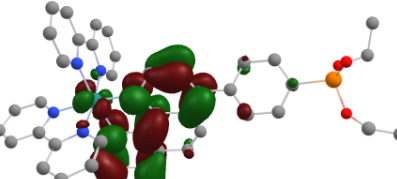
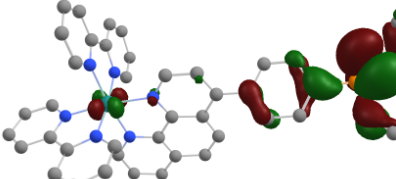
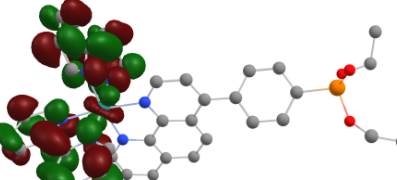
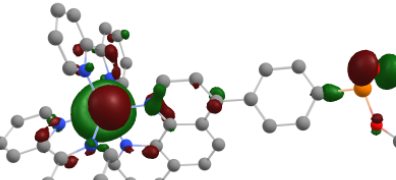
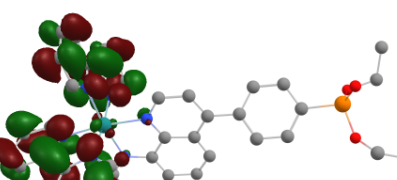
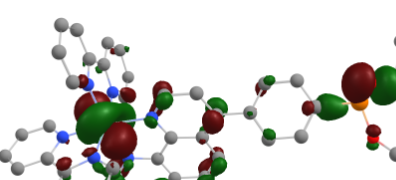
1	44	5.362254351	26.964976703	-1.955949430
2	7	6.224576452	28.201608373	-3.439611469
3	7	7.420327481	26.698917686	-1.575792657
4	7	5.187048182	25.448261008	-3.403339900
5	7	3.368710440	27.188226410	-2.590457174
6	7	4.682748631	25.845823427	-0.311534737
7	7	5.320764683	28.408612757	-0.427368411
8	6	5.595879042	28.961834294	-4.340915538
9	6	6.285448272	29.758652808	-5.264983893
10	6	7.667904801	29.750099541	-5.278560065
11	6	8.374121416	28.930923007	-4.367590504
12	6	9.826220956	28.853347635	-4.305811583
13	6	10.404330313	28.102749277	-3.309838867

14	6	9.639526902	27.366507102	-2.352624998
15	6	10.217192674	26.578822706	-1.329756928
16	6	9.393422992	25.883581155	-0.466269330
17	6	7.999082619	25.967708073	-0.618108289
18	6	8.228489942	27.396135383	-2.433424935
19	6	7.595922486	28.186790278	-3.443366438
20	6	6.172182321	24.609249429	-3.781953472
21	1	7.117016249	24.724251572	-3.265508703
22	6	6.005103044	23.646713487	-4.770543598
23	1	6.832442322	22.997932696	-5.034546696
24	6	4.767014367	23.542936895	-5.402936593
25	6	3.744878997	24.405937751	-5.020410902
26	1	2.778201854	24.340538575	-5.503682369
27	6	3.972922036	25.354248724	-4.018187903
28	6	2.951336935	26.309526455	-3.547469526
29	6	1.638603591	26.337940382	-4.028584309
30	1	1.317555101	25.634042686	-4.786135727
31	6	0.737556487	27.272870069	-3.529048636
32	6	1.171574351	28.167055063	-2.551344411
33	1	0.506785184	28.912868447	-2.130648339
34	6	2.487832118	28.089832411	-2.111423135
35	1	2.865181687	28.765731082	-1.353720511
36	6	4.358755421	24.537166594	-0.333174820
37	1	4.483693155	24.033294388	-1.283769504
38	6	3.895826477	23.855621472	0.786253663
39	1	3.653227854	22.801712261	0.711691214
40	6	3.753515951	24.553245355	1.984985445
41	6	4.083978573	25.904394276	2.016980169
42	1	3.976617935	26.462205555	2.938820158
43	6	4.549123932	26.534968659	0.858713940
44	6	4.928621661	27.959779197	0.799835436

45	6	4.900037205	28.816751149	1.904622864
46	1	4.594623766	28.449005462	2.876159239
47	6	5.270941791	30.149636349	1.756805659
48	6	5.667452562	30.600930789	0.498676546
49	1	5.964547655	31.630349809	0.333492087
50	6	5.681156620	29.701003476	-0.560377815
51	1	5.985784008	30.007663159	-1.553313552
52	1	5.251376859	30.821112841	2.608441069
53	1	3.391943850	24.056782153	2.879064543
54	1	11.486135694	28.032826969	-3.261020953
55	1	-0.282938496	27.299927672	-3.895721318
56	1	4.598773380	22.805106781	-6.180071350
57	1	7.333244283	25.428939016	0.045710990
58	1	4.512404939	28.946416725	-4.314895678
59	6	10.688519159	29.565641914	-5.283746594
60	6	11.749958229	30.364811091	-4.824511328
61	6	10.504707236	29.411179272	-6.669085535
62	6	12.608035728	30.989062427	-5.725620221
63	6	11.364617216	30.036544593	-7.568958224
64	6	12.425918610	30.822400268	-7.104066609
65	1	11.891753354	30.509349460	-3.757570251
66	1	9.713441782	28.769296734	-7.045765792
67	1	13.417554588	31.611835696	-5.359338867
68	1	11.227835401	29.915213016	-8.638638128
69	15	13.538846413	31.576590006	-8.330233078
70	8	12.932791718	31.650211886	-9.683923021
71	8	14.845784608	30.674387933	-8.108212027
72	8	14.002757478	32.989719567	-7.695768448
73	6	13.399802045	34.240302670	-8.138914327
74	6	14.321351278	35.372587247	-7.732344817
75	6	16.059517826	30.910946207	-8.888765361

76	6	16.017201376	30.174196487	-10.215158692
77	1	16.190813506	31.989061605	-9.023133730
78	1	16.867755486	30.549036277	-8.249519592
79	1	16.964751317	30.319398585	-10.744094933
80	1	15.874149827	29.101734871	-10.056370075
81	1	15.204497380	30.547340935	-10.842496988
82	1	13.252778169	34.196872554	-9.220877121
83	1	12.418000452	34.337480813	-7.660741393
84	1	15.298007659	35.272035890	-8.213087908
85	1	14.468509070	35.388272064	-6.648850355
86	1	13.886065226	36.329623535	-8.035746935
87	1	8.214555286	30.371066194	-5.977818252
88	1	11.297205055	26.527653833	-1.232234516
89	1	9.802534588	25.270436811	0.328725806
90	1	5.724055294	30.377487262	-5.955722896

Table S12. The electron-cloud distribution of the HOMO and LUMO calculated by DFT of the complex **Ru-4PPh**

Orbital	E(eV)	The electron-cloud distribution	Orbital	E(eV)	The electron-cloud distribution
LUMO+3	-6.89		HOMO	-10.36	
LUMO+2	-7.04		HOMO-1	-10.50	
LUMO+1	-7.20		HOMO-2	-10.74	
LUMO	-7.29		HOMO-3	-10.81	

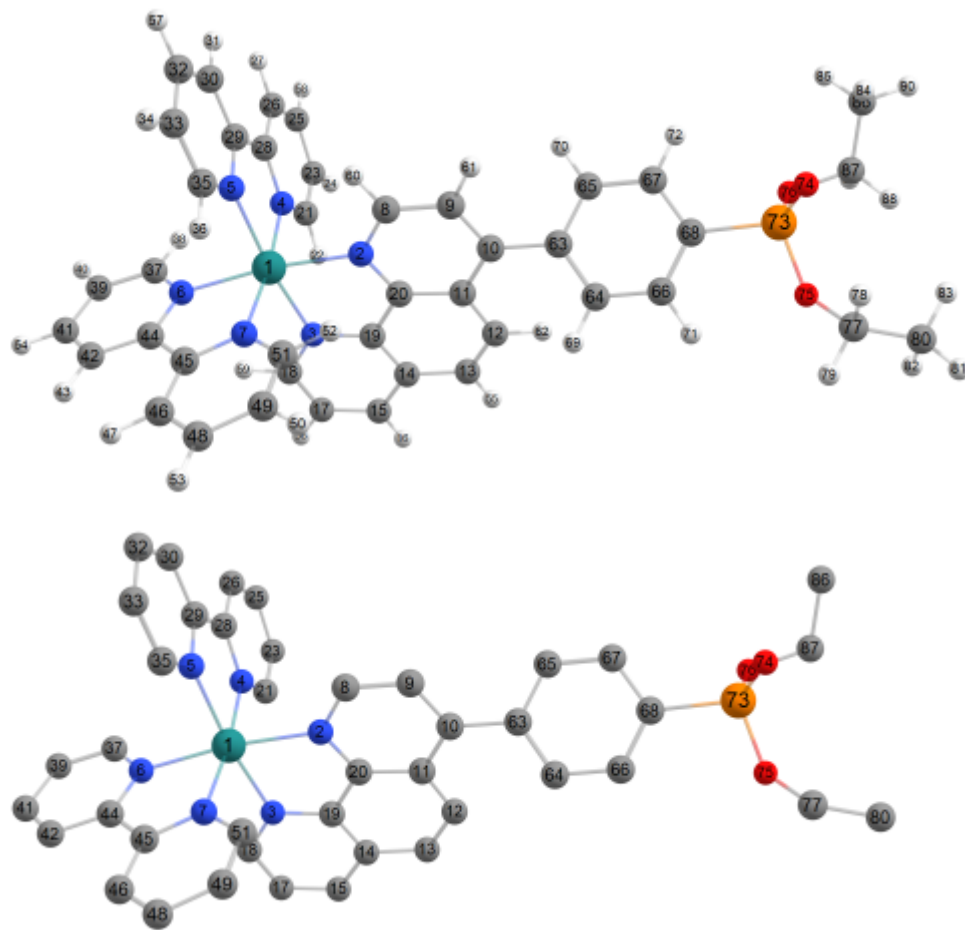


Figure S31. Optimized structure of the complex **Ru-4PPh**.

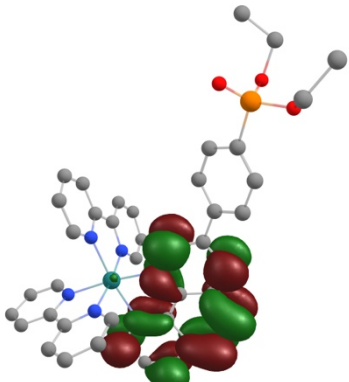
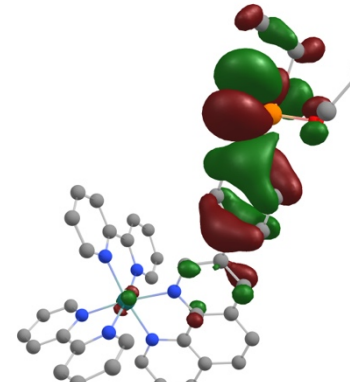
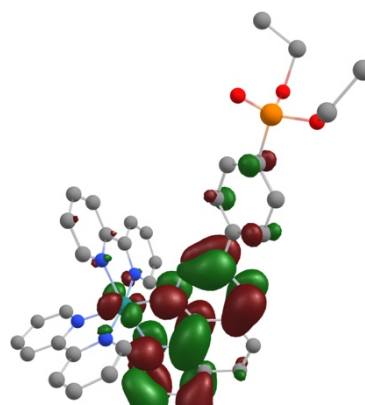
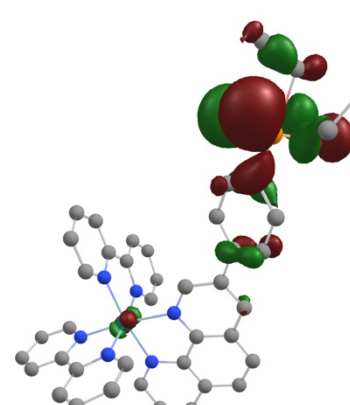
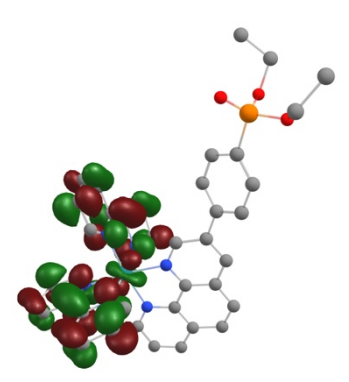
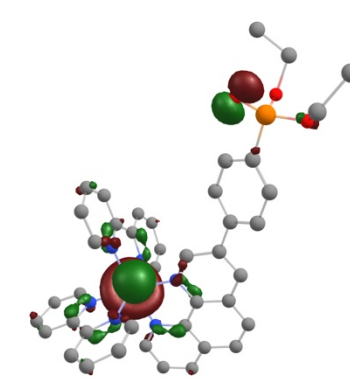
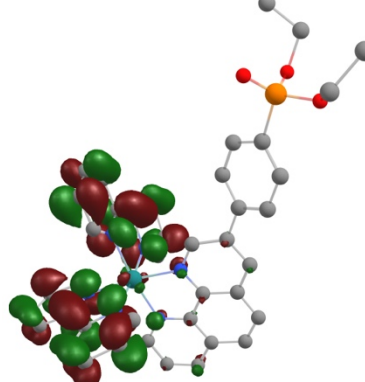
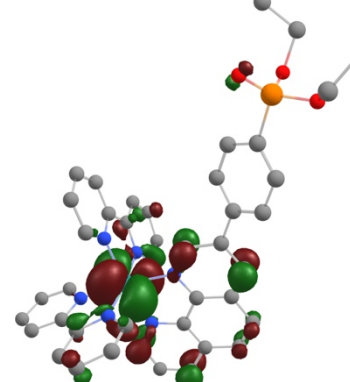
1	44	10.614529083	26.208703574	0.540285325
2	7	12.684769050	25.934990933	0.846052517
3	7	10.624798112	24.778892678	2.091927365
4	7	10.728597259	24.834085688	-1.046638158
5	7	10.796369848	27.476093665	-1.126215123
6	7	8.531300689	26.492731585	0.505090654
7	7	10.351595397	27.713433167	1.984644036
8	6	13.702650613	26.511274799	0.197058636
9	6	15.040628242	26.253249646	0.502420750
10	6	15.392888349	25.362861694	1.517291506
11	6	14.319766602	24.695262320	2.191189407
12	6	14.510931607	23.676573815	3.187803135
13	6	13.456241677	23.079410651	3.813715572

14	6	12.105997080	23.436167100	3.494423908
15	6	10.974701882	22.858371472	4.112921953
16	1	11.106758671	22.110769824	4.888933865
17	6	9.712191130	23.254620512	3.716289919
18	6	9.576548035	24.216207578	2.701800648
19	6	11.882685884	24.404788837	2.487619224
20	6	12.991013841	25.027957563	1.825124776
21	6	10.703166417	23.491534534	-0.925020601
22	1	10.581336263	23.109036241	0.080715104
23	6	10.820520200	22.632838700	-2.011427391
24	1	10.792097566	21.560535989	-1.854666669
25	6	10.975630432	23.179748307	-3.284404354
26	6	11.003971172	24.564193748	-3.420011942
27	1	11.126126435	25.005411016	-4.401264654
28	6	10.878019033	25.377280580	-2.289224484
29	6	10.891824724	26.852168060	-2.335986246
30	6	10.993933046	27.589326845	-3.519956520
31	1	11.064229377	27.084372221	-4.475148768
32	6	11.001430308	28.979804067	-3.472477946
33	6	10.904812647	29.609440035	-2.232381511
34	1	10.906324085	30.689924359	-2.143658994
35	6	10.802184702	28.823941362	-1.090454475
36	1	10.723819443	29.273082889	-0.108160058
37	6	7.663644816	25.842085322	-0.296126227
38	1	8.094630964	25.103237961	-0.960546634
39	6	6.295466309	26.085958525	-0.283124794
40	1	5.644026065	25.531763625	-0.949176134
41	6	5.794316807	27.046844414	0.594081466
42	6	6.681969304	27.725357778	1.423213851
43	1	6.309381760	28.476478080	2.108344309
44	6	8.048981486	27.436150853	1.365018417

45	6	9.063165270	28.105233278	2.202961070
46	6	8.759702612	29.080708841	3.157855788
47	1	7.733776434	29.383719989	3.324992650
48	6	9.781423647	29.665546662	3.899492162
49	6	11.095267998	29.259880823	3.669349764
50	1	11.924993594	29.686716366	4.221212790
51	6	11.335114213	28.284330433	2.708848719
52	1	12.339759378	27.940104504	2.496421225
53	1	9.554551519	30.422920920	4.642084378
54	1	4.732676215	27.265850317	0.632474999
55	1	13.627572551	22.310050150	4.559723943
56	1	8.821828758	22.834101235	4.169884053
57	1	11.079978939	29.558631089	-4.386391649
58	1	11.073192935	22.541983730	-4.156248314
59	1	8.596298333	24.535403113	2.367245680
60	1	13.440722558	27.222735273	-0.577884875
61	1	15.812910901	26.788906798	-0.037665602
62	1	15.522097200	23.374726059	3.429298915
63	6	16.819355959	25.152805997	1.846118331
64	6	17.283947302	25.220144187	3.171124228
65	6	17.749015510	24.938331786	0.811775432
66	6	18.640290567	25.073448195	3.451711419
67	6	19.100114140	24.781106171	1.097676846
68	6	19.559963945	24.849409285	2.421139977
69	1	16.591684154	25.426107588	3.981777037
70	1	17.406156113	24.865701725	-0.216113219
71	1	18.989222510	25.128709073	4.476690755
72	1	19.801405880	24.598197854	0.290559668
73	15	21.347320333	24.763256678	2.754809756
74	8	22.123336042	25.945013526	2.297209242
75	8	21.428570297	24.473161814	4.339990444

76	8	21.667308692	23.353158148	2.055302785
77	6	22.163344151	25.349147315	5.250082075
78	1	22.479608530	26.240855640	4.703974509
79	1	21.447703172	25.639231282	6.025468831
80	6	23.343435435	24.606646026	5.845798190
81	1	23.837660293	25.239726188	6.589639415
82	1	23.019456544	23.685797731	6.338181225
83	1	24.079754843	24.353477156	5.077576053
84	1	23.750402549	24.415119854	0.610306276
85	1	23.100965040	22.974999699	-0.209531745
86	6	23.681856022	23.325542917	0.648548382
87	6	23.043543353	22.872866585	1.948670406
88	1	23.614868739	23.213261244	2.818209415
89	1	22.960752903	21.785419126	2.005269235
90	1	24.690961029	22.908334436	0.570620098

Table S13. The electron-cloud distribution of the HOMO and LUMO calculated by DFT of the complex **Ru-3PPh**

Orbital	E(eV)	The electron-cloud distribution	Orbital	E(eV)	The electron-cloud distribution
LUMO+3	-6.91		HOMO	-10.44	
LUMO+2	-7.09		HOMO-1	-10.62	
LUMO+1	-7.22		HOMO-2	-10.78	
LUMO	-7.30		HOMO-3	-10.89	

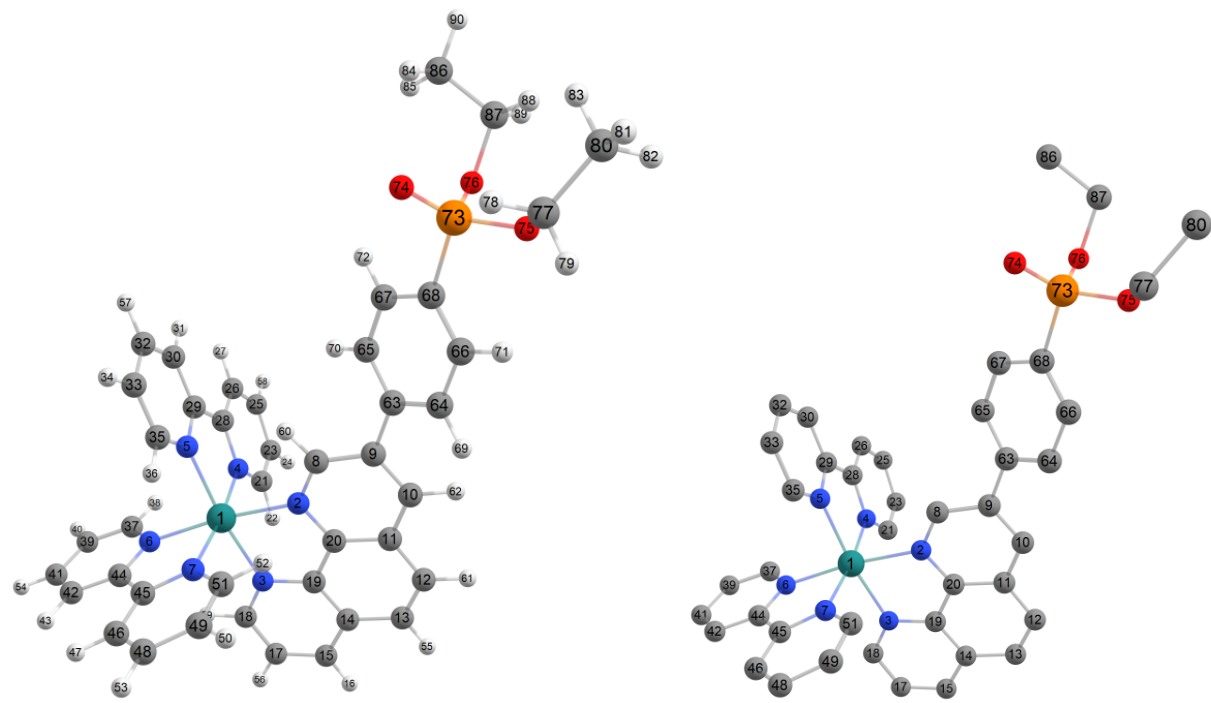


Figure S32. Optimized structure of the complex **Ru-3PPh**.

1	44	10.491884507	26.468217163	0.226464736
2	7	12.578876026	26.241705716	0.476944300
3	7	10.565993298	25.039802736	1.787011936
4	7	10.586201043	25.095571886	-1.364064480
5	7	10.625364633	27.737946622	-1.441548412
6	7	8.404326887	26.716195014	0.241434853
7	7	10.237674385	27.966221537	1.679226807
8	6	13.562098881	26.858119105	-0.180142176
9	6	14.939459936	26.639366218	0.071851942
10	6	15.268709087	25.722056169	1.066713614
11	6	14.256885163	25.051966718	1.782626865
12	6	14.518858486	24.091981893	2.820317698
13	6	13.499828820	23.481116350	3.489272127
14	6	12.127035209	23.771233238	3.179065264
15	6	11.030823990	23.176253509	3.840076172
16	1	11.204308147	22.454527408	4.632231067

17	6	9.745269990	23.524735515	3.467324506
18	6	9.551874553	24.459798243	2.438265564
19	6	11.842659802	24.705407420	2.153705164
20	6	12.912695356	25.342448031	1.452746904
21	6	10.562644655	23.752794076	-1.244172393
22	1	10.458518819	23.368981507	-0.236872540
23	6	10.660125354	22.895937857	-2.334076050
24	1	10.634711211	21.823344449	-2.179154159
25	6	10.791598716	23.445218824	-3.608658962
26	6	10.816043619	24.829898995	-3.742538468
27	1	10.916244027	25.272401228	-4.725694915
28	6	10.711415621	25.641150158	-2.608183596
29	6	10.720293718	27.116340715	-2.652544447
30	6	10.819202405	27.856264604	-3.835089261
31	1	10.892762552	27.353503055	-4.791231687
32	6	10.820821416	29.246829312	-3.784938379
33	6	10.719912118	29.873938856	-2.544009167
34	1	10.717191365	30.954234167	-2.453157322
35	6	10.622484353	29.085722913	-1.403487264
36	1	10.543847664	29.532552312	-0.420259871
37	6	7.529402055	26.054992368	-0.543020792
38	1	7.956142086	25.322222648	-1.216731008
39	6	6.158796341	26.281856707	-0.503395725
40	1	5.501603053	25.719936738	-1.157264394
41	6	5.662660559	27.236318442	0.383513210
42	6	6.557530527	27.924618408	1.196682357
43	1	6.188697808	28.671410864	1.888547906
44	6	7.926647866	27.652339609	1.112158379
45	6	8.948330884	28.334405108	1.930187532
46	6	8.651135601	29.298689070	2.898459058
47	1	7.624251770	29.581655353	3.092941122

48	6	9.680311175	29.897168844	3.618791850
49	6	10.995212770	29.516889910	3.353869697
50	1	11.831006888	29.955883021	3.886750894
51	6	11.228359175	28.550962363	2.382270529
52	1	12.233474997	28.226202684	2.143445080
53	1	9.458581189	30.646166919	4.371312019
54	1	4.599468663	27.443397362	0.440907578
55	1	13.711428029	22.761061851	4.273352382
56	1	8.881059520	23.089096791	3.955849048
57	1	10.898872416	29.828016363	-4.697397692
58	1	10.872915087	22.808876845	-4.483217337
59	1	8.553636502	24.746325687	2.127631336
60	1	13.259084973	27.582190422	-0.926874850
61	1	15.551332505	23.863211178	3.064840830
62	1	16.309805496	25.504494054	1.283657315
63	6	15.957007430	27.387219476	-0.697806784
64	6	17.128355586	27.848188277	-0.076162728
65	6	15.766506075	27.657251913	-2.065017102
66	6	18.077107178	28.568760416	-0.798347212
67	6	16.714697353	28.374788779	-2.783750378
68	6	17.878096119	28.843697514	-2.155802647
69	1	17.287961253	27.670205053	0.983221543
70	1	14.890270659	27.271454919	-2.578722843
71	1	18.978099168	28.920260594	-0.308303767
72	1	16.558987429	28.563059249	-3.840818544
73	15	19.036794341	29.879031011	-3.102236584
74	8	18.479305427	31.194003080	-3.515225794
75	8	20.352221241	29.960804804	-2.173537029
76	8	19.415287020	28.833399316	-4.261523400
77	6	20.896049872	31.237870708	-1.713960801
78	1	20.181693688	32.030922033	-1.947119186

79	1	20.987363918	31.145136798	-0.627866132
80	6	22.244747579	31.491682456	-2.358561747
81	1	22.687140336	32.401178677	-1.939619549
82	1	22.930281864	30.660358271	-2.173973764
83	1	22.145841469	31.633882697	-3.438723855
84	1	19.243800874	30.859820799	-6.135315525
85	1	18.841435618	29.290296835	-6.866713357
86	6	19.654314648	29.903602032	-6.467366648
87	6	20.351575780	29.186049873	-5.325187397
88	1	21.163694942	29.785896898	-4.902110056
89	1	20.771517383	28.230041007	-5.645057030
90	1	20.369961669	30.088412924	-7.274956832

Table S14. The electron-cloud distribution of the HOMO and LUMO calculated by DFT of the complex **Ru-4,7(PPh)₂**

Orbital	E(eV)	The electron-cloud distribution	Orbital	E(eV)	The electron-cloud distribution
LUMO+3	-6.67		HOMO	-10.20	
LUMO+2	-6.81		HOMO-1	-10.27	
LUMO+1	-7.05		HOMO-2	-10.39	
LUMO	-7.14		HOMO-3	-10.41	

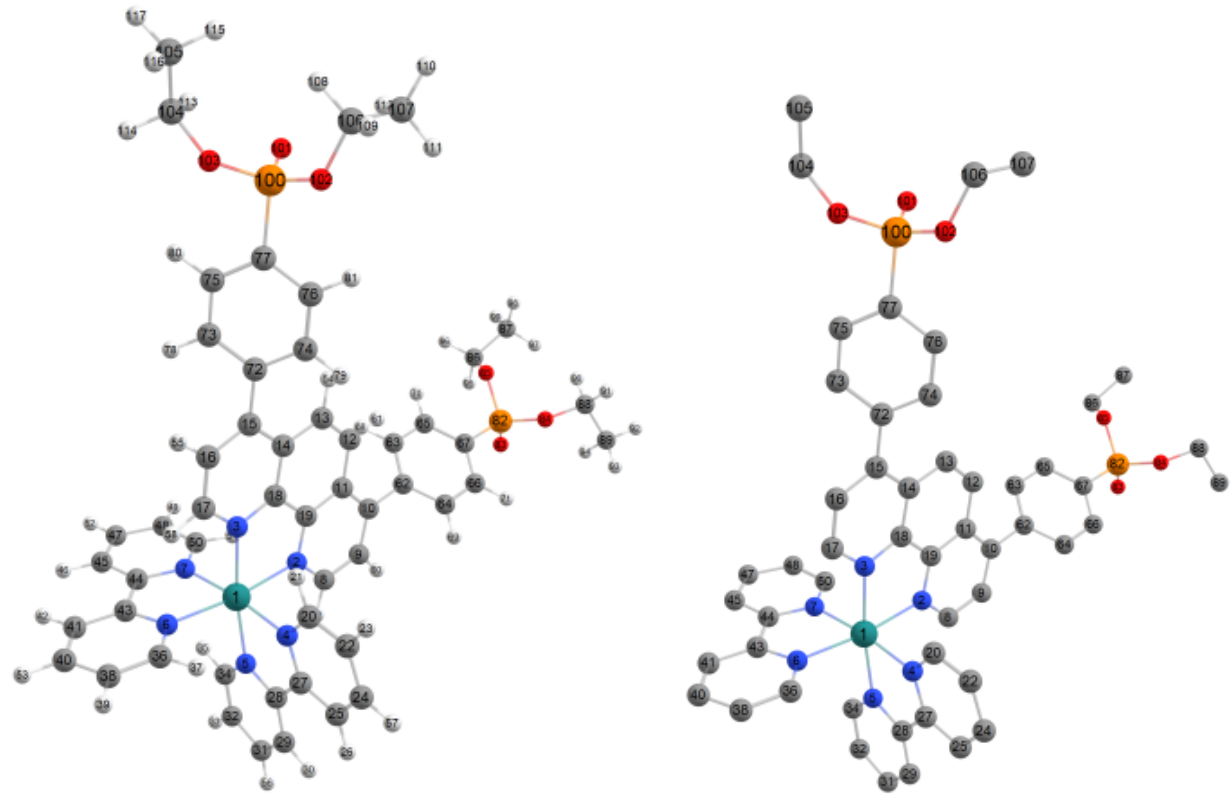


Figure S33. Optimized structure of the complex **Ru-4,7(PPh)₂**.

1	44	10.231479450	26.227411225	0.418182725
2	7	12.310797962	26.010226581	0.682495001
3	7	10.323274896	24.839837559	2.000672534
4	7	10.321647320	24.821565651	-1.140882224
5	7	10.337956454	27.460552069	-1.281234392
6	7	8.141085505	26.468700248	0.438675647
7	7	9.977841892	27.754485292	1.840968631
8	6	13.292572040	26.597679940	-0.009384835
9	6	14.645516674	26.409947888	0.282752418
10	6	15.049159747	25.589777276	1.335423780
11	6	14.015546326	24.912713947	2.059641235
12	6	14.259619527	23.979458183	3.121090551
13	6	13.239352000	23.354586263	3.777436366
14	6	11.866292958	23.581610965	3.429340068
15	6	10.759330844	22.946752745	4.080156615

16	6	9.483591383	23.339765862	3.678147376
17	6	9.304254106	24.271517536	2.653367680
18	6	11.594214680	24.510775998	2.394413028
19	6	12.668078196	25.158437652	1.695240269
20	6	10.323953198	23.481986833	-0.987857340
21	1	10.249960079	23.122994347	0.031116424
22	6	10.411603603	22.600650479	-2.058914306
23	1	10.407526855	21.531899642	-1.877309568
24	6	10.505370647	23.120399195	-3.349269011
25	6	10.506100818	24.501537104	-3.516944911
26	1	10.581191877	24.922059639	-4.511890200
27	6	10.412996292	25.338326893	-2.400299538
28	6	10.402874067	26.811812829	-2.479913220
29	6	10.457602964	27.524206958	-3.682192444
30	1	10.506235653	26.999690080	-4.628116829
31	6	10.447761275	28.915253025	-3.664691251
32	6	10.383136596	29.570447078	-2.435793416
33	1	10.373514895	30.652481025	-2.370135483
34	6	10.328179054	28.808858820	-1.274656795
35	1	10.278104298	29.278145599	-0.299856867
36	6	7.261757725	25.776429888	-0.313719337
37	1	7.686502562	25.027448666	-0.970725620
38	6	5.889507597	25.990260419	-0.261218748
39	1	5.229020431	25.401242547	-0.887392282
40	6	5.395946453	26.967182974	0.602479003
41	6	6.295004502	27.688204742	1.381615525
42	1	5.928876136	28.452003851	2.056180297
43	6	7.665347384	27.424547020	1.288383928
44	6	8.688927144	28.130310582	2.083155798
45	6	8.392191966	29.118226303	3.027567991
46	1	7.365797461	29.408721215	3.213166871

47	6	9.420828368	29.729193728	3.737607695
48	6	10.734886098	29.337555460	3.485751992
49	1	11.570056843	29.782396346	4.014738384
50	6	10.968048706	28.351238223	2.534753118
51	1	11.972745810	28.017498073	2.307230597
52	1	9.199116512	30.494142335	4.473962744
53	1	4.331657966	27.165560610	0.668789659
54	1	13.463742491	22.671830685	4.586839061
55	1	8.609079415	22.890557226	4.134845435
56	1	10.489127458	29.475108161	-4.592705045
57	1	10.576540719	22.464294120	-4.210055253
58	1	8.308110013	24.550790202	2.329842196
59	1	12.988055840	27.261611797	-0.810227801
60	1	15.385580452	26.947345957	-0.299154242
61	1	15.283919633	23.767871185	3.399860428
62	6	16.490281344	25.454141964	1.645668317
63	6	16.984763956	25.633777601	2.948953205
64	6	17.401420310	25.197615441	0.605056229
65	6	18.352736305	25.556444696	3.201637803
66	6	18.764349964	25.109482034	0.863496435
67	6	19.254642767	25.290776101	2.165098968
68	1	16.305826435	25.870920470	3.762359581
69	1	17.035247141	25.039602399	-0.405012134
70	1	18.723919226	25.699125325	4.210245988
71	1	19.451150635	24.892408871	0.052470509
72	6	10.913993043	21.920900861	5.135211331
73	6	10.162433068	22.021395232	6.318803643
74	6	11.757585047	20.808582799	4.961915759
75	6	10.272995736	21.052327878	7.310744141
76	6	11.859764825	19.837728931	5.953657282
77	6	11.125515156	19.953755226	7.141835440

78	1	9.511362805	22.876487583	6.474341658
79	1	12.307343990	20.681744648	4.034393107
80	1	9.689164376	21.146830384	8.219834582
81	1	12.498038001	18.974757380	5.801818887
82	15	21.051985052	25.294979558	2.450968330
83	8	21.762573332	26.488767195	1.922981183
84	8	21.409382345	23.868201665	1.802727628
85	8	21.193940788	25.079816278	4.044559707
86	6	21.942512986	26.015643651	4.880760521
87	6	23.242349155	25.387494388	5.344917691
88	6	22.786756789	23.386603564	1.747103403
89	6	23.511505564	23.899575649	0.515390994
90	1	23.302037945	23.671890829	2.669779847
91	1	22.694205283	22.298316257	1.737730919
92	1	24.522512160	23.480062464	0.485570789
93	1	22.989597300	23.593355153	-0.395638533
94	1	23.584027349	24.989355207	0.530881488
95	1	22.120588331	26.932682245	4.314279144
96	1	21.286455666	26.237201355	5.727306504
97	1	23.918252523	25.212576500	4.502749329
98	1	23.059615956	24.437551592	5.854536851
99	1	23.746720369	26.062410994	6.043936779
100	15	11.370910984	18.777413584	8.507711997
101	8	12.423395580	19.152857750	9.488333064
102	8	11.611332078	17.435525806	7.654678038
103	8	9.891436842	18.639850821	9.135592974
104	6	9.631680748	18.799377526	10.563592509
105	6	9.273052481	17.465558913	11.190071165
106	6	12.054276094	16.204680200	8.303322189
107	6	13.568079937	16.141744706	8.395446369
108	1	11.588175506	16.126998597	9.290685545

109	1	11.650406306	15.405375762	7.678020224
110	1	13.869576972	15.183651404	8.831204658
111	1	14.019256928	16.220764860	7.401910721
112	1	13.949658088	16.949078960	9.024387050
113	1	10.510391001	19.245194694	11.035855985
114	1	8.795579935	19.501710919	10.629305603
115	1	10.124527084	16.778719844	11.178270655
116	1	8.437332993	16.997166499	10.663305711
117	1	8.981073945	17.618151188	12.234092179

8. Oxidation of sulfides

Table S15. Redox potentials relevant to photoredox catalysis of **Ru-cat** and referenced compounds **Ru(bpy)₃** and **Ru(phen)₃**, **Ru-phen** (vs Ag⁺/Ag)^a

Compound	$E_{1/2}(\text{PC}^+/\text{PC})$, (V)	$E_{1c}(\text{PC}/\text{PC}^-)$, (V)	E_{00} , (eV)	$E_{1/2}(\text{PC}^+/*\text{PC})$, (V) ^b	$E_{1/2}(*\text{PC}/\text{PC}^-)$, (V) ^c
Ru(bpy)₃^b	0.97 0.99 ^d	-1.64 -1.64 ^d	2.036 2.11 ^d	-1.07 -1.08 ^d	0.40 0.47 ^d
Ru(phen)₃	0.96 ^d	-1.06 ^d	2.02 ^d	-1.17 ^d	0.52 ^d
Ru-phen	0.975 0.977 ^e	-1.645 -1.683 ^e	2.049 2.016 ^e	-1.074 -1.039	0.404 0.333
Ru-3P	1.03	-1.45	1.934	-0.904	0.484
Ru-4P	1.025	-1.415	1.925	-0.90	0.51
Ru-5P	1.005	-1.55	2.056	-1.051	0.506
Ru-3,8P₂	1.08	-1.23	1.779	-0.699	0.549
Ru-4,7P₂	1.08	-1.335	1.905	-0.825	0.57
Ru-3PPh	0.995	-1.525	2.019	-1.024	0.494
Ru-5PPh	0.985	-1.60	2.046	-1.061	0.446
Ru-4,7(PPh)₂	0.98	-1.55	1.990	-0.92	0.44

^a In MeCN containing 0.1 M TBAPF₆. ^b Calculated value ($E_{1/2}(\text{PC}^+/*\text{PC}) = E_{1/2}(\text{PC}^+/\text{PC}) - E_{00}$ where E_{00} is the one-electron potential corresponding to the zero-zero spectroscopic energy of the excited state.^{15, 16} An approximative value of E_{00} corresponding to the emission maximum was used as low temperature luminescence spectra were not recorded in this work. ^c Calculated value ($E_{1/2}(*\text{PC}/\text{PC}^-) = E_{1/2}(\text{PC}/\text{PC}^-) + E_{00}$ where E_{00} is the one-electron potential corresponding to the zero-zero spectroscopic energy of the excited state).^{15, 16} An approximative value of E_{00} corresponding to the emission maximum was used as low temperature luminescence spectra were not recorded in this work. ^d Reported values.¹⁷ E_{00} was calculated from reported $E_{1/2}$. The potentials given versus SCE were converted using the conversion constant given in the ref.¹⁸ ^e Reported values.¹⁹ E_{00} was calculated from the reported emission maximum. The potentials given versus Fc^{+/Fc} were converted using the conversion constant given in the ref.¹⁸

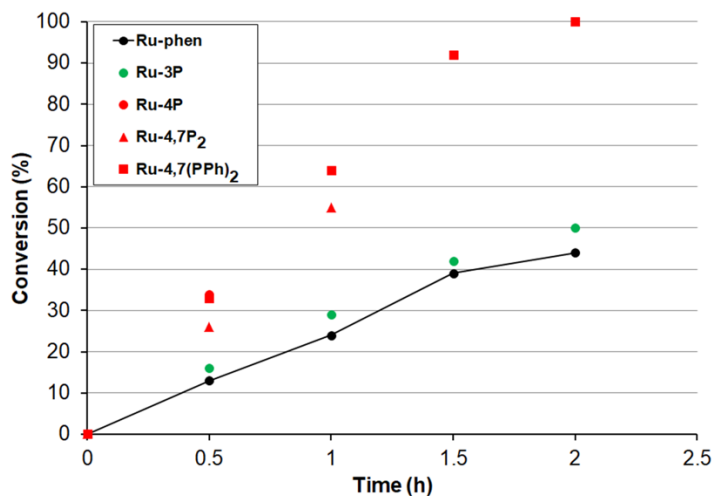


Figure S34. Photooxidation of benzyl methyl sulfide by molecular oxygen in the presence of 0.05 mol% **Ru-Pcat** and referenced photocatalysts **Ru-(bpy)₃** and **Ru-phen** in MeCN/H₂O (10:1 v/v) under irradiation of blue LED.

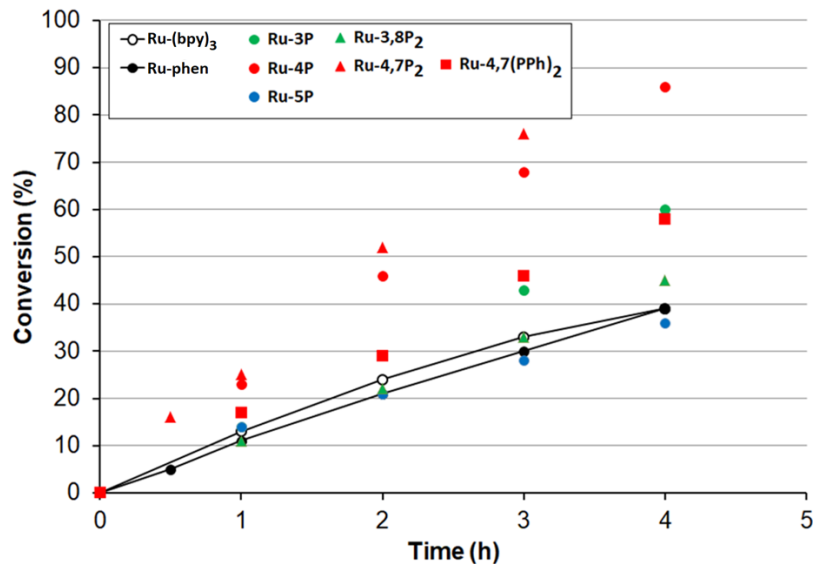


Figure S35. Photooxidation of 4-chlorothioanisol by molecular oxygen in the presence of 0.05 mol% **Ru-Pcat** and referenced photocatalysts **Ru-(bpy)₃** and **Ru-phen** in MeCN/H₂O (10:1 v/v) under irradiation of blue LED.

Methyl phenyl sulfoxide,²⁰ methyl 4-methylphenyl sulfoxide, ²⁰4-methoxyphenyl methyl sulfoxide,²⁰} 4-chlorophenyl methyl sulfoxide,²⁰ methyl 4-nitrophenyl sulfoxide,²¹ benzyl methyl sulfoxide,²⁰ thian-4-one S-oxide,²² dibutyl sulfoxide²⁰ are known compounds and their spectral data were consistent with those in the literature.

Methyl phenyl sulfoxide. ¹H NMR (CDCl₃, 400 MHz): 2.70 (s, 3 H, CH₃), 7.50–7.59 (m, 3 H, Ar), 7.64–7.71 (m, 3 H, Ar).

Methyl 4-methylphenyl sulfoxide. ¹H NMR (CDCl₃, 300 MHz): 2.38 (s, 3H, CH₃), 2.72 (s, 3H, OCH₃), 7.26–7.33 (m, 2H, Ar), 7.50–7.58 (m, 2H, Ar).

4-Methoxyphenyl methyl sulfoxide. ¹H NMR (CDCl₃, 300 MHz): 2.71 (s, 3H, CH₃), 3.82 (s, 3H, OCH₃), 7.04–7.09 (m, 2H, Ar), 7.59–7.66 (m, 2H, Ar).

4-Chlorophenyl methyl sulfoxide. ¹H NMR (CDCl₃, 300 MHz): 2.71 (s, 3H, CH₃), 7.49–7.55 (m, 2H, Ar), 7.57–7.63 (m, 2H, Ar).

Methyl 4-nitrophenyl sulfoxide. ¹H NMR (CDCl₃, 300 MHz): 2.81 (s, 3H, CH₃), 7.82–7.90 (m, 2H, Ar), 8.38–8.44 (m, 2H, Ar).

Dibutyl sulfoxide. 0.96 (t, *J* = 7.3 Hz, 3H, CH₃), 1.35–1.61 (m, 2H, CH₂), 1.65–1.82 (m, 2H, CH₂), 2.60–2.78 (m, 2H, CH₂).

Benzyl methyl sulfoxide. ¹H NMR (CDCl₃, 300 MHz): 2.46 (s, 3H, CH₃), 3.93 and 4.02 (AB-system, *J* = 14 Hz, 2H, CH₂), 7.29–7.41 (m, 5H, Ar).

Thian-4-one S-oxide. ¹H NMR (CDCl₃, 300 MHz): 2.43–2.57 (m, 2H, CH₂), 2.78–2.95 (m, 2H, CH₂), 3.19–3.38 (m, 4H, 2CH₂).

9. NMR-spectra

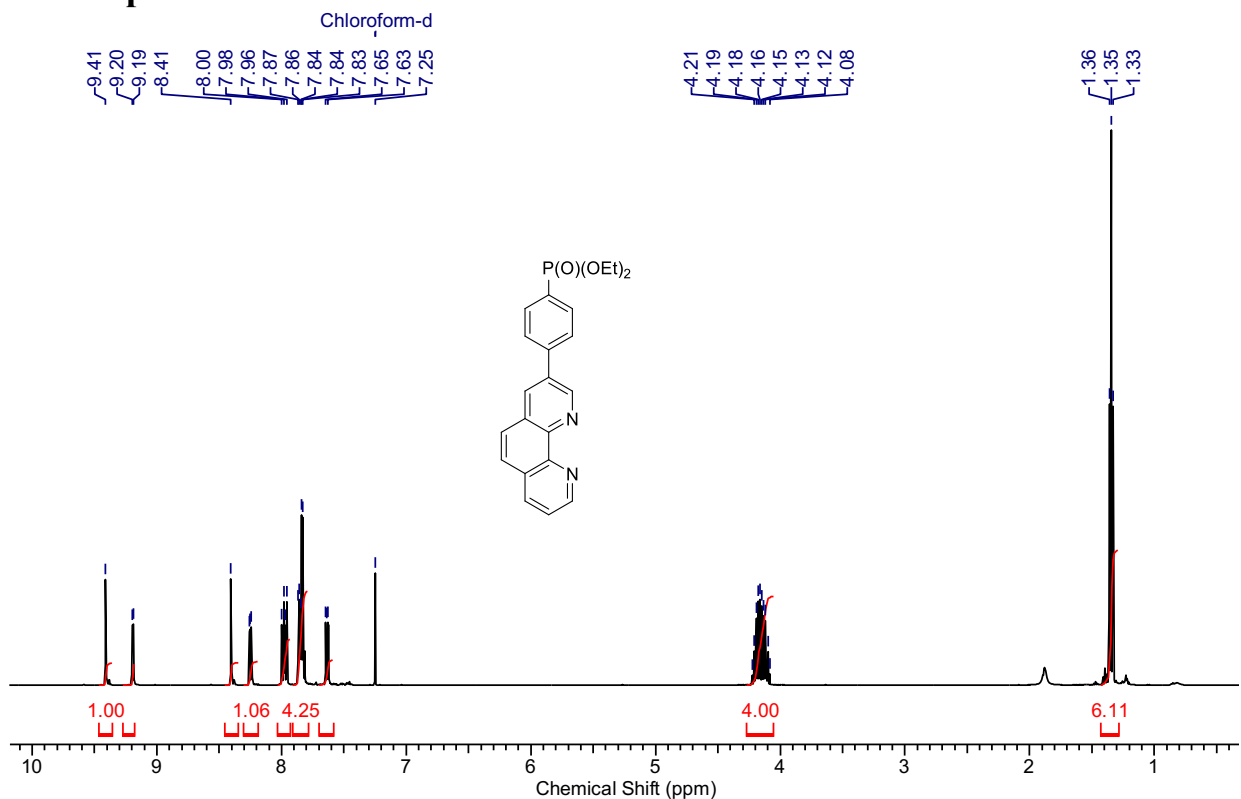


Figure S36. ^1H NMR spectrum of **3PPh** (CDCl_3 , 400 MHz, 300 K).

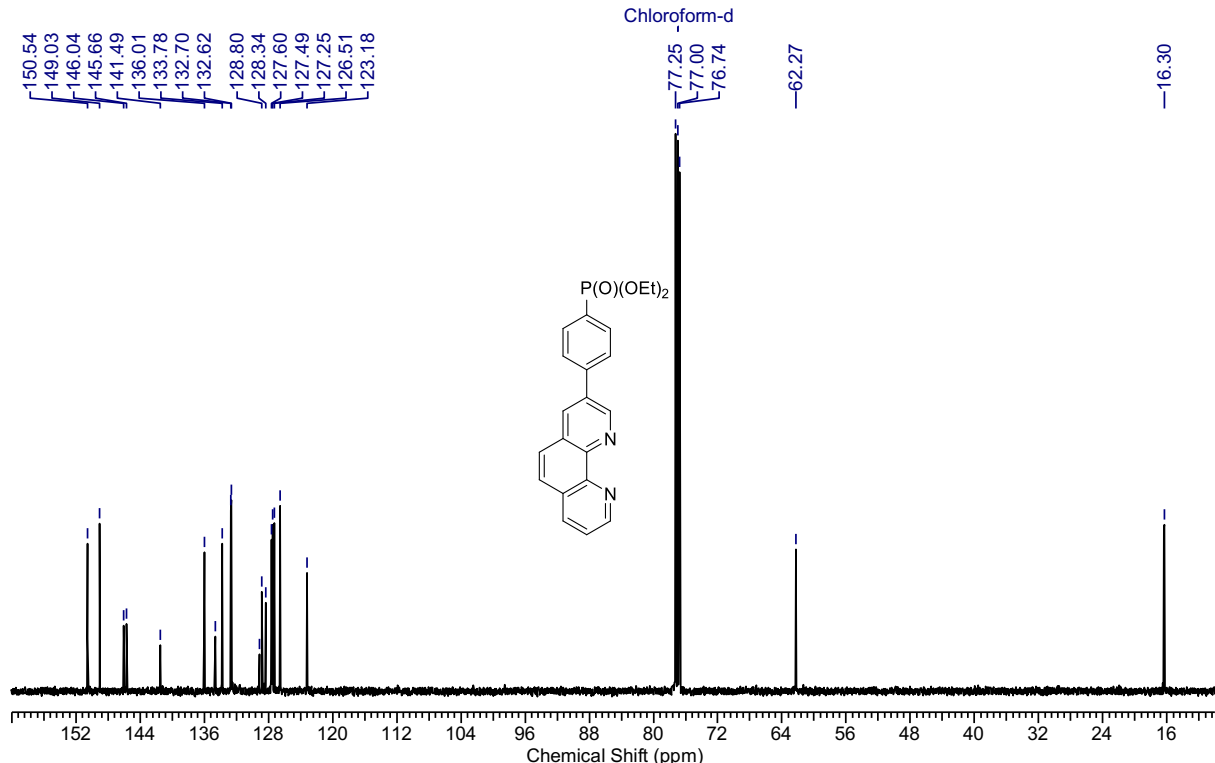


Figure S37. ^{13}C NMR spectrum of **3PPh** (CDCl_3 , 100.6 MHz, 300 K).

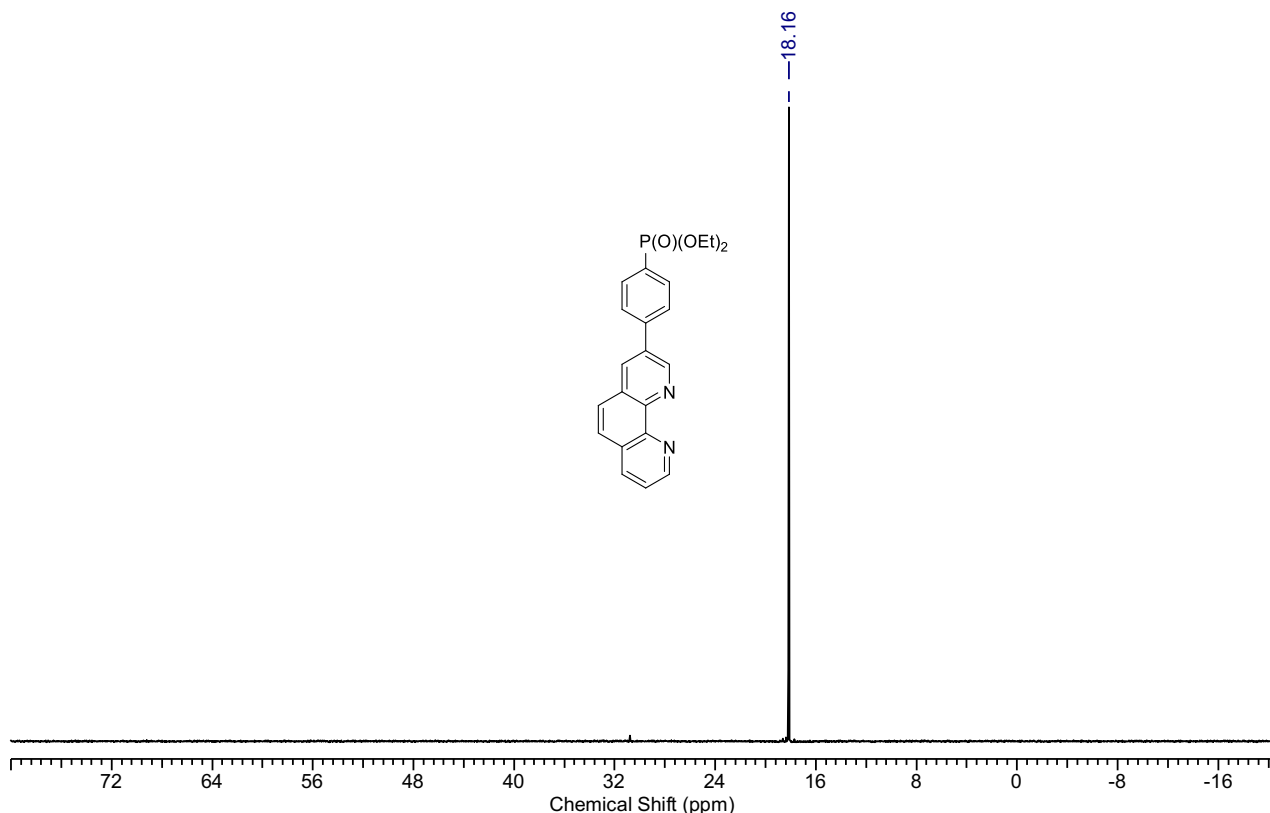


Figure S38. ^{31}P NMR spectrum of **3PPh** (CDCl_3 , 162.5 MHz, 300 K).

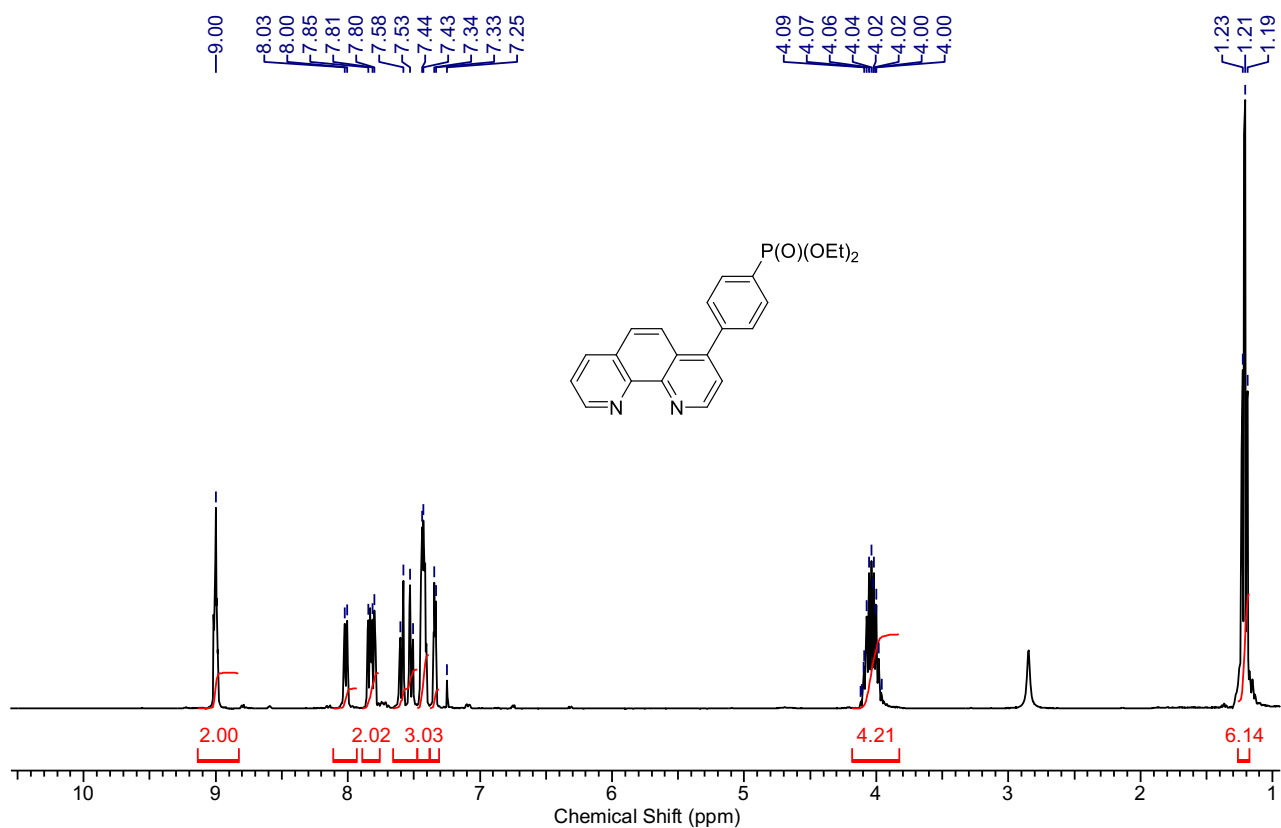


Figure S39. ^1H NMR spectrum of **4PPh** (CDCl_3 , 400 MHz, 300 K).

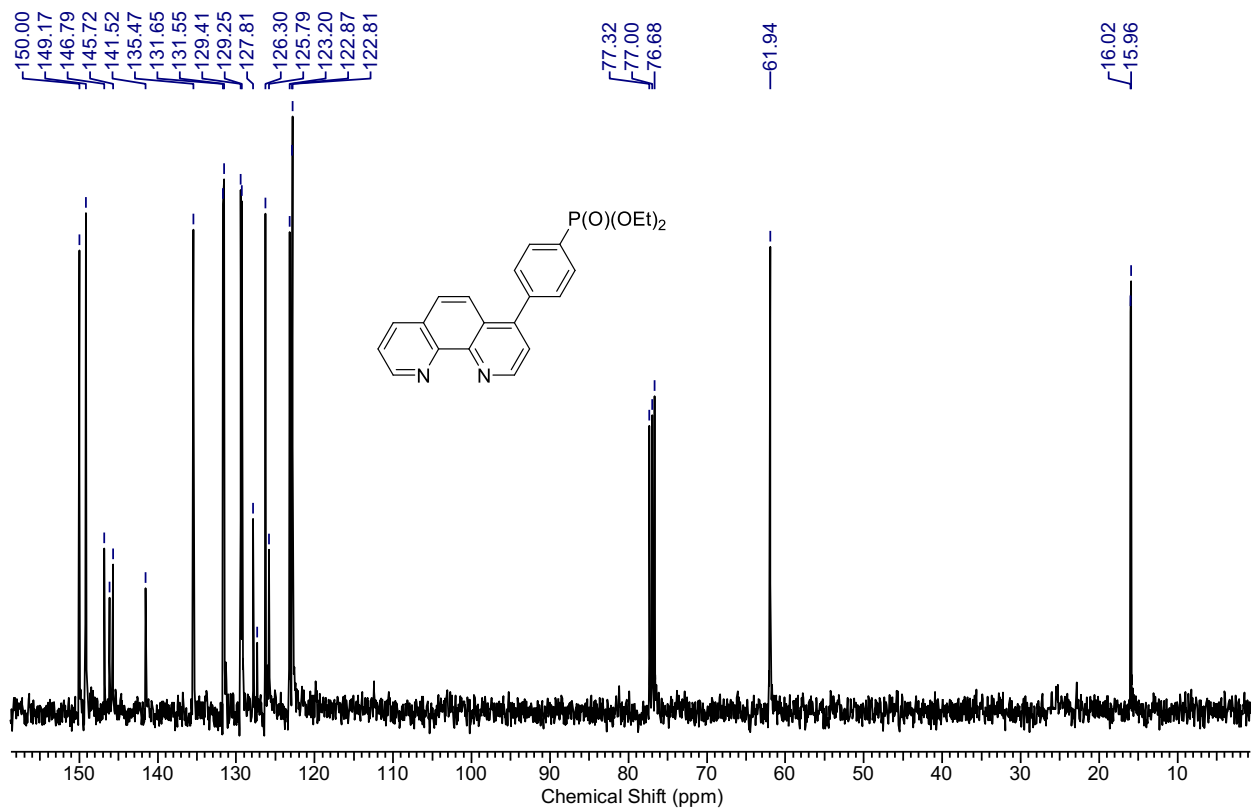


Figure S40. ^{13}C NMR spectrum of **4PPh** (CDCl_3 , 100.6 MHz, 300 K).

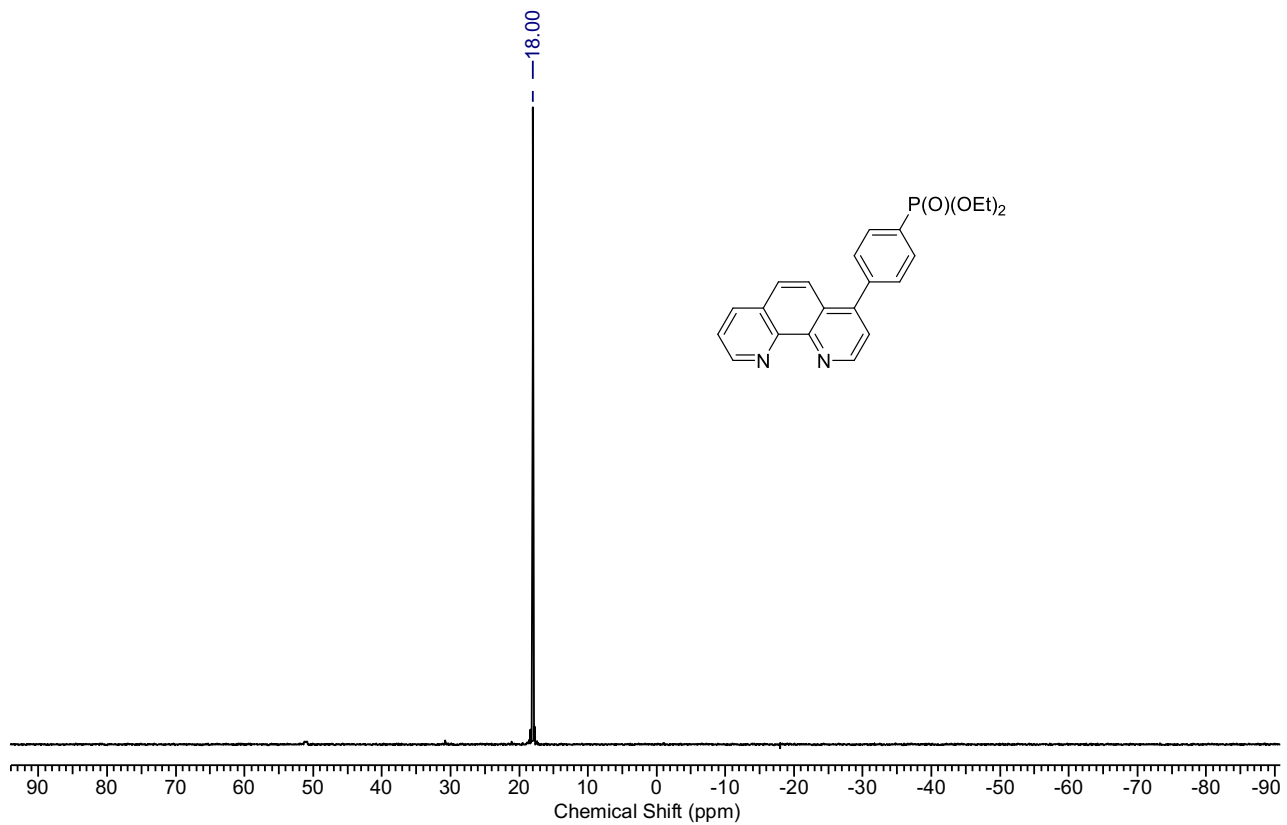


Figure S41. ^{31}P NMR spectrum of **4PPh** (CDCl_3 , 162.5 MHz, 300 K).

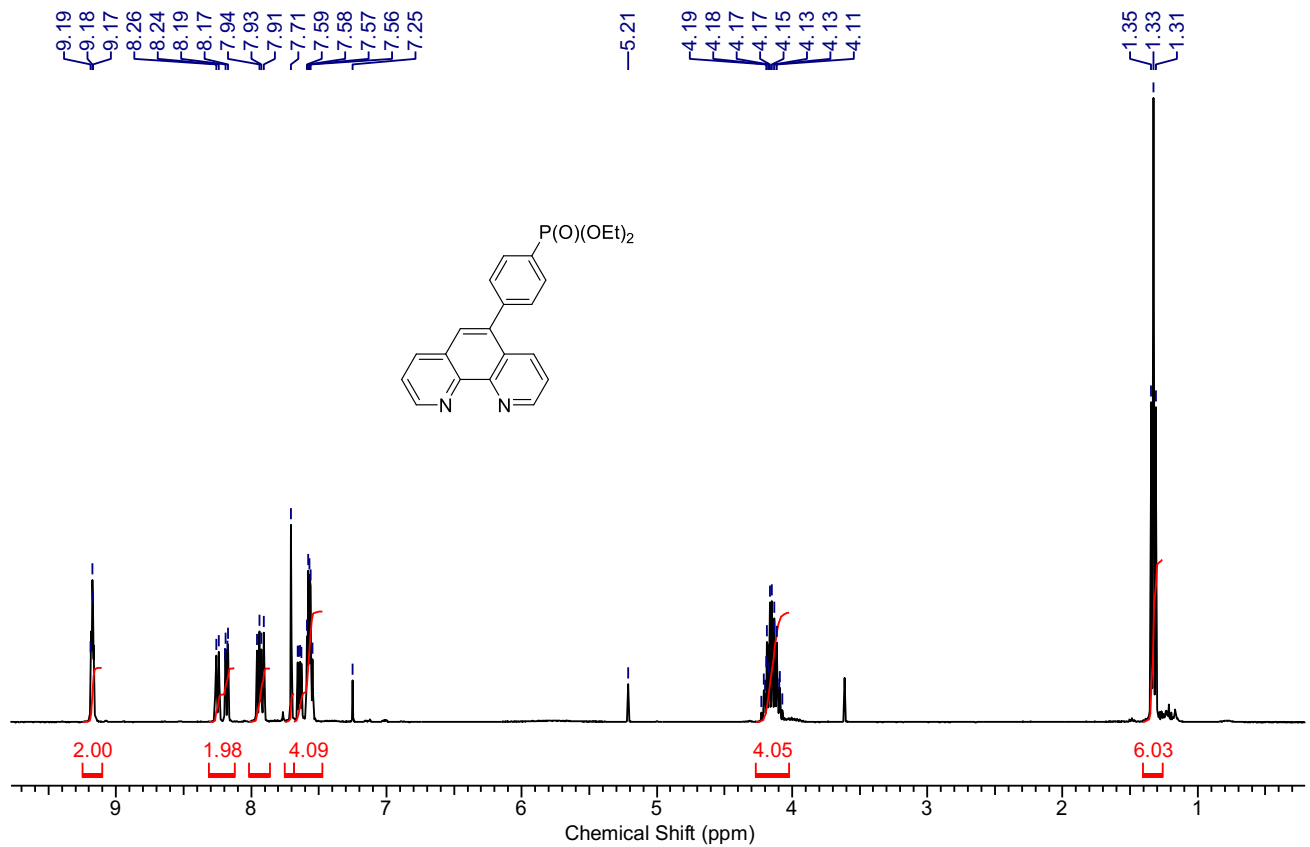


Figure S42. ^1H NMR spectrum of **5PPh** (CDCl_3 , 400 MHz, 300 K).

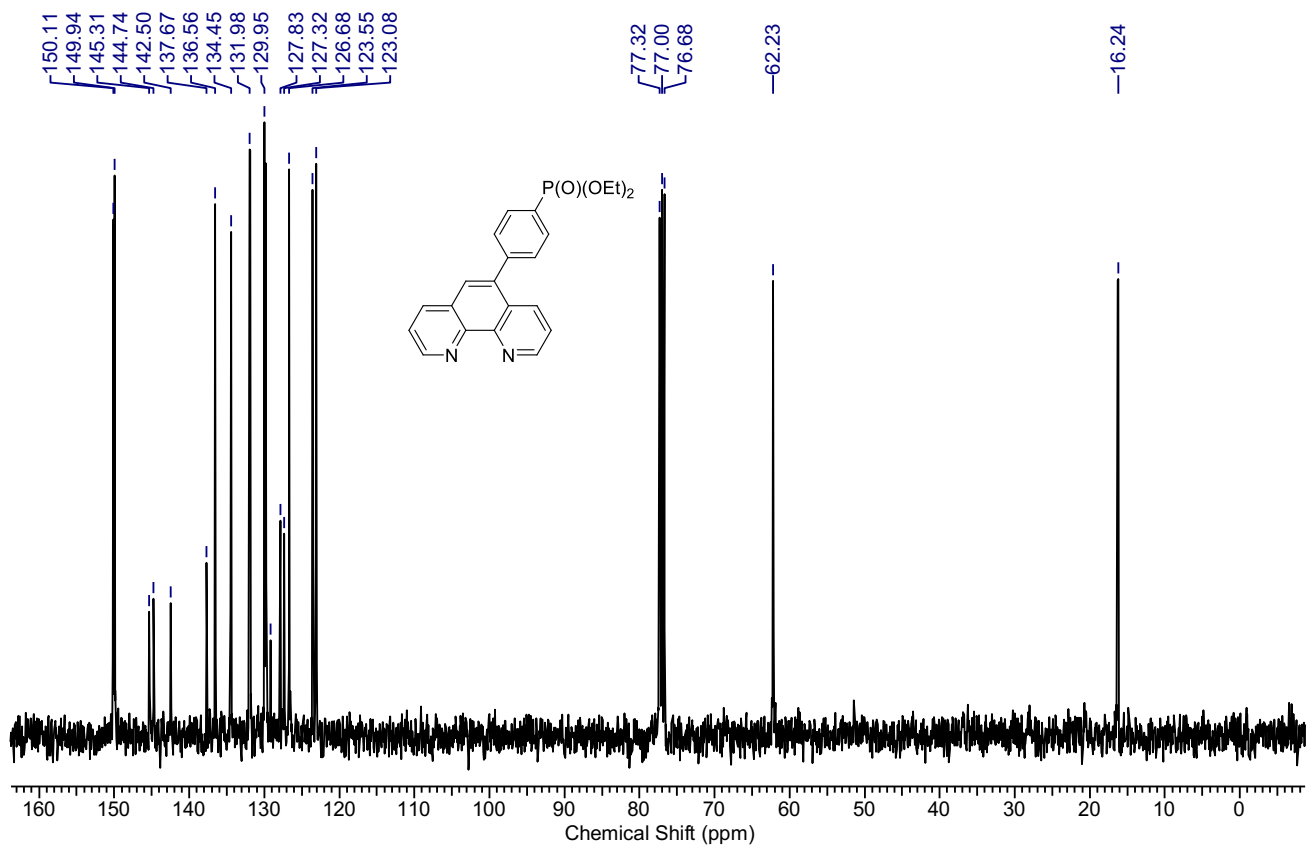


Figure S43. ^{13}C NMR spectrum of **5PPh** (CDCl_3 , 100.6 MHz, 300 K).

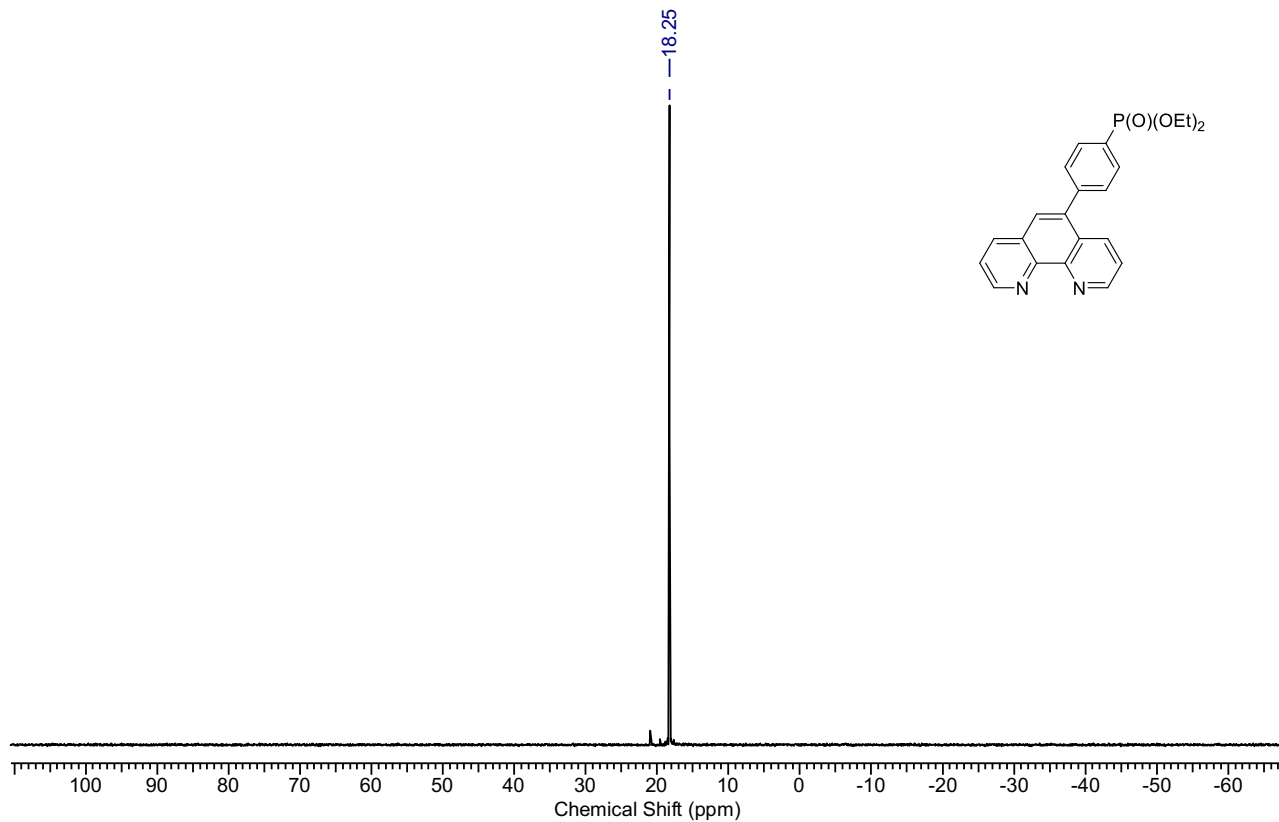


Figure S44. ^{31}P NMR spectrum of **5PPh** (CDCl_3 , 162.5 MHz, 300 K).

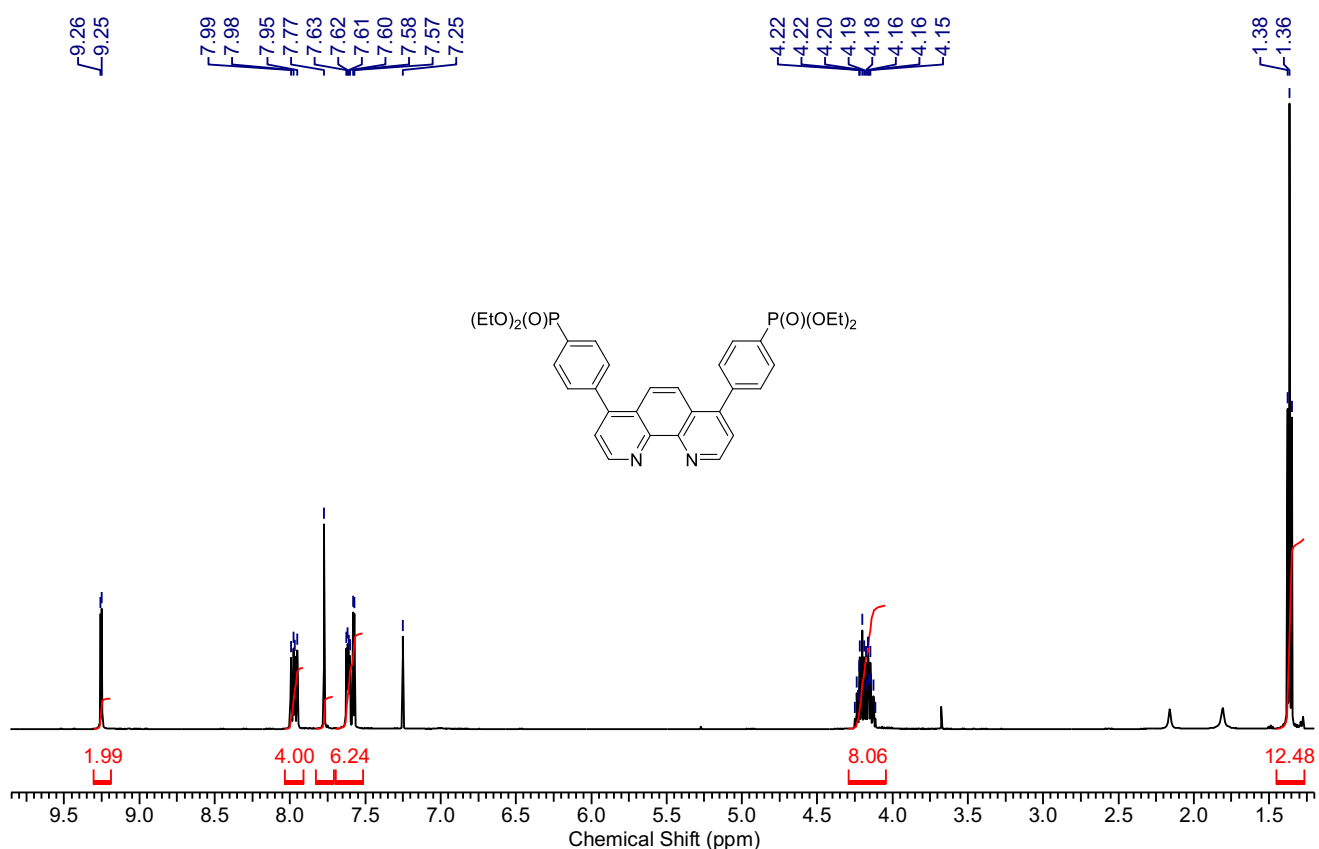


Figure S45. ^1H NMR spectrum of **4,7(PPh)₂** (CDCl_3 , 400 MHz, 300 K).

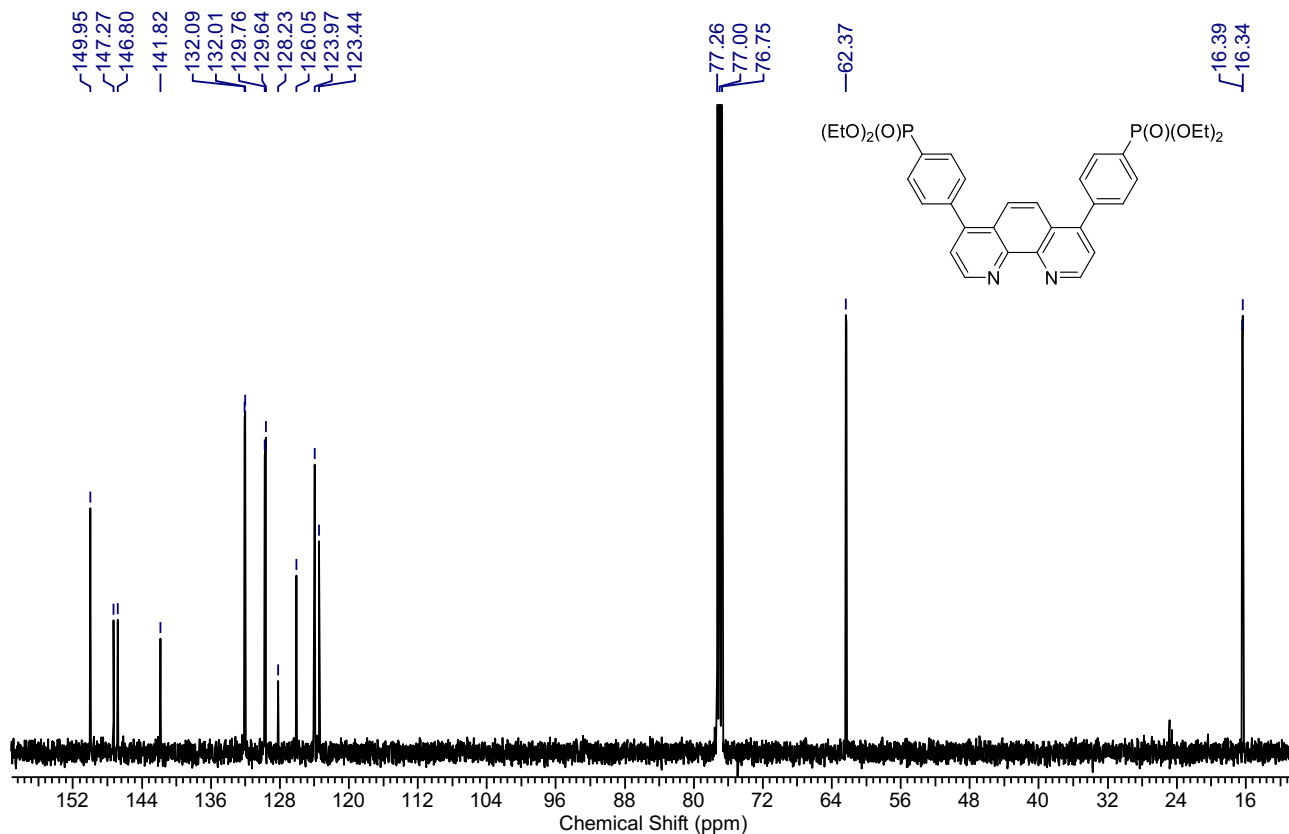


Figure S46. ^{13}C NMR spectrum of **4,7(PPh)₂** (CDCl_3 , 100.6 MHz, 300 K).

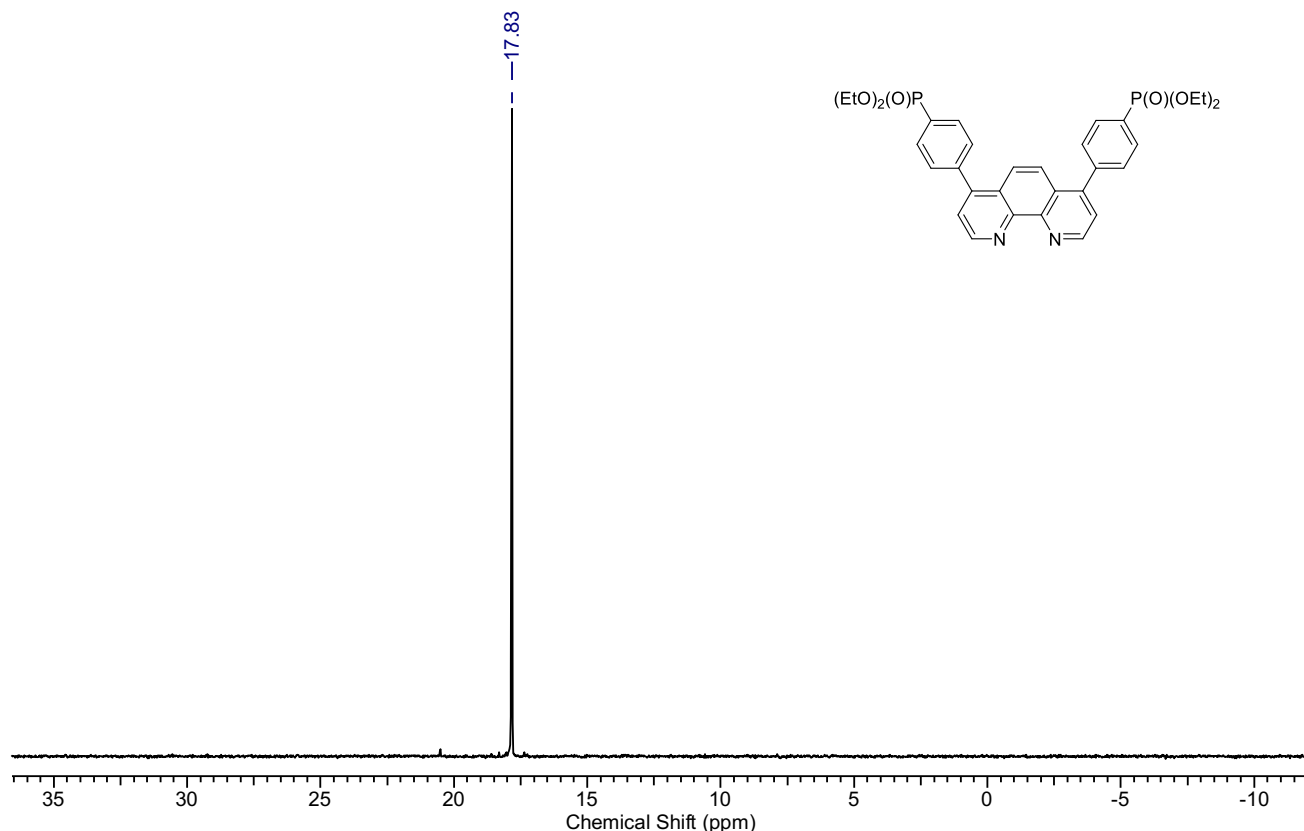


Figure S47. ^{31}P NMR spectrum of **4,7(PPh)₂** (CDCl_3 , 162.5 MHz, 300 K).

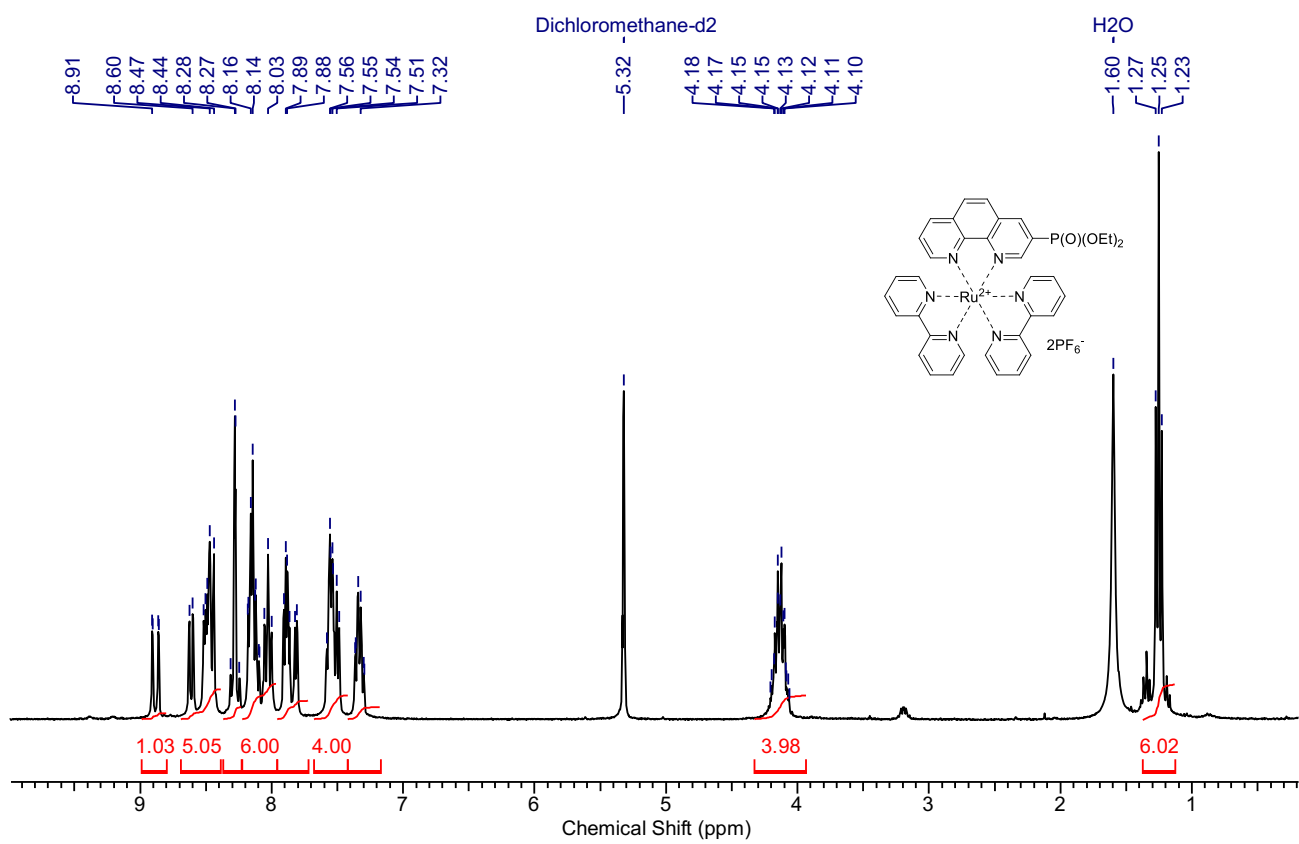


Figure S48. ¹H NMR spectrum of Ru-3P (CD₂Cl₂, 400 MHz, 300 K).

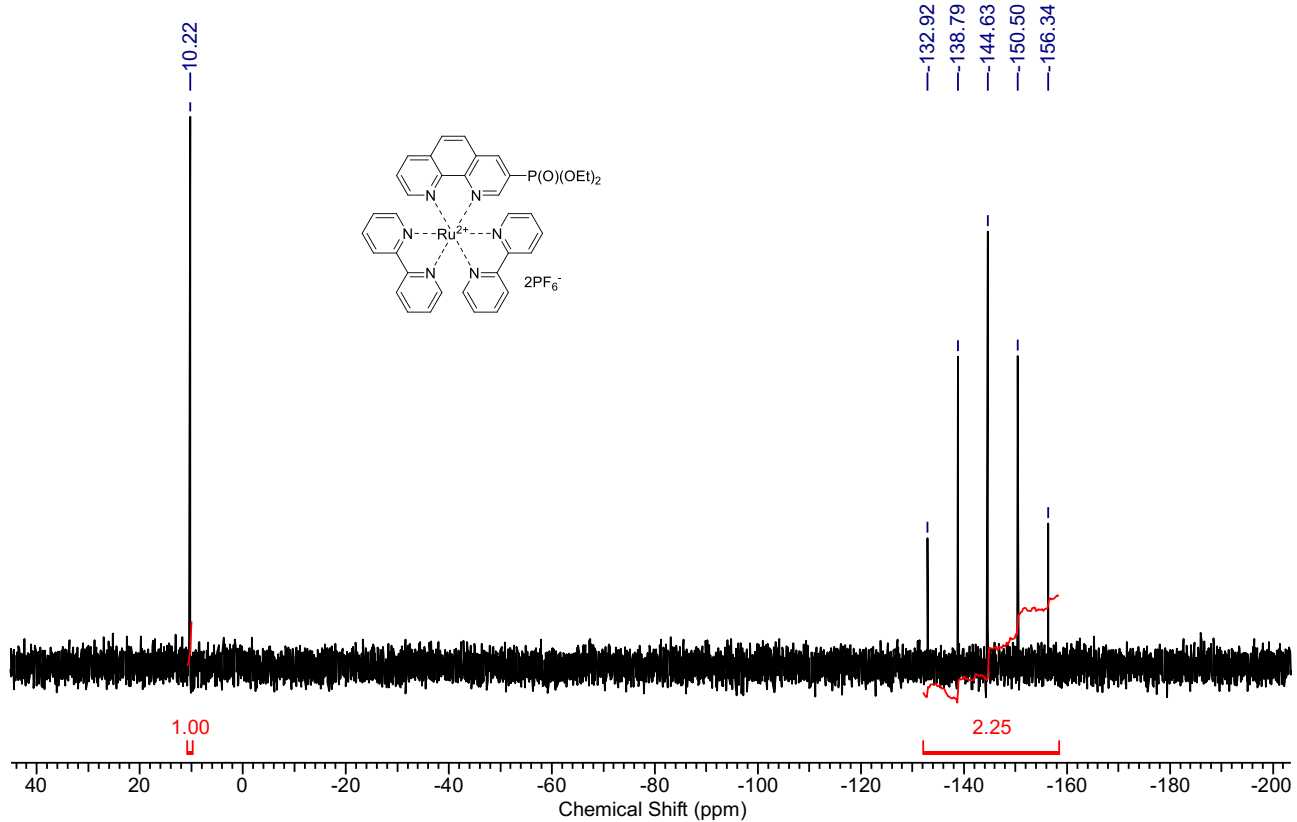


Figure S49. ³¹P NMR spectrum of Ru-3P (CD₂Cl₂, 162.5 MHz, 300 K).

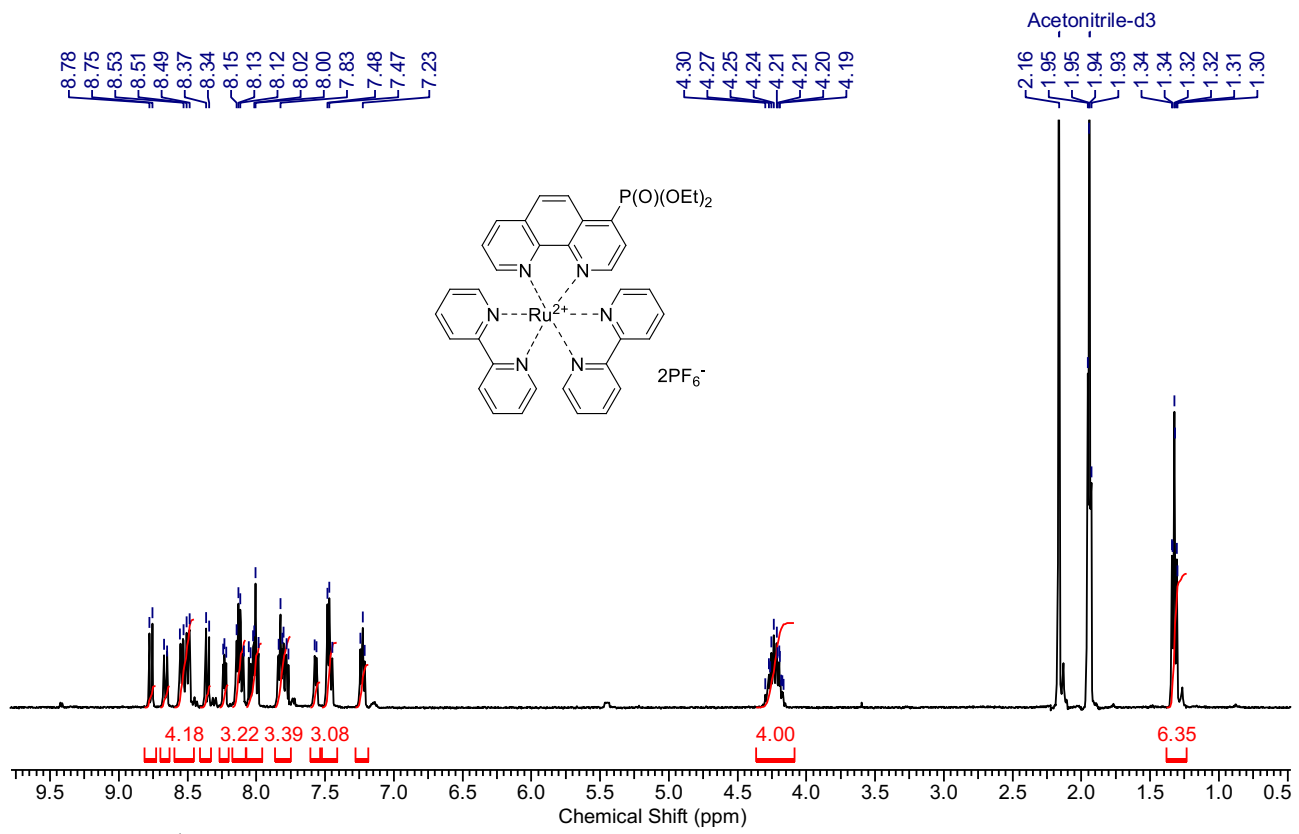


Figure S50. ^1H NMR spectrum of Ru-4P (CD_3CN , 400 MHz, 300 K).

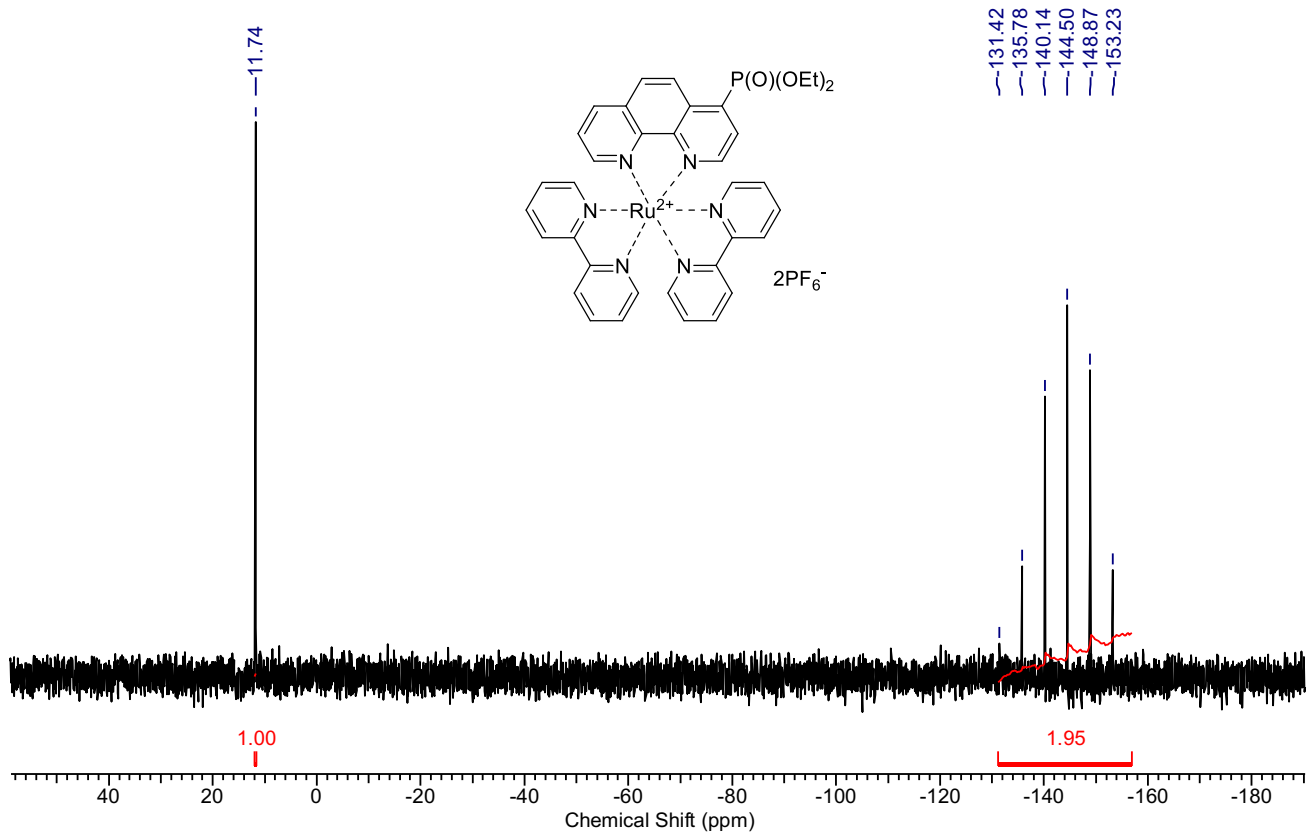


Figure S51. ^{31}P NMR spectrum of Ru-4P (CD_3CN , 162.5 MHz, 300 K).

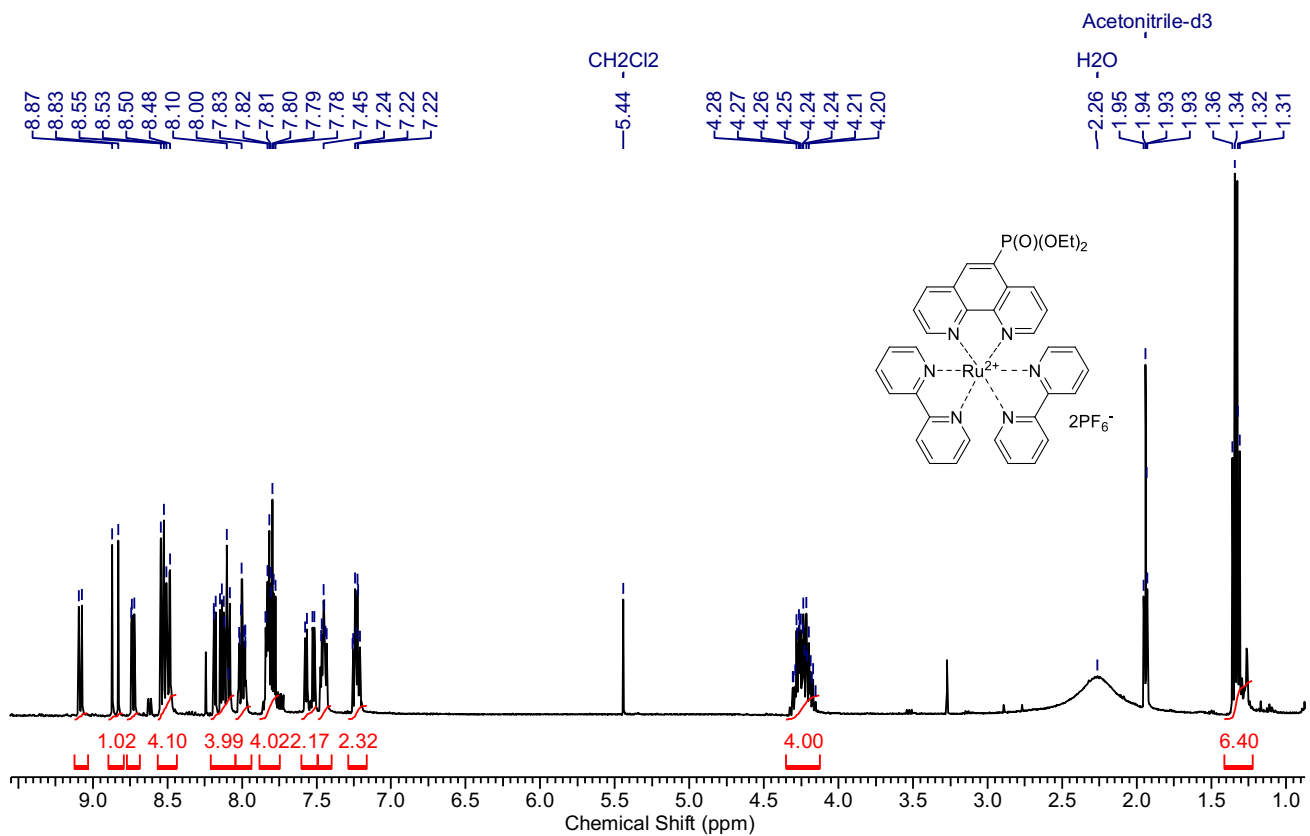


Figure S52. ^1H NMR spectrum of **Ru-5P** (CD_3CN , 400 MHz, 300 K).

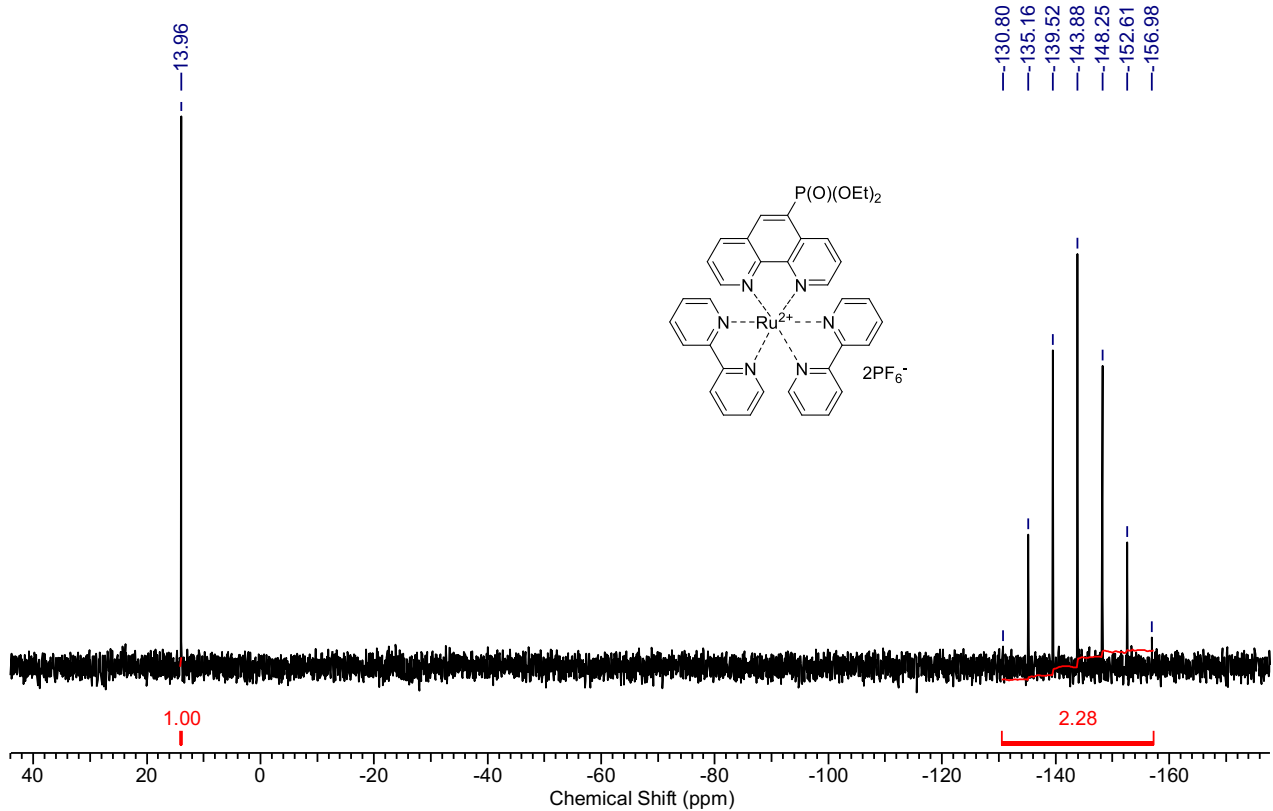


Figure S53. ^{31}P NMR spectrum of **Ru-5P** (CD_3CN , 162.5 MHz, 300 K).

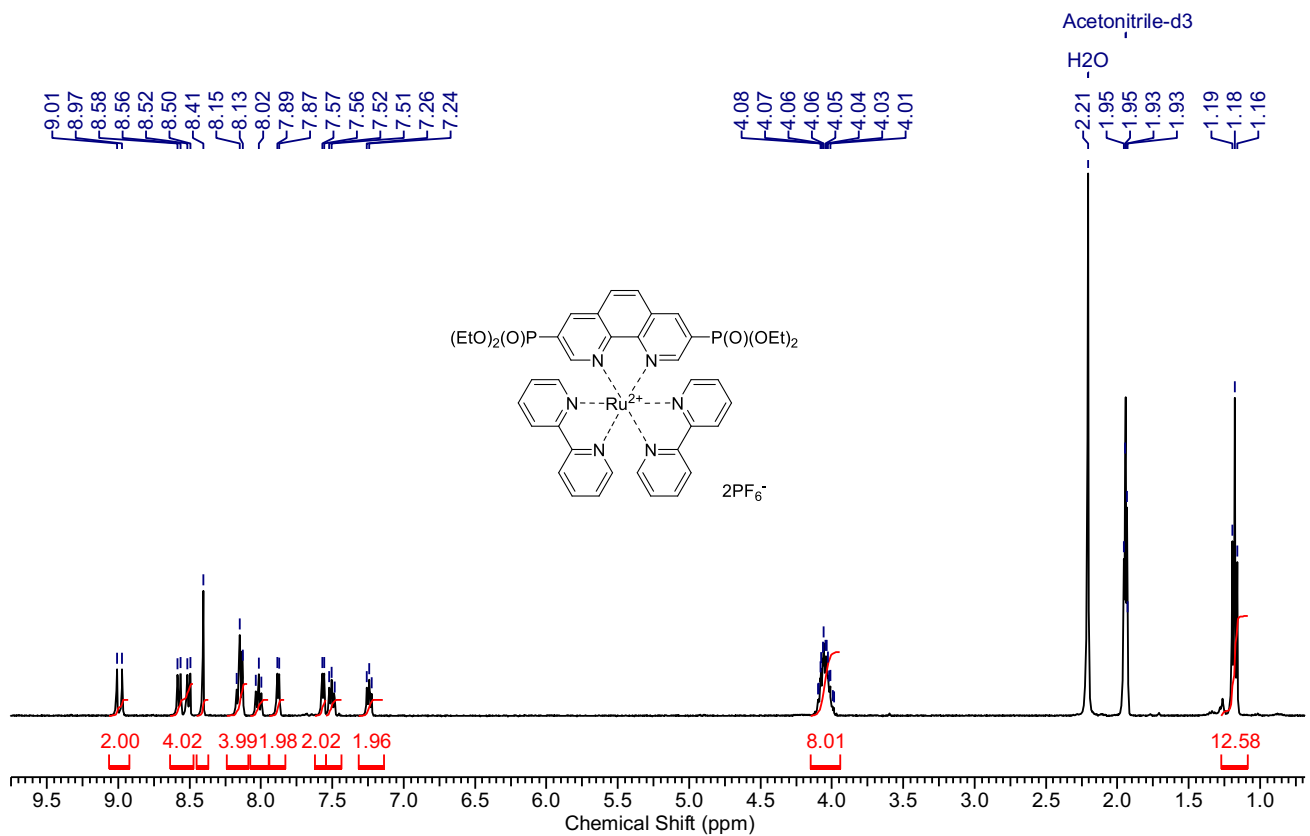


Figure S54. ^1H NMR spectrum of Ru-3,8P₂ (CD₃CN, 400 MHz, 300 K).

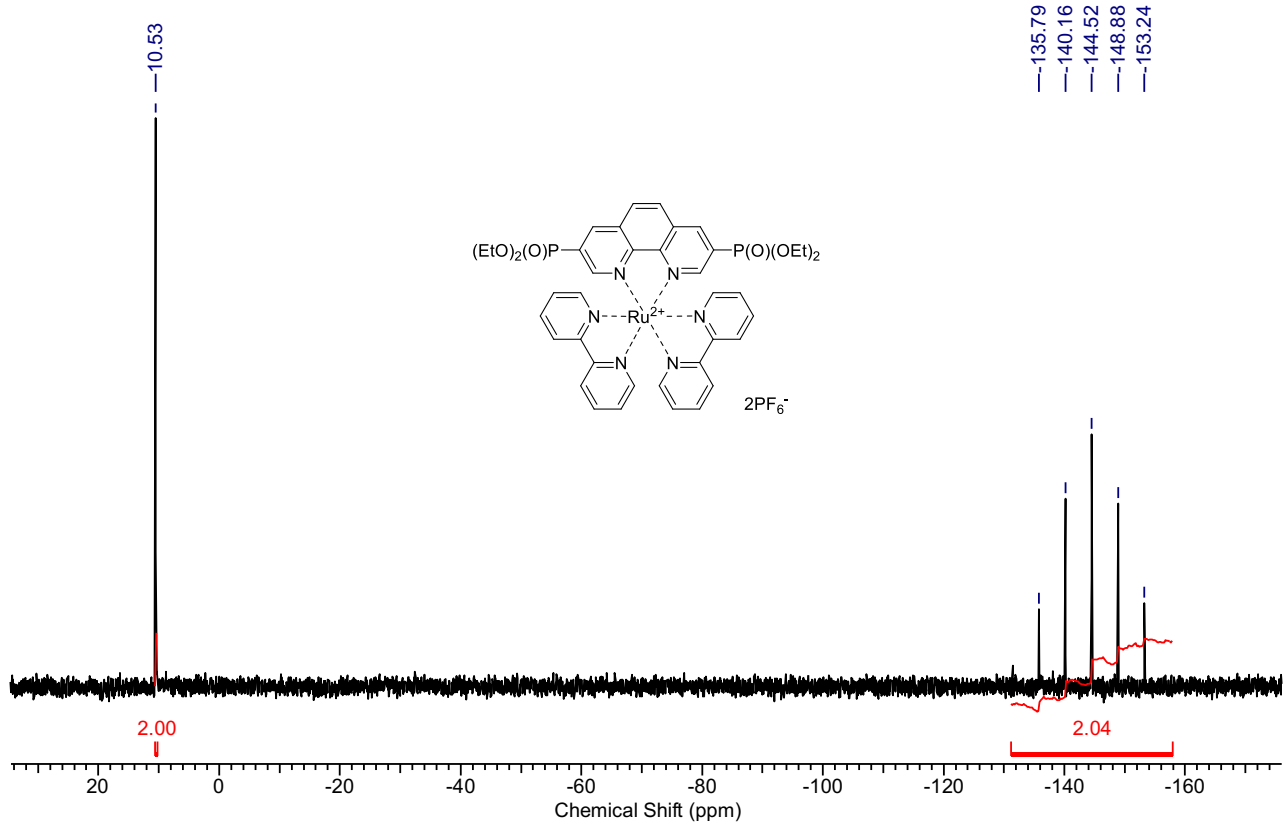


Figure S55. ^{31}P NMR spectrum of Ru-3,8P₂ (CD₃CN, 162.5 MHz, 300 K).

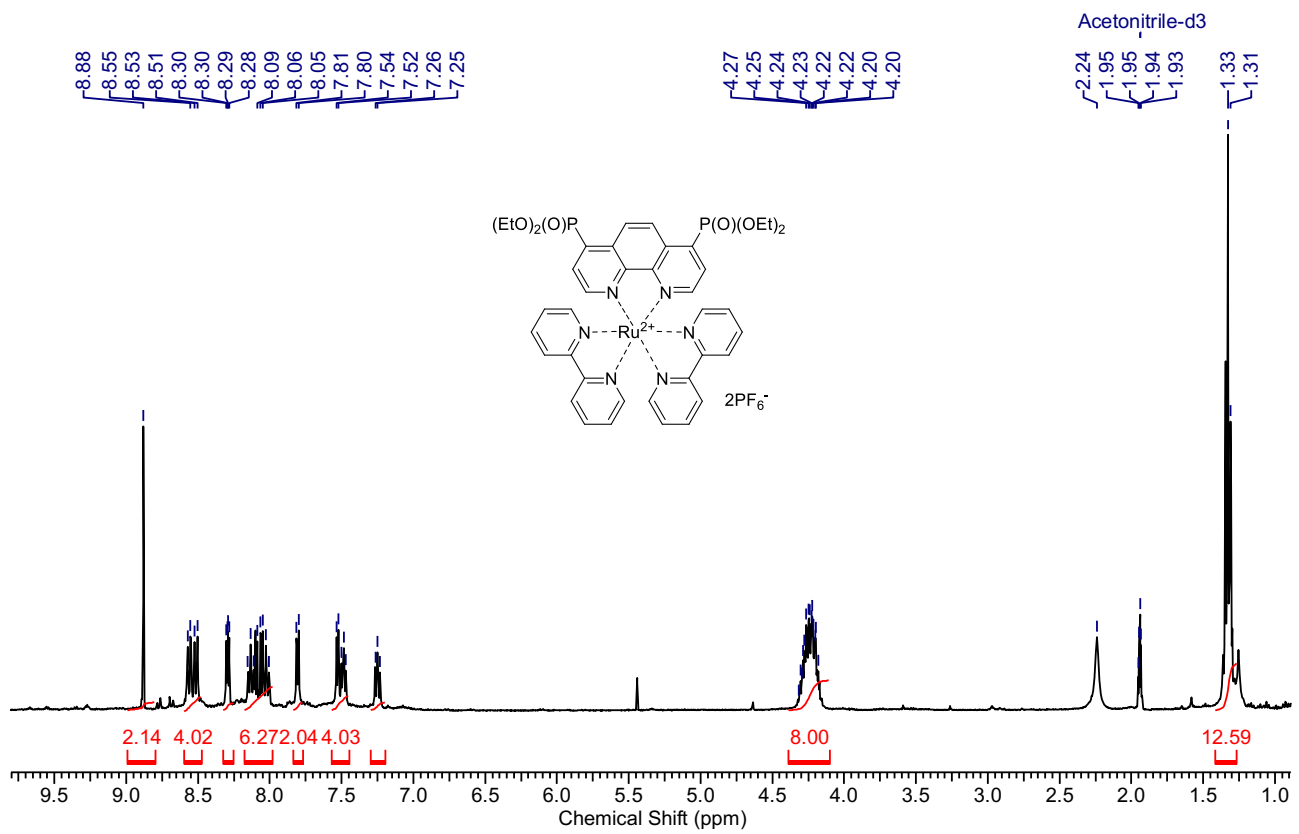


Figure S56. ^1H NMR spectrum of **Ru-4,7P₂** (CD_3CN , 400 MHz, 300 K).

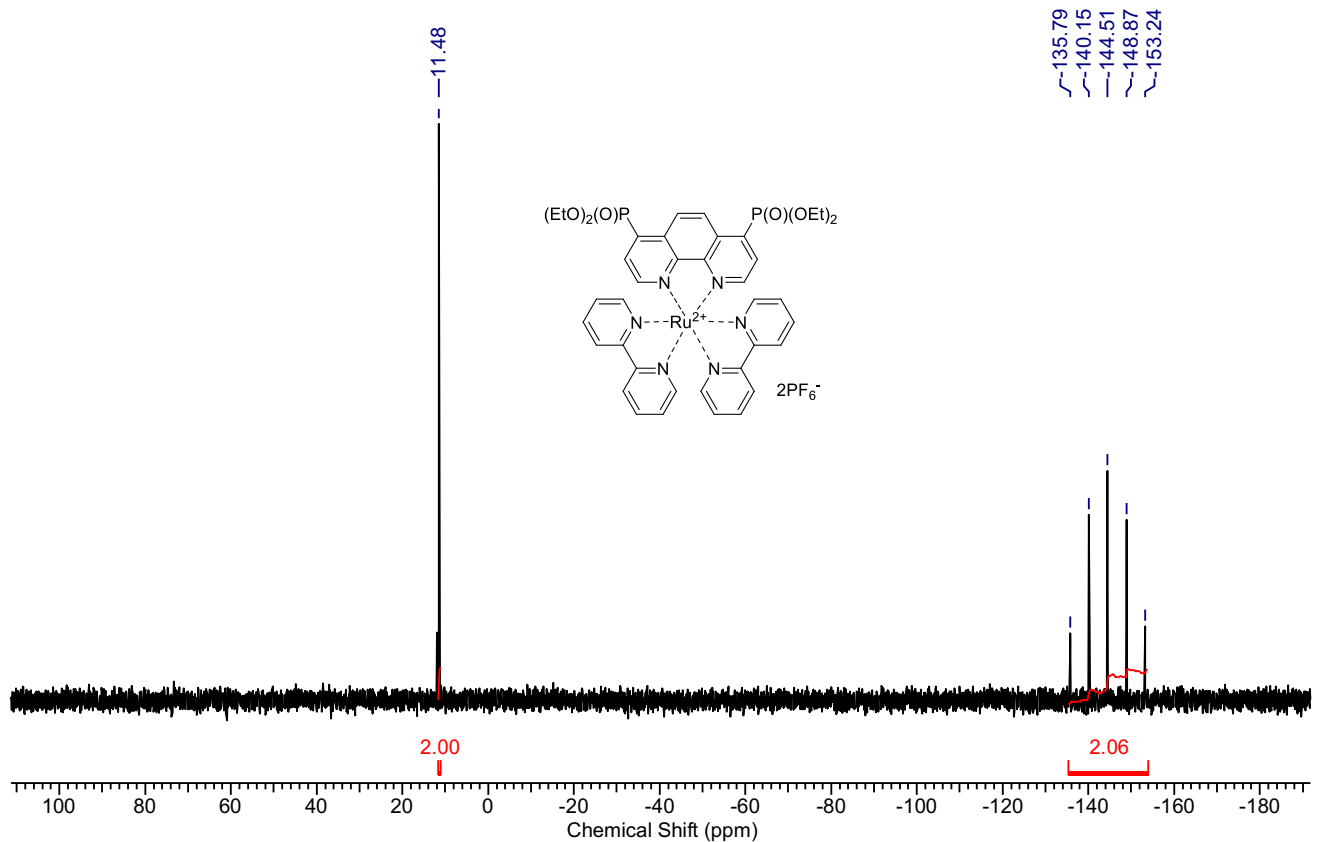


Figure S57. ^{31}P NMR spectrum of **Ru-4,7P₂** (CD_3CN , 162.5 MHz, 300 K).

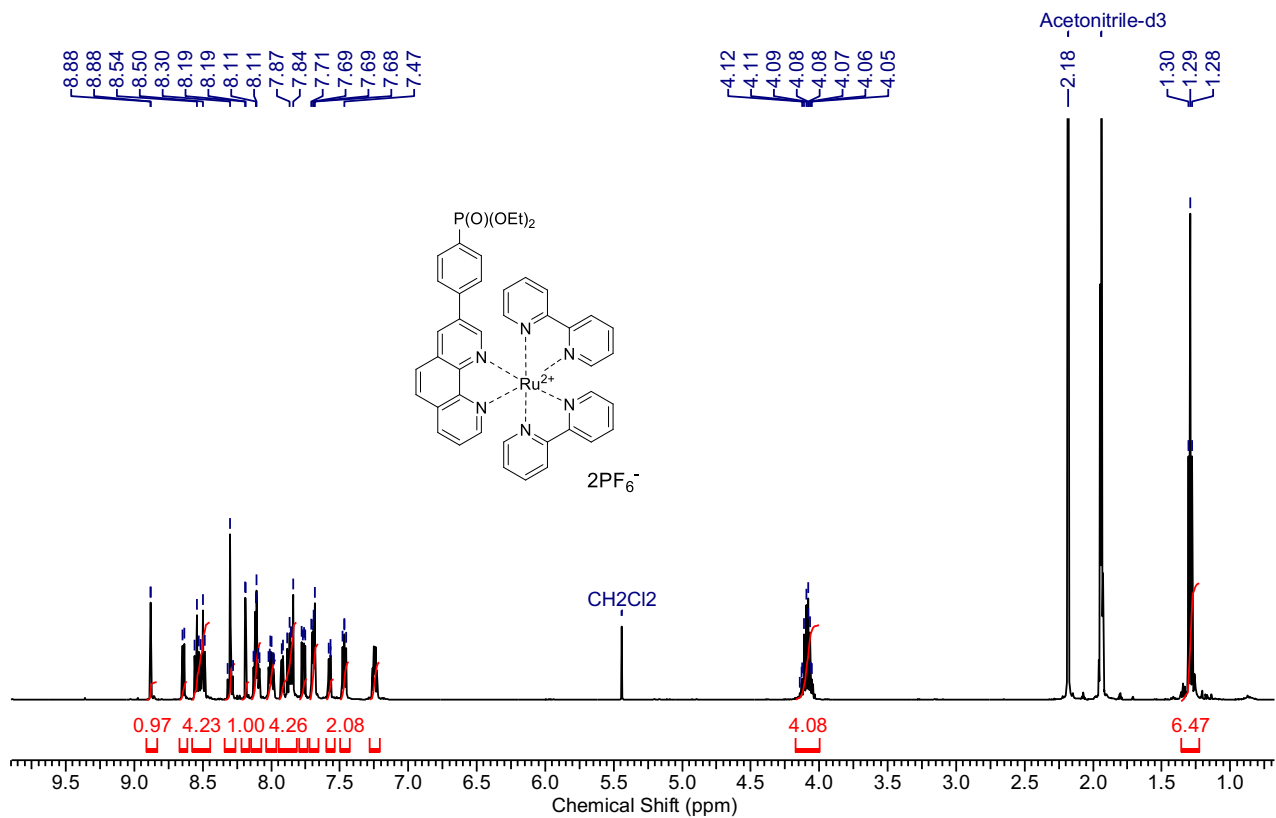


Figure S58. ^1H NMR spectrum of **Ru-3PPh** (CD_3CN , 400 MHz, 300 K).

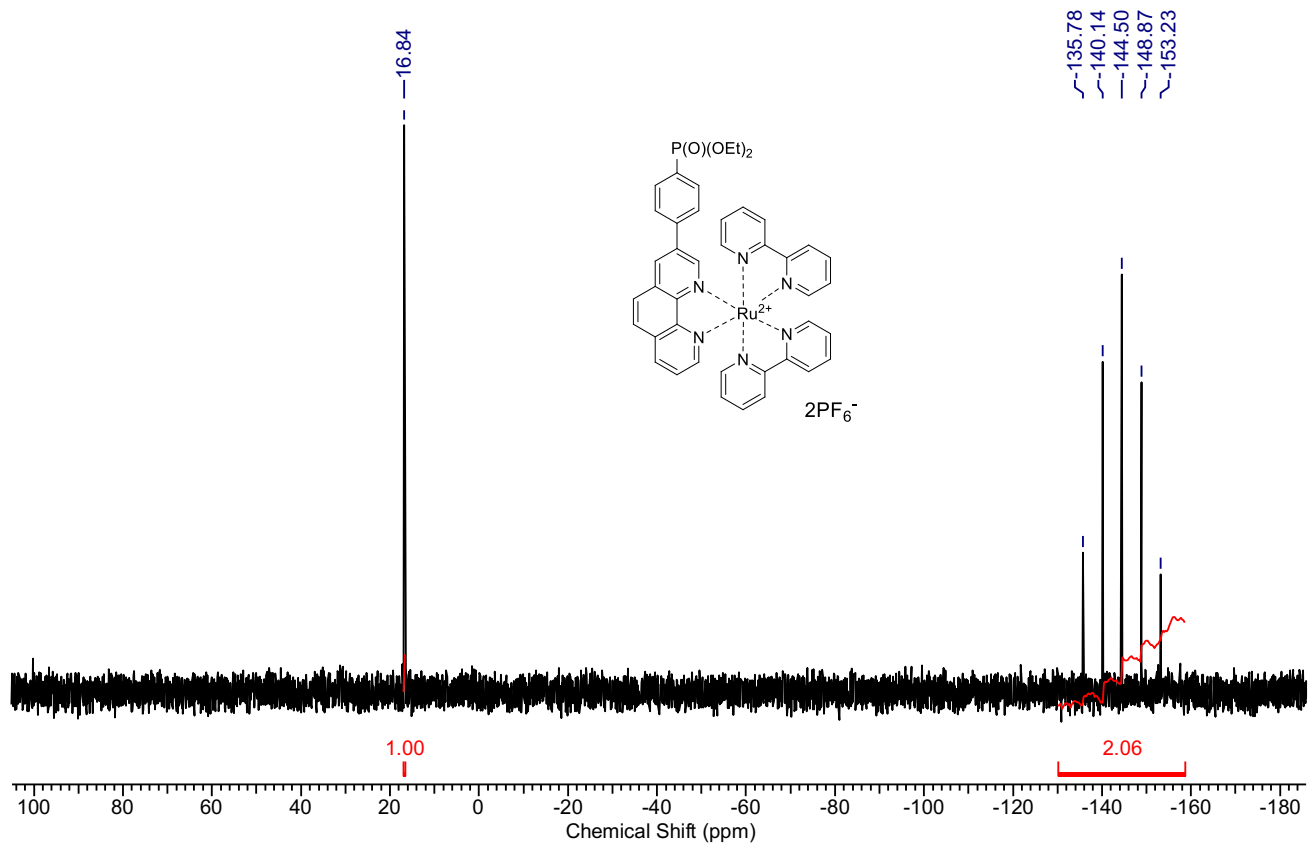


Figure S59. ^{31}P NMR spectrum of **Ru-3PPh** (CD_3CN , 162.5 MHz, 300 K).

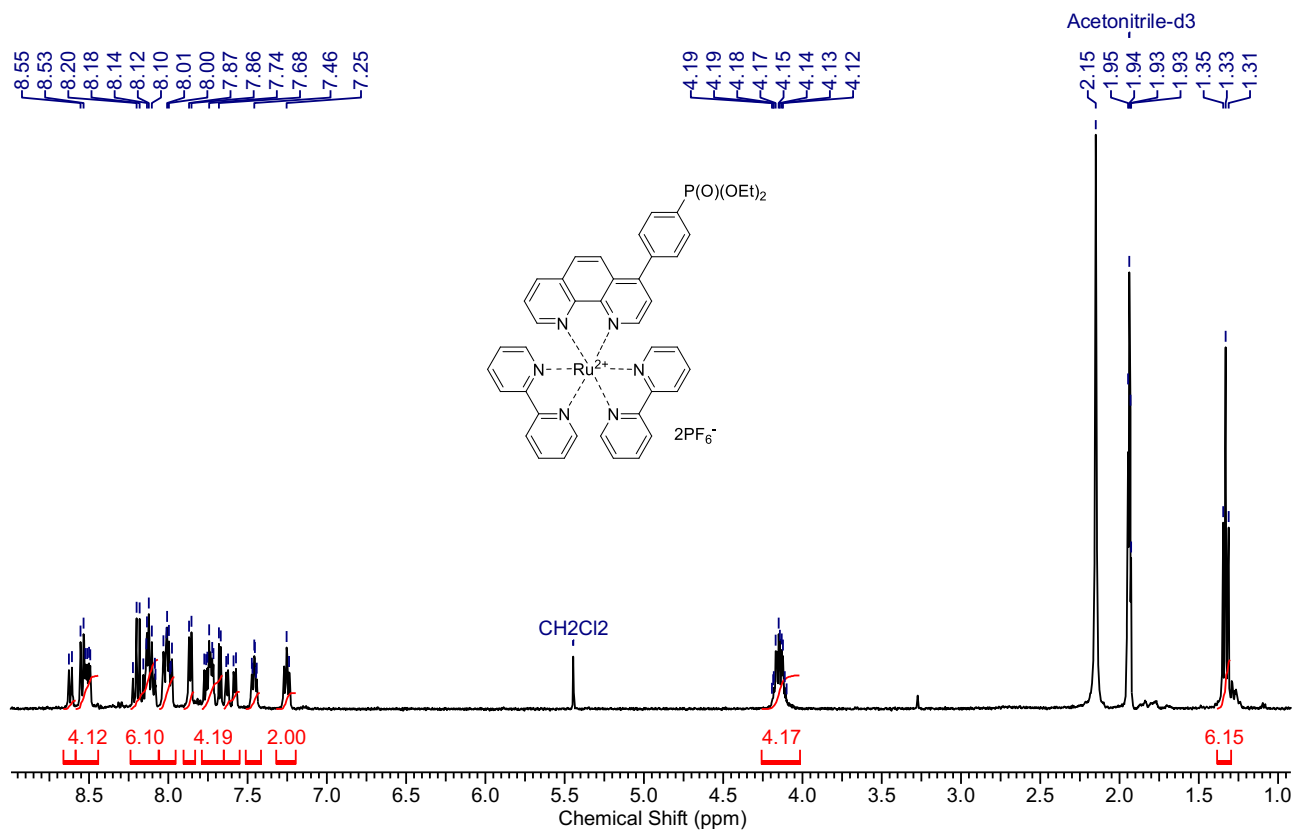


Figure S60. ¹H NMR spectrum of Ru-4PPh (CD₃CN, 400 MHz, 300 K).

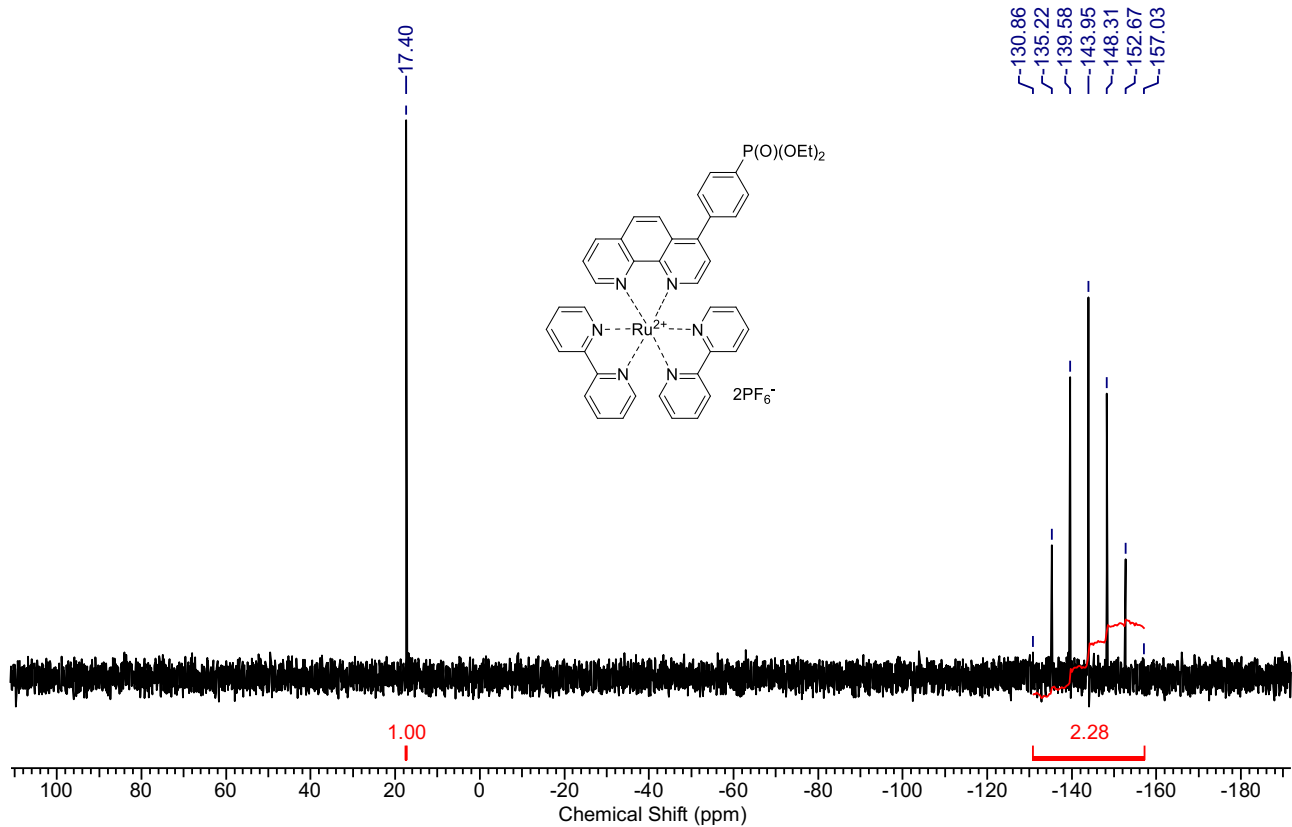


Figure S61. ³¹P NMR spectrum of Ru-4PPh (CD₃CN, 162.5 MHz, 300 K).

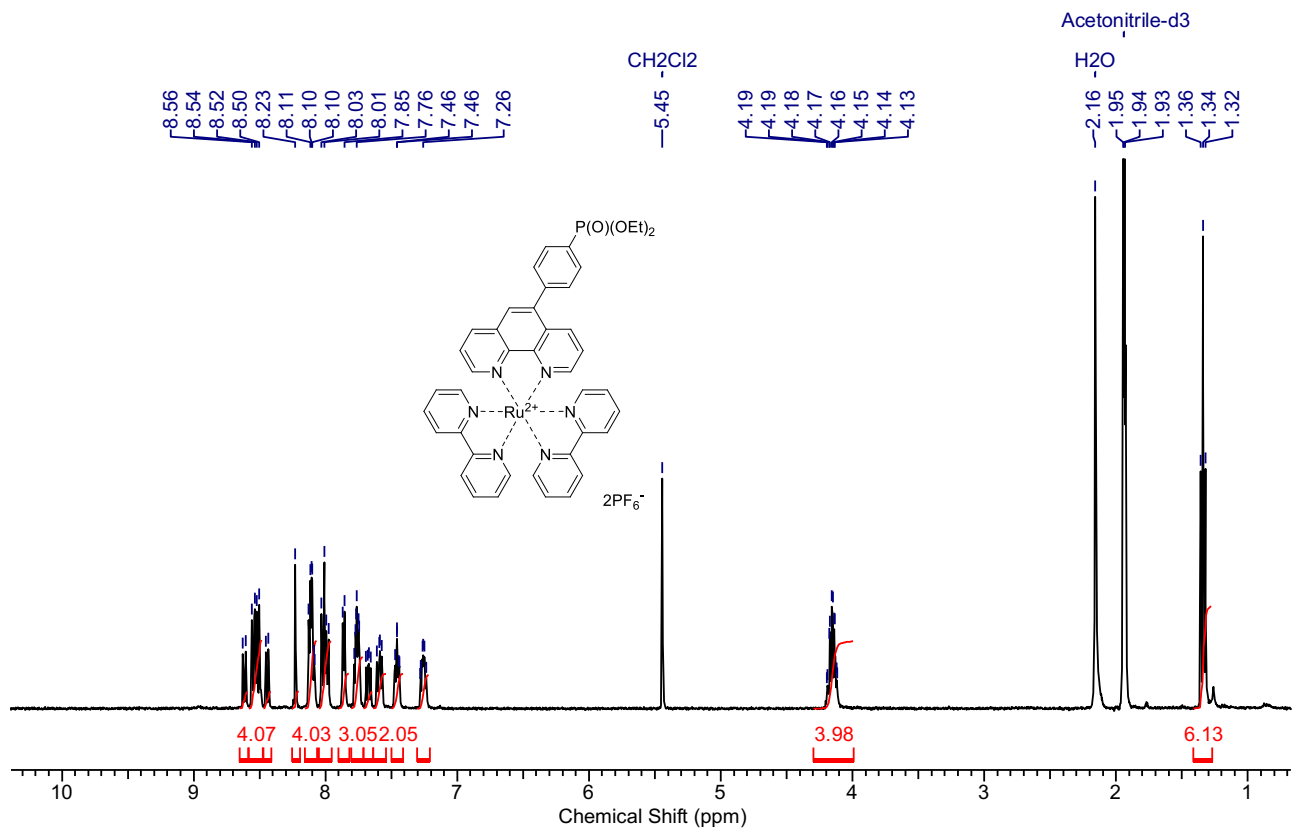


Figure S62. ^1H NMR spectrum of **Ru-5PPh** (CD_3CN , 400 MHz, 300 K).

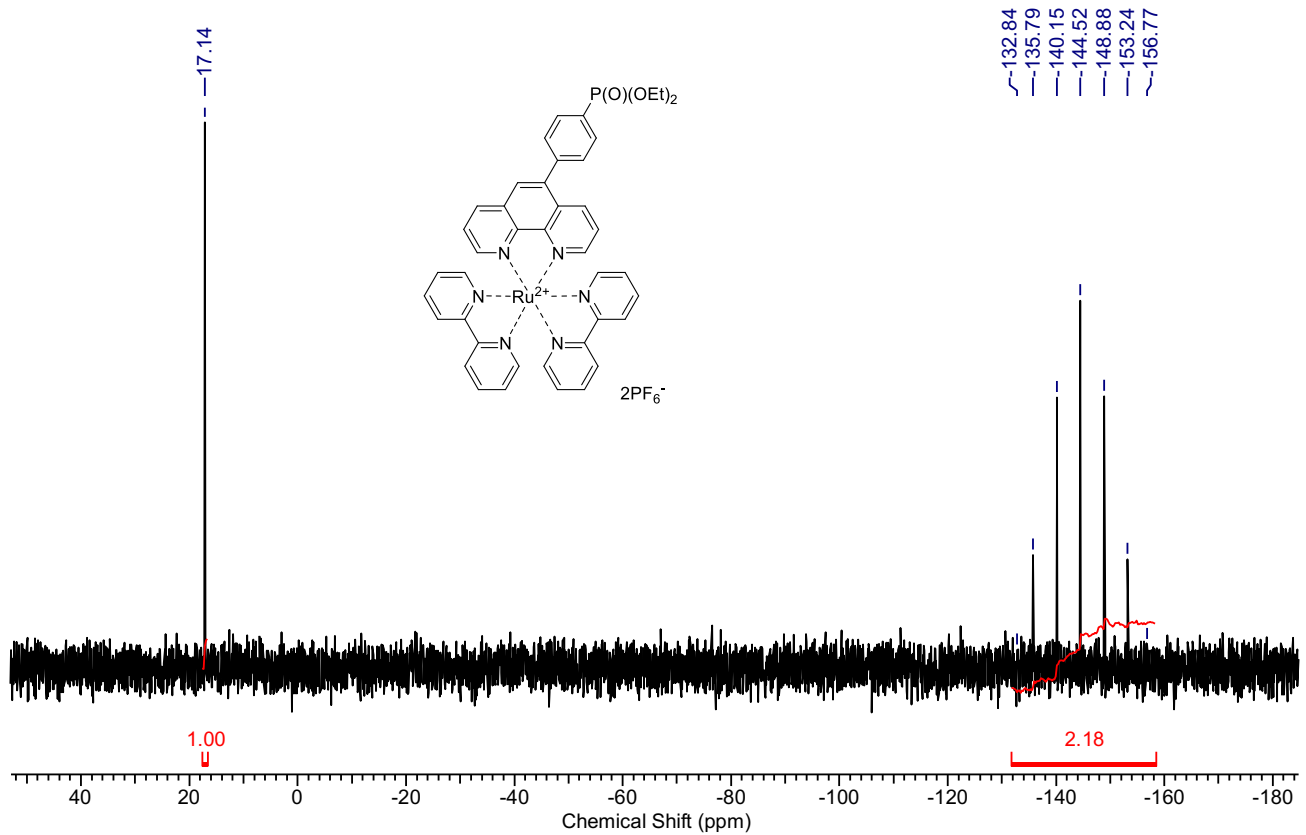


Figure S63. ^{31}P NMR spectrum of **Ru-5PPh** (CD_3CN , 162.5 MHz, 300 K).

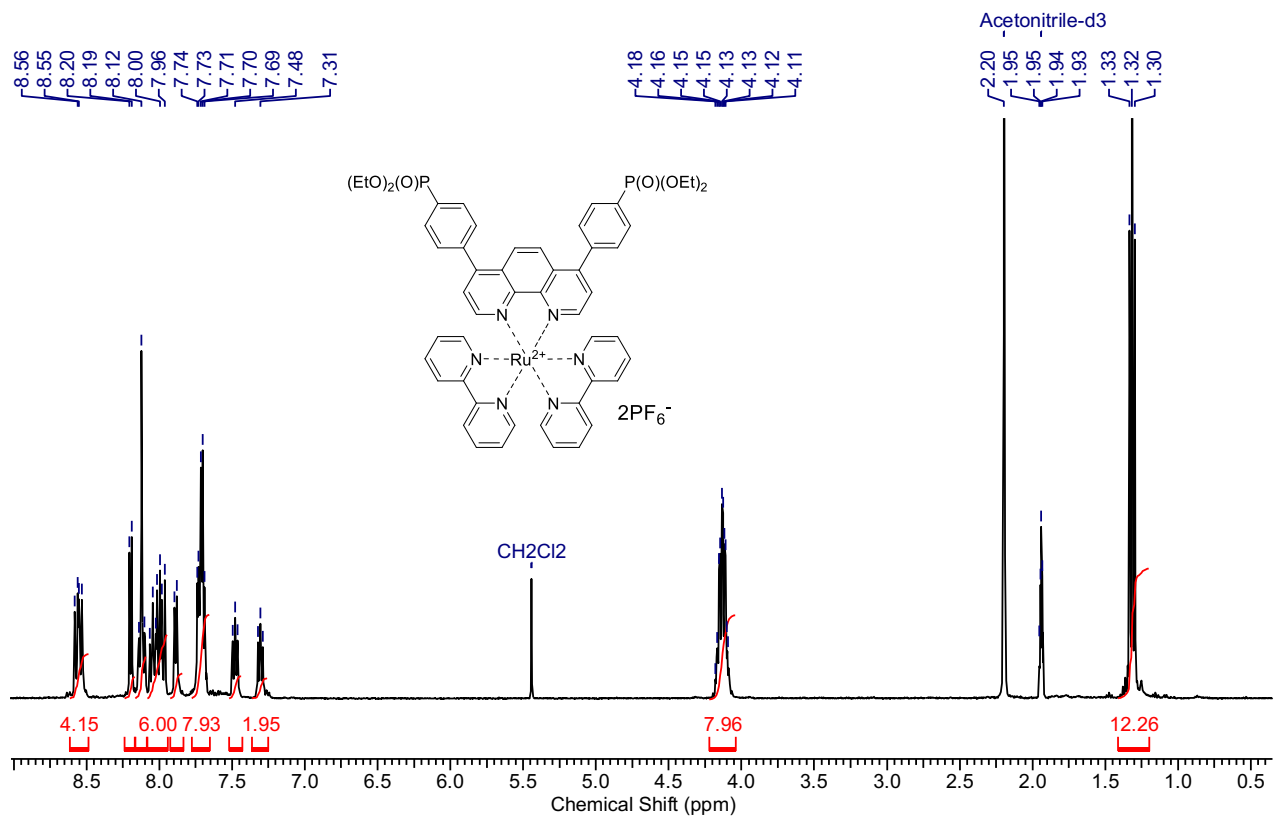


Figure S64. ^1H NMR spectrum of $\text{Ru-4,7}(\text{PPh})_2$ (CD_3CN , 400 MHz, 300 K).

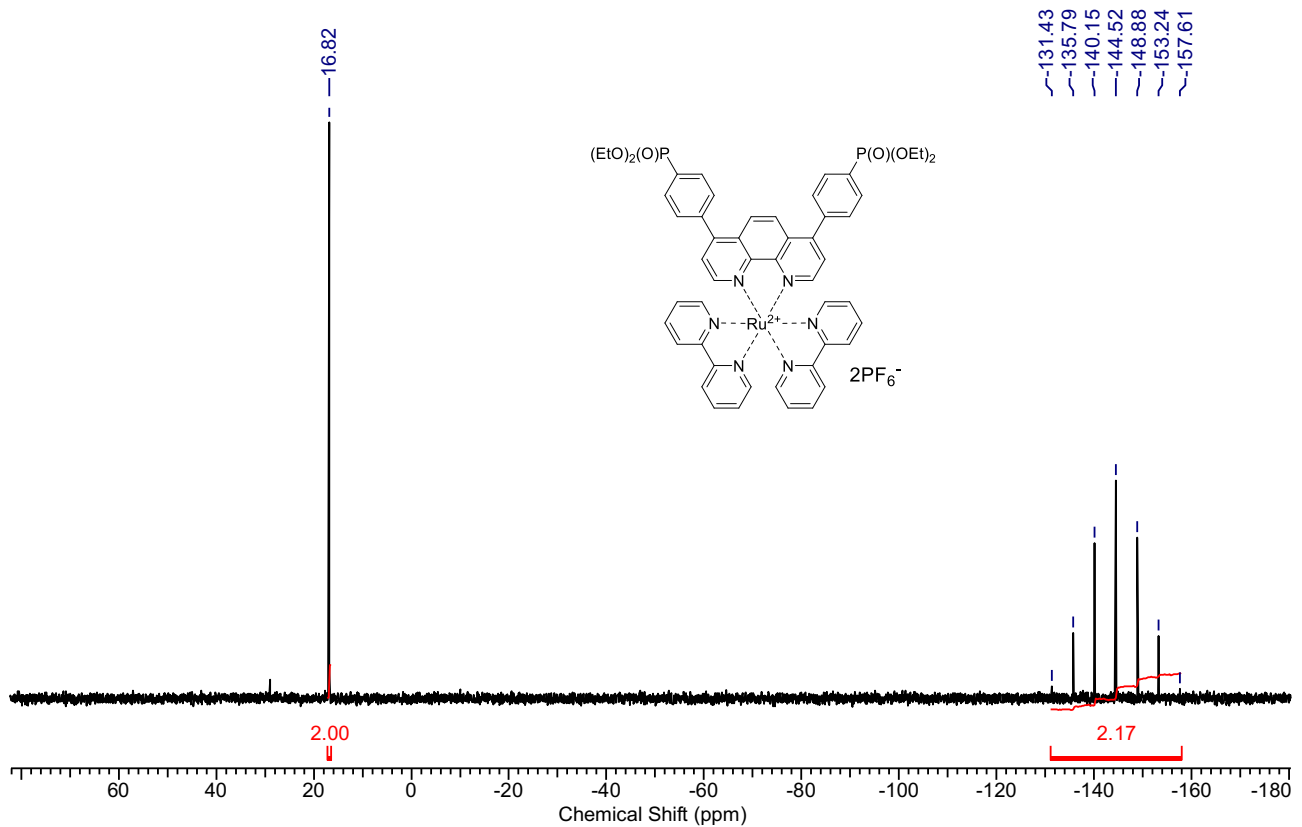


Figure S65. ^{31}P NMR spectrum of $\text{Ru-4,7}(\text{PPh})_2$ (CD_3CN , 162.5 MHz, 300 K).

10. Mass-spectra of the complexes

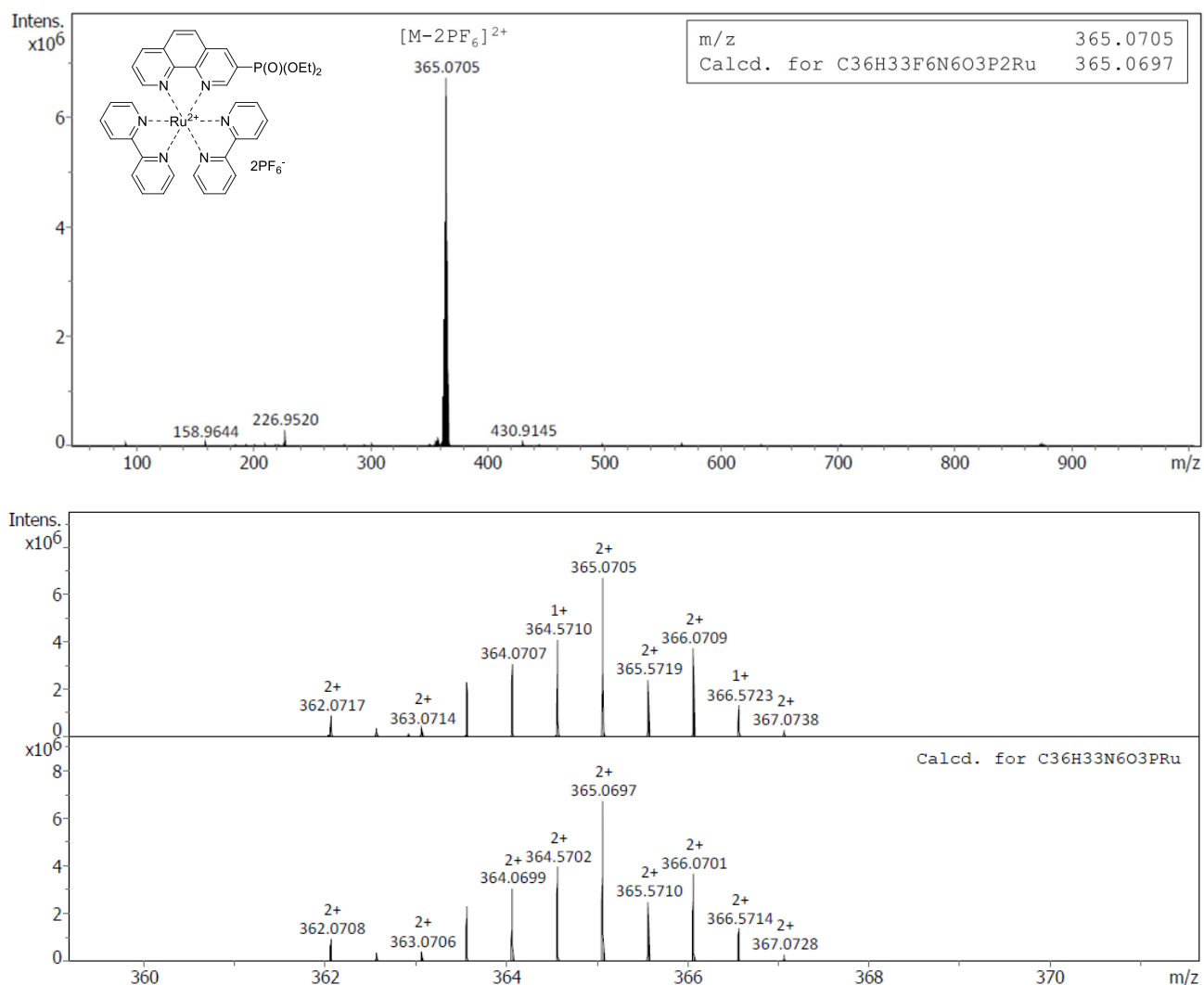


Figure S66. Mass-spectrum (ESI) of the complex **Ru-3P**. Set Capillary: 1500 V. Set End Plate Offset: -500 V. Set Collision Cell RF: 750.0 Vpp. Set Nebulizer: 0.3 Bar. Set Dry Heater: 200 °C. Set Dry Gas: 4.0 l/min.

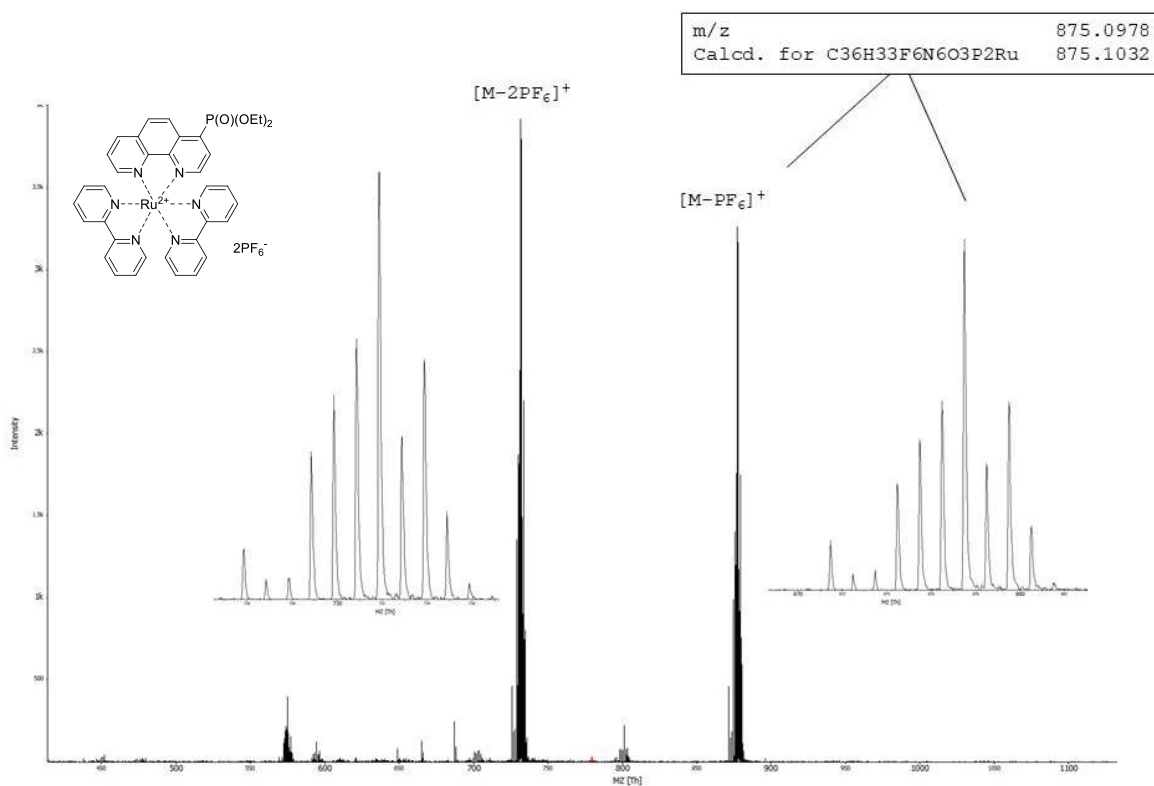


Figure S67. Mass-spectrum (MALDI-TOF) of the complex **Ru-4P**. Matrix: 1,8,9-trihydroxyanthracene. Calibration standard: PEG-600 + PEG-1000.

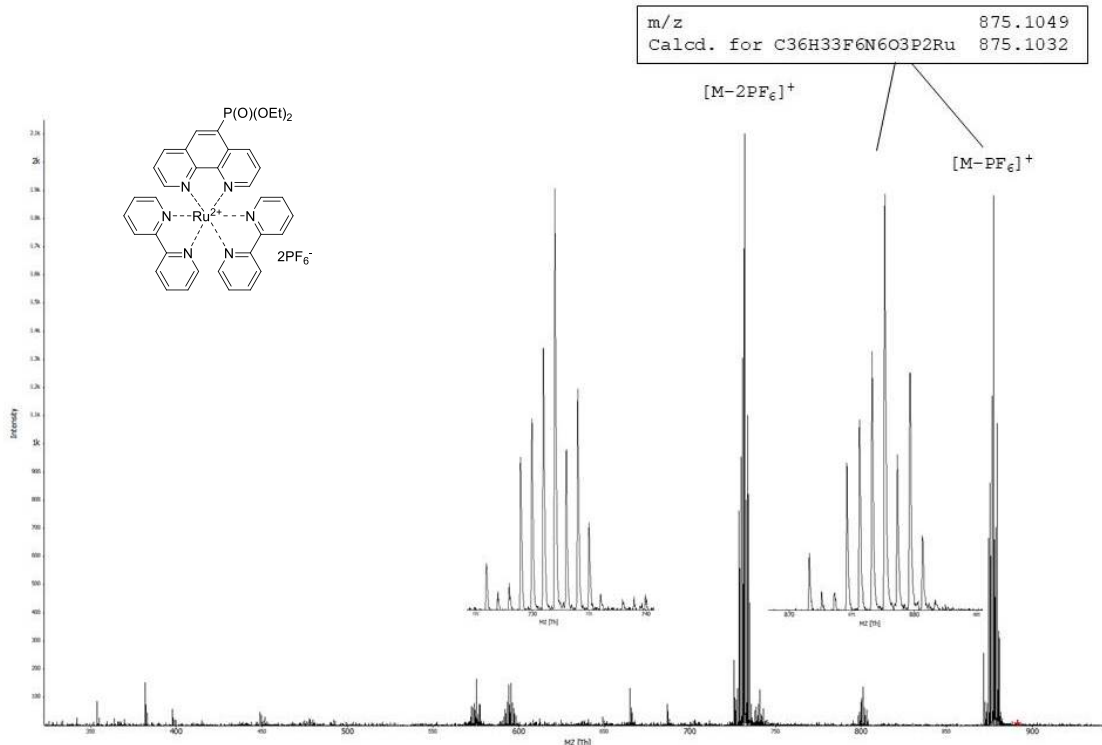


Figure S68. Mass-spectrum (MALDI-TOF) of the complex **Ru-5P**. Matrix: 1,8,9-trihydroxyanthracene. Calibration standard: PEG-600 + PEG-1000.

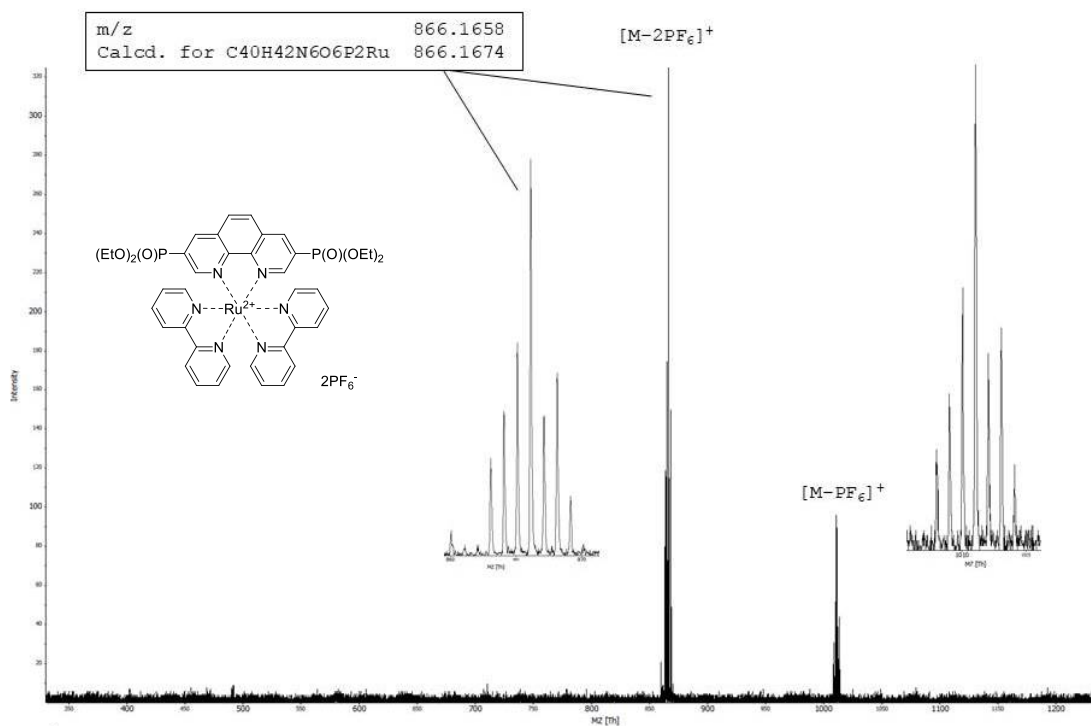


Figure S69. Mass-spectrum (MALDI-TOF) of the complex **Ru-3,8P₂**. Matrix: 1,8,9-trihydroxyanthracene. Calibration standard: PEG-600 + PEG-1000.

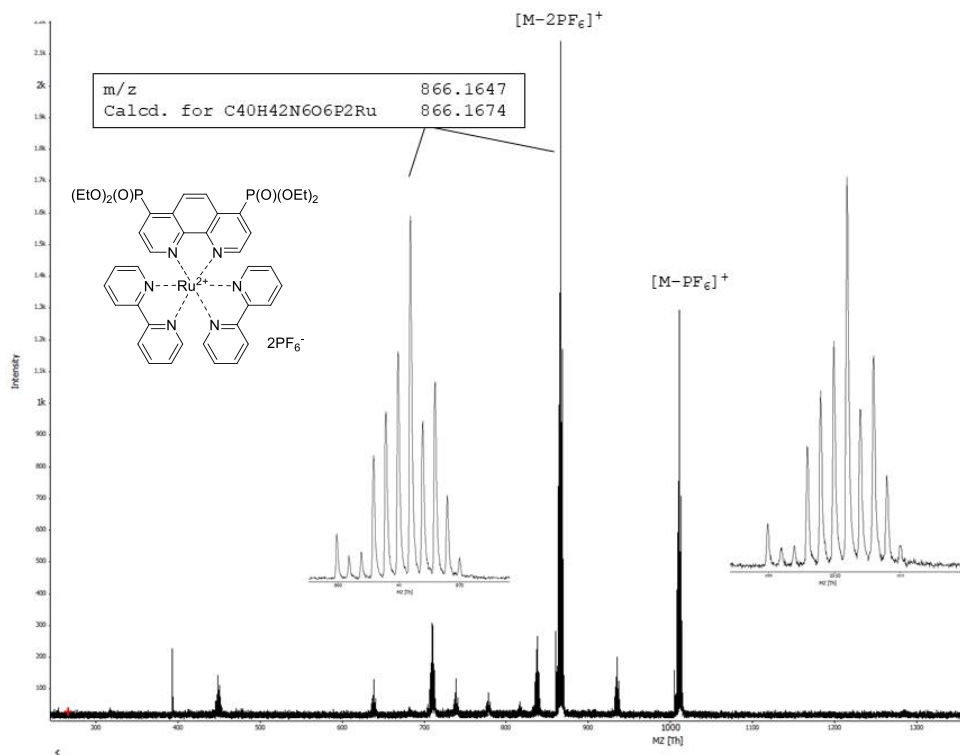


Figure S70. Mass-spectrum (MALDI-TOF) of the complex **Ru-4,7P₂**. Matrix: 1,8,9-trihydroxyanthracene. Calibration standard: PEG-600 + PEG-1000.

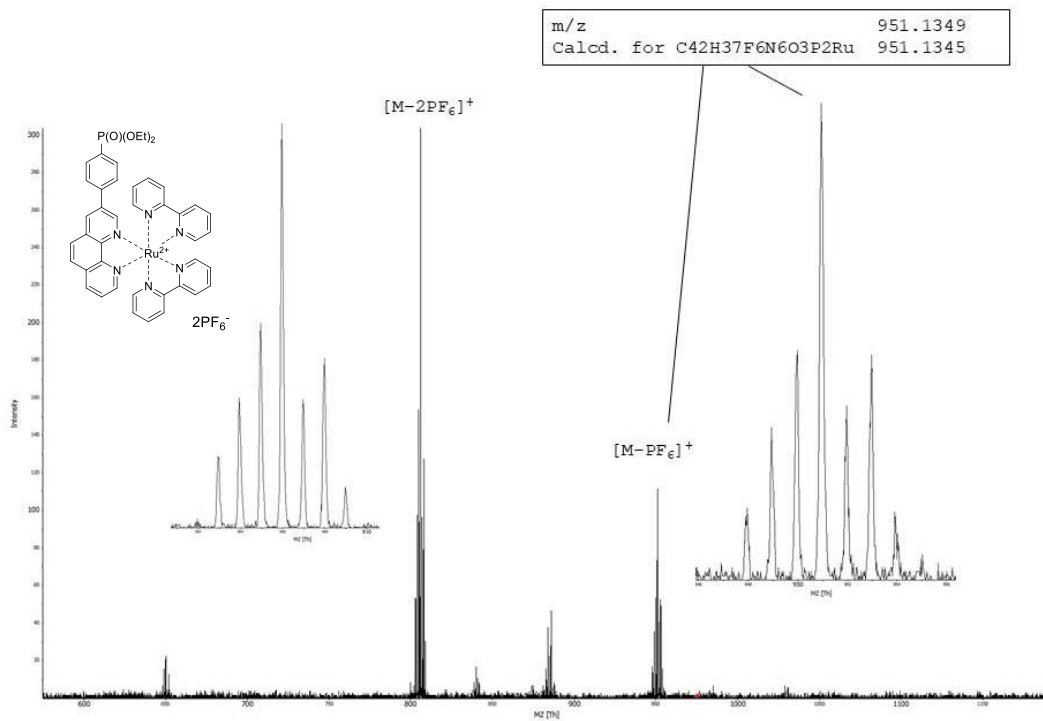


Figure S71. Mass-spectrum (MALDI-TOF) of the complex **Ru-3PPh**. Matrix: 1,8,9-trihydroxyanthracene. Calibration standard: PEG-600 + PEG-1000.

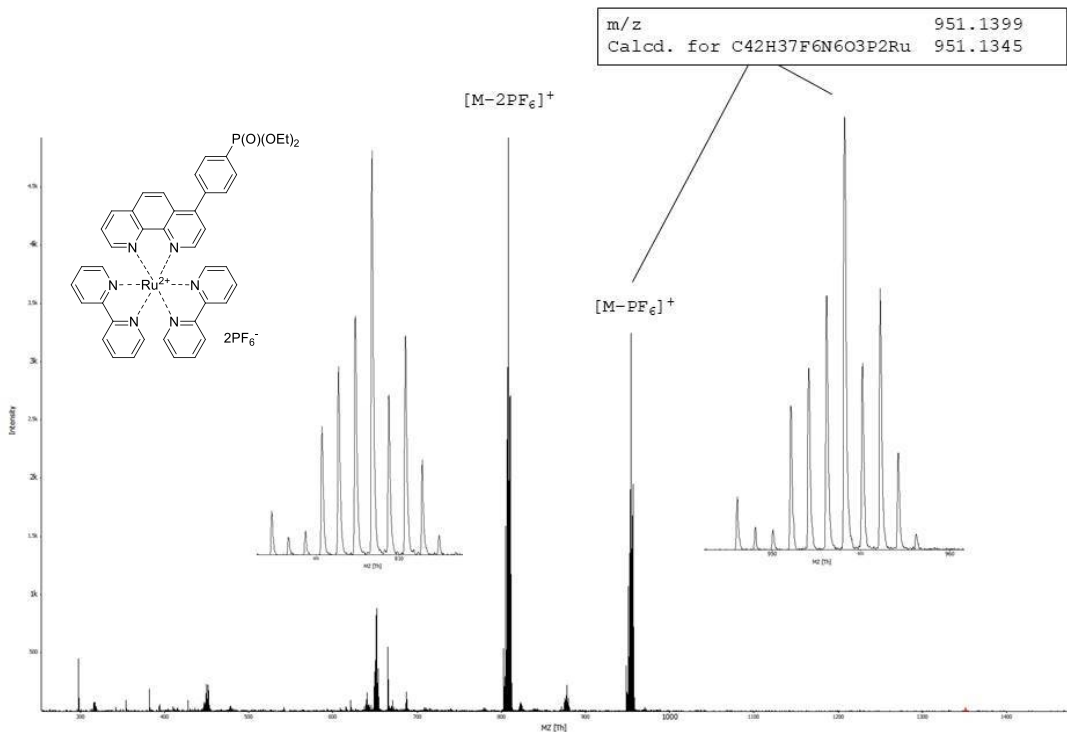


Figure S72. Mass-spectrum (MALDI-TOF) of the complex **Ru-4PPh**. Matrix: 1,8,9-trihydroxyanthracene. Calibration standard: PEG-600 + PEG-1000.

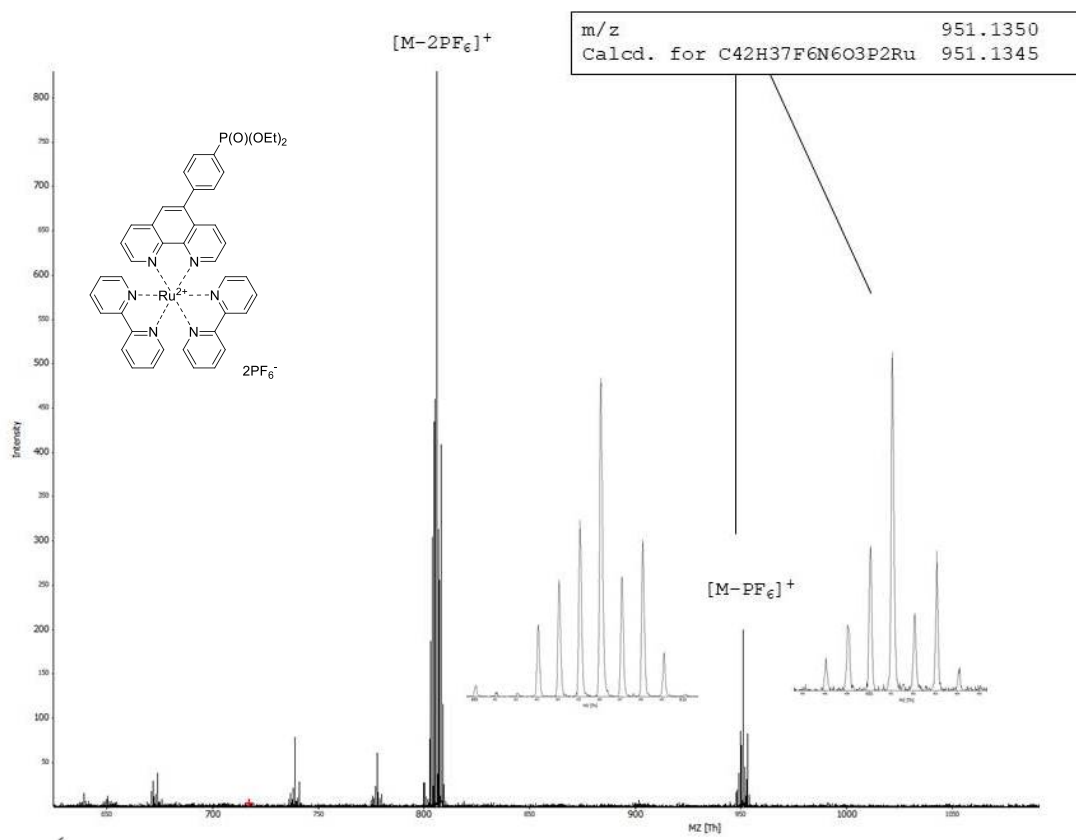


Figure S73. Mass-spectrum (MALDI-TOF) of the complex **Ru-5PPh**. Matrix: 1,8,9-trihydroxyanthracene. Calibration standard: PEG-600 + PEG-1000.

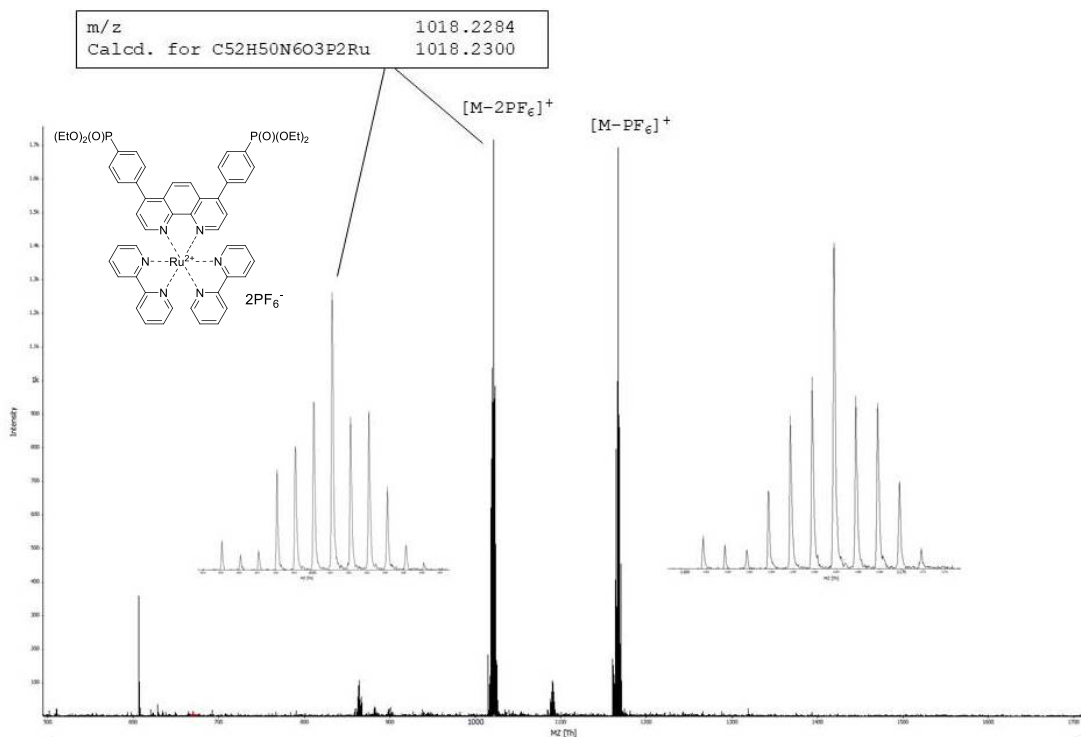


Figure S74. Mass-spectrum (MALDI-TOF) of the complex **Ru-4,7(PPh)₂**. Matrix: 1,8,9-trihydroxyanthracene. Calibration standard: PEG-1000 + PEG-1500.

11. References

1. D. Tzalis, Y. Tor, F. Salvatorre and S. Jay Siegel, *Tetrahedron Lett.*, 1995, **36**, 3489-3490.
2. J. Mlochowski, *Roczn. Chem.*, 1974, **48**, 2145-2155.
3. G. I. Graf, D. Hastreiter, L. E. da Silva, R. A. Rebelo, A. G. Montalban and A. McKillop, *Tetrahedron*, 2002, **58**, 9095-9100.
4. F. Ferretti, E. Gallo and F. Ragagni, *J. Organomet. Chem.*, 2014, **771**, 59-67.
5. A. Mitrofanov, A. B. Lemeune, C. Stern, R. Guillard, N. Gulyukina and I. Beletskaya, *Synthesis*, 2012, **44**, 3805-3810.
6. M. E. Hoque, R. Bisht, C. Haldar and B. Chattopadhyay, *J. Am. Chem. Soc.*, 2017, **139**, 7745-7748.
7. P. A. Lay, A. M. Sargeson, H. Taube, M. H. Chou and C. Creutz, *Inorganic Syntheses*, 1986, DOI: 10.1002/9780470132555.ch78, 291-299.
8. A. S. Abel, I. S. Zenkov, A. D. Averin, A. V. Cheprakov, A. G. Bessmertnykh-Lemeune, B. S. Orlinson and I. P. Beletskaya, *ChemPlusChem*, 2019, **84**, 498-503.
9. S. Amthor, P. Keil, D. Nauroozi, D. Perleth and S. Rau, *Eur. J. Inorg. Chem.*, 2021, **2021**, 4790-4798.
10. B.-H. Ye, X.-M. Chen, T.-X. Zeng and L.-N. Ji, *Inorg. Chim. Acta*, 1995, **240**, 5-11.
11. A. A. Granovsky, *Firefly version 8*, [www *http://classic.chem.msu.su/gran/firefly/index.html*](http://classic.chem.msu.su/gran/firefly/index.html).
12. M.W.Schmidt, K.K.Baldridge, J.A.Boatz, S.T.Elbert, M.S.Gordon, J.H.Jensen, S.Koseki, N.Matsunaga, K.A.Nguyen, S.Su, T.L.Windus, M.Dupuis and J.A.Montgomery, *J.Comput.Chem.* , 1993, **14**, 1347-1363
13. M. Dolg, H. Stoll, H. Preuss and R. M. Pitzer, *J. Phys. Chem.*, 1993, **97**, 5852-5859.
14. W. Huang and T. Ogawa, *Polyhedron*, 2006, **25**, 1379-1385.
15. V. Balzani, F. Bolletta, M. T. Gandolfi and M. Maestri, Berlin, Heidelberg, 1978.
16. J. W. Tucker and C. R. J. Stephenson, *J. Org. Chem.*, 2012, **77**, 1617-1622.
17. K. Kalyanasundaram, *Coordination Chemistry Reviews*, 1982, **46**, 159-244.
18. V. V. Pavlishchuk and A. W. Addison, *Inorg. Chim. Acta*, 2000, **298**, 97-102.
19. Y. Zhang, P. Traber, L. Zedler, S. Kupfer, S. Gräfe, M. Schulz, W. Frey, M. Karnahl and B. Dietzek, *Phys. Chem. Chem. Phys.*, 2018, **20**, 24843-24857.
20. T. Neveselý, E. Svobodová, J. Chudoba, M. Sikorski and R. Cibulka, *Adv. Synth. Catal.*, 2016, **358**, 1654-1663.
21. K. Kamata, T. Hirano and N. Mizuno, *Chem. Commun.*, 2009, DOI: 10.1039/b907952a, 3958-3960.
22. Y. Gao and Y. Lam, *Adv. Synth. Catal.*, 2008, **350**, 2937-2946.